12-27-2013

Volatization of Extraterrestrial Materials as Determined by Zinc Isotopic Analysis

Randal Christopher Paniello
Washington University in St. Louis

WASHINGTON UNIVERSITY IN ST. LOUIS

Department of Earth and Planetary Sciences

Dissertation Examination Committee:

Frederic Moynier, Chair
Alex Bradley
Jeffrey G. Catalano
Bruce Fegley
Christine Floss
Brad Joliff
Ernst Zinner

Volitization of Extraterrestrial Materials as Determined by Zinc Isotopic Analysis

by

Randal C Paniello

A dissertation presented to the
Graduate School of Arts and Sciences
of Washington University in
partial fulfillment of the
requirements for the degree
of Doctor of Philosophy

December 2013

St. Louis, Missouri

TABLE OF CONTENTS

LIST OF FIGURES

Chapter 1

Chapter 2

Chapter 3

Manuscript

Chapter 4

Manuscript

Chapter 5

Manuscript

Chapter 6

Manuscript

LIST OF TABLES

Manuscript

Chapter 6

Manuscript

Acknowledgement

The author would like to thank Dr. Fred Moynier, who has been both mentor and friend for the past several years, and who helped with this work in so many ways. He was instrumental in stimulating the scientific curiosity that led to this work, he was diligent in his encouragement to seeing it completed, and he provided many editorial and scientific contributions to creating the final thesis product.

Dr. Moynier's grants provided all of the funding used in this project.

Thanks are also extended to Dr. Frank Podosek, who introduced me to the world of meteorites and encouraged me to pursue this work.

Many thanks also go to the faculty of the Dept. of Earth and Planetary Sciences at Washington University, who have always been welcoming and helpful. Their collective brilliance is astounding. Special thanks specifically go, alphabetically, to: Drs. Ray Arvidson, Jeff Catalano, Bob Criss, Bruce Fegley, Brad Jolliff, Katarina Lodders, Bill McKinnon (who still owes me a grade), Jill Pasteris, Roger Phillips, Slava Solamatov, and Doug Wiens. Their input and encouragement has been extremely valuable and stimulating. The suggestions and patience of the thesis committee members was also very much appreciated.

Finally, I thank my wonderful wife Jane, who reluctantly indulged my whim to pursue this course of study and, ultimately, encouraged me to finish. Without her support this project could not have happened.

Statement Regarding Role of Candidate in Co-Authored Work

All four subprojects described in this thesis include work that has already been published (3) or has been submitted for publication (1), and each includes one or more coauthors. The Candidate performed the majority of the work for all of these papers. Specifically, he formulated hypotheses and designed the experiments with consultation from his Mentor (Dr. Moynier); he obtained the samples to be studied from the source collections; he personally performed 75-100% of the individual chemistries/analyses and mass spectrometry for each project; he carried out all of the data analysis and error calculations; and he wrote the initial drafts and most of the revisions of all of the manuscripts, in consultation with his coauthors.

1. Introduction

Much has been learned over the past two or three decades about the origins of the materials that make up the orbiting bodies in our solar system. There is strong evidence for the sun forming as a result of condensation within a molecular cloud, with the remainder forming a solar nebula; and that the elemental makeup of that nebula was primarily hydrogen, with lesser amounts of other elements resembling the current solar abundances (e.g., Burbridge et al. 1957), with some material inherited from other stars after supernova. At first order, the process of accretion of dust, ice and other nebular elements into chondrules (Desch et al. 2012, Hewins and Zanda 2012), planetesimals and eventually asteroids and planets is generally understood and accepted (e.g., Edvardsson et al. 1993).

With the availability of high-precision mass spectrometry, analysis of stable isotopes has enabled a number of advances in our understanding of these formation processes. After their original accretion, planetary bodies were subjected to a number of secondary processes that may have resulted in changes in their elemental composition (Brearley and Jones 1998). Prolonged heating from decay of short-lived radioisotopes, such as ^{26}Al, may have allowed for moderately volatile elements to slowly evaporate away. Impacts from other bodies added frictional heating acutely and created ejecta that could later land on Earth as meteorites. But once the body had cooled, and post-accretionary activity had subsided, the composition of stable isotopes is presumed to have remained unchanged to the present day because these elements, by definition, do not undergo any radioactive decay. Analysis of stable isotopes can thus provide evidence of planetary formation processes that took place billions of years ago.

Fractionation of isotopes in planetary formation may occur by several mechanisms: volatization, mineral-silicate melt or mineral-liquid metal segregation, and thermal or shock metamorphism are the most important (Luck et al. 2005), and each of these is a mass-dependent process (Young et al. 2002). Fractionation that occurs by a simple Rayleigh distillation process is given, for Zn isotopes for example, by

$$\delta^{66}Zn = 10^3 \times \left(\frac{[Zn]}{[Zn]_0}\right)^{\alpha-1} - 10^3 \qquad \text{(Eq. 1)}$$

where α is the fractionation factor that can be approximated by

$$\alpha \cong \sqrt{\frac{M^{64}Zn}{M^{66}Zn}} \qquad \text{(Eq. 2)}$$

with $M\,^{x}Zn$ is the atomic mass of the zinc isotope. The Rayleigh equation assumes that it is an open system from which the evaporating material is instantly removed, and that the residue element is instantaneously re-equilibrated. These assumptions may not be valid in planetary processes. While a body in space may seem to be an open system, evaporated material may be retained near the surface by the body's gravity. Instantaneous re-equilibration is unlikely due to the large mass of the body relative to its surface area and the limited movement of material through a solid solution or a melt; on a small scale this has been referred to as a "diffusion-limited regime" (Moynier et al. 2009, 2010) and helps explain the discrepancy between measured fractionation and that predicted by the Rayleigh model in small volume samples such as chondrules or tektites. But based on their velocities, we would still expect the lighter isotopes to be preferentially lost during evaporation, leaving a relatively heavier isotopic ratio in the residual.

Multi-collector inductively-coupled plasma mass spectrometry (MC-ICP-MS) has enabled resolution of stable isotopes at precision less than 0.1 *per mille* (‰) per atomic mass unit. Studies of stable isotopes of Fe (Zhu et al. 2001, Poitrasson et al. 2004, Weyer et al. 2005, Moynier et al. 2007, Wang et al. 2013), Mg (Young and Galy 2004, Teng et al. 2007), Si (Fitoussi et al. 2009, Savage and Moynier 2013, Pringle et al. 2013) and Cd (Wombacher et al. 2008) have all been used to show homogeneity of their respective reservoirs in the solar nebula.

Zinc has five stable isotopes with established solar abundances: ^{64}Zn (48.63%), ^{66}Zn (27.9%), ^{67}Zn (4.10%), ^{68}Zn (18.75%), and ^{70}Zn (0.62%) (Lodders 2003), with very limited isotopic fractionation in terrestrial rock (Chen et al. 2013). It is classified as moderately volatile, with a 50% condensation temperature T_c of 726K (Figure 1), suggesting that it could be preferentially lost by evaporative processes. For example, Albarede (2004) showed that Zn became isotopically heavier with increasing shock stage in Cococino sandstones from Meteor Crater, Arizona, which implied loss of lighter isotopes with increased impact heating, presumably by volatization. Moynier et al. (2009) found enrichment of heavy Zn isotopes by 1‰ or more in a series of tektites, most likely due to evaporation (with loss of light isotopes) caused by intense heating from the impact that formed them.

Luck et al. (2005) was the first to report high-precision Zn isotopic data in planetary materials, studying a small series of carbonaceous and ordinary chondrites. Their data suggest a single common nebular reservoir for Zn, which was found to be consistent with the terrestrial fractionation line. They concluded that moderately volatile element abundance variability in chondrites was not caused by volatization, but by pre-accretion processes in the nebula.

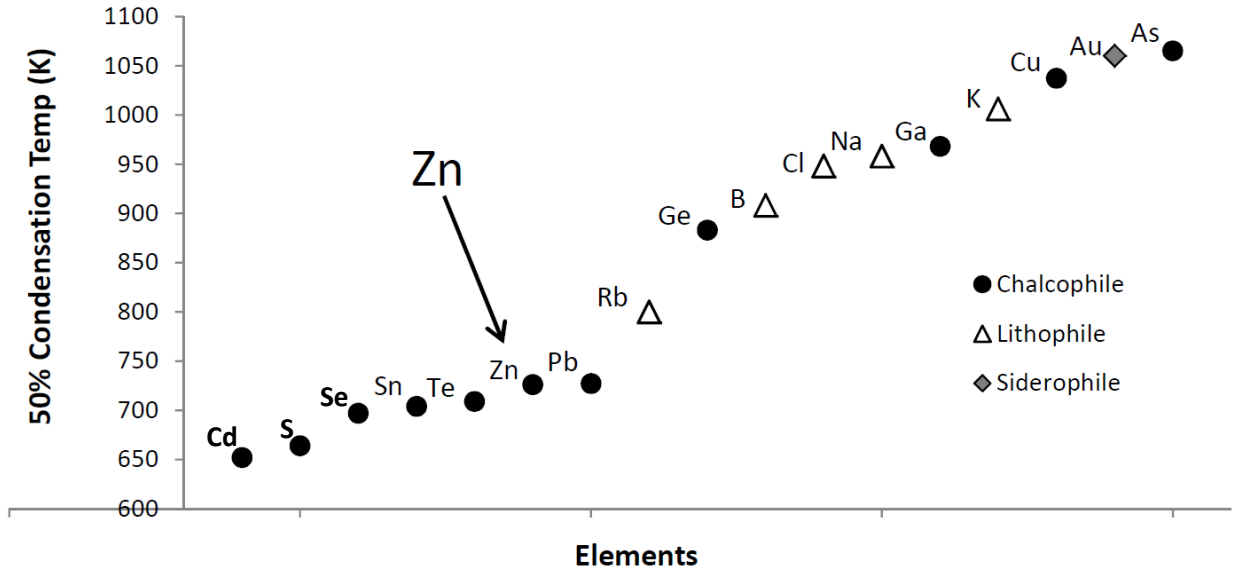

Figure 1-1. 50% condensation temperatures (in K) at 10^{-4} bar for moderately volatile elements. Some elements with T_c<1100K, with very low abundances, were omitted: Tl, In, Cs, Sb, and Ag. (compiled from Lodders 2003).

Moynier et al. (2010) studied Zn volatization in ureilites, which are igneous ultramafic achondrite meteorites. They found a very strong correlation of lower zinc content with heavier isotopic fractionation, which would be expected with volatization. The more depleted samples also exhibited a higher shock state, suggesting an impact may have been responsible for the heating event. The degree of fractionation was much less than expected for a simple Rayleigh distillation model, and a model of diffusion-limited evaporation was proposed.

In order to test evaporative loss of volatiles in meteoritic materials, Wulf et al. (1995) carried out a series of heating experiments at various oxygen fugacities on small pieces of two carbonaceous chondrites, Allende and Murchison. Among the interesting findings was that Zn was lost by volatization in reducing conditions, but retained in oxidizing conditions.

Samples of extraterrestrial material available for direct chemical analysis include lunar samples, collected by the Apollo and Luna missions, and meteorites. Meteorites can be identified and classified by chemical signatures, and some can be linked to their parent body, such as Mars or the Moon, principally by correlation of oxygen isotope ratios that are unique to each body. The vast majority of meteorites come from the asteroid belt that resides between the orbits of Mars and Jupiter. Meteorites can be broadly subdivided into chondrites, so named because they are largely comprised of chondrules (Scott 2007), and achondrites, which do not have chondrules. The presence of chondrules constrains the thermal history of these meteorites to temperatures below ~950^{o}C; higher temperatures would cause the minerals to melt and lose their chondrule structures, so they would no longer be recognizable as chondrites (Brearley and Jones 1998). Meteorites are grouped into subcategories based on chemical or other properties. It is assumed that meteorites within a single class originated from the same parent body, although it is possible that multiple bodies may have accreted with similar chemical makeup. Meteoroids are expelled from their parent body as ejecta from impacts, then they may spend thousands or millions of years in space before they are drawn into Earth's gravitational field and reach the ground as meteorites.

The database maintained by the Meteoritical Society lists nearly 47,000 approved meteorite names and classifications. Only about one thousand of these are observed falls; the rest are finds with the majority (about two-thirds) of all meteorites found in Antarctica (Figure 2), although recently many new finds come from the desert in northwest Africa. Table 1-1 shows the numbers of confirmed meteorites in the worldwide collection as of early November, 2013; the numbers change frequently as new falls and finds are added. It can be seen that nearly seven of every eight meteorites that have been recovered have been classified as ordinary chondrites; this

proportion is even higher (92%) among the meteorites from Antarctica. Among the non-ordinary chondrites, the largest groups are the carbonaceous chondrites, the howardites-eucrites-diogenites (HEDs), and the irons.

In this thesis, zinc isotopes are used to determine the role of volatization in the histories of several groups of meteorites, as well as some lunar materials. In the first group, Martian meteorites and Apollo lunar samples are reported (chapter 3). The second group is a set of HED meteorites, which are believed to have originated from asteroid 4-Vesta (chapter 4). Next, a large series of ordinary chondrites, including the H, L and LL subclasses, is examined (chapter 5). Finally, a group of enstatite chondrites and achondrites are studied (chapter 6). Each of these subgroups was found to have unique characteristics and thermal histories that were manifested in the zinc isotopic measurements.

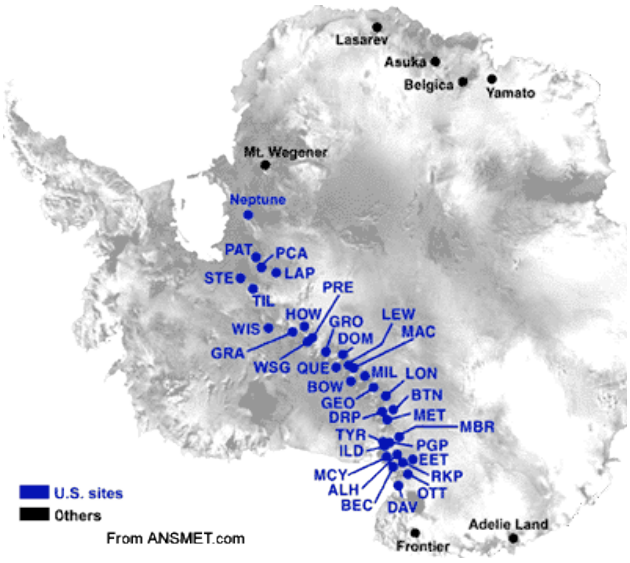

# finds	Abbr.	Site Name
1841	ALH	Allan Hills
2	BEC	Beckett Nunatak
1	BOW	Bowden Neve
15	BTN	Bates Nunataks
10	DAV	David Glacier
951	DOM	Dominion Range
27	DRP	Derrick Peak
2204	EET	Elephant Moraine
32	GEO	Geologists Range
355	GRA	Graves Nunataks
406	GRO	Grosvenor Mountains
5	HOW	Mount Howe
1	ILD	Inland Forts
1664	LAP	LaPaz Icefield
1960	LEW	Lewis Cliff
10	LON	Lonewolf Nunataks

# finds	Abbr.	Site Name
1061	MAC	MacAlpine Hills
2	MBR	Mount Baldr
1133	MET	Meteorite Hills
2043	MIL	Miller Range
1	OTT	Outpost Nunatak
182	PAT	Patuxent Range
633	PCA	Pecora Escarpment
1	PGP	Purgatory Peak
17	PRE	Mount Prestrud
3480	QUE	Queen Alexandra Range
138	RKP	Reckling **Peak**
1	STE	Stewart Hills
83	TIL	Thiel Mountains
3	TYR	Taylor Glacier
33	WIS	Wisconsin Range
9	WSG	Mount Wisting

Figure 1-2. Antarctic meteorite search locations from US expeditions and the number of meteorites found. (Map from ANSMET.com)

	Ant.	Non-Ant.	Falls	Total	%	Non-OC
Chondrites						
Ordinary	28846	11953	867	40799	87.33%	
Carbonaceous	1033	630	44	1663	3.56%	28.09%
Enstatite	383	152	17	535	1.15%	9.04%
Rumuruti	41	103	1	144	0.31%	2.43%
Kakangari	1	2	1	3	0.01%	0.05%
Achondrites						
HEDs	553	714	61	1267	2.71%	21.40%
Irons	146	934	49	1080	2.31%	18.24%
Ureilites	117	225	6	342	0.73%	5.78%
Mesosiderites	53	142	7	195	0.42%	3.29%
Primitive	62	117	3	179	0.38%	3.02%
Pallisites	31	67	4	98	0.21%	1.66%
Aubrites	43	35	9	78	0.17%	1.32%
Lunar	33	133	0	166	0.36%	2.80%
Martian	28	97	5	125	0.27%	2.11%
Total	31370	15304	1074	46674		

Table 1-1. Confirmed meteorites by type as of November, 2013. Primitive group includes acapulcoites, brachinites, lodranites, and winonaites Ant., Antarctica. OC, ordinary chondrite. Compiled from the Meteoritical Society database at http://www.lpi.usra.edu/meteor/metbull.php.

REFERENCES

Albarede F (2004). The stable isotope geochemistry of copper and zinc. In: Johnson, C.M., Beard, B., Albarede, F. (eds.), Geochemistry of Non-traditional Stable Isotopes. *Reviews in Mineralogy and Geochemistry*, Mineralogical Society of America, Geochemical Society, vol. 55, pp. 409–427.

Brearley AJ, Jones RH (1998). Chondritic meteorites. In: Papike JJ, ed., *Rev. Mineral. 36: Planetary Materials*. Mineralogical Soc. Amer., Washington DC.

Burbidge EM, Burbidge GR, Fowler WA, Hoyle F (1957). Synthesis of the elements in stars. *Rev. Mod. Phys.* 29, 547-650.

Chen H, Savage P, Teng F-Z, Helz RT, Moynier F (2013). Zinc isotope fractionation during magmatic differentiation and the isotopic composition of the bulk Earth. *Earth Plan. Sci. Lett.* 369-370, 34-42.

Desch SJ, Morris MA, Connolly HC, Boss AP (2012). The importance of experiments: Constraints on chondrule formation models. *Meteoritics Planet. Sci*. 47, 1139–1156.

Edvardsson B, Anderson J, Gustafsson B, Lambert DL, Nissen PE, Tomkin J (1993). The chemical evolution of the galactic disk – part one – analysis and results. *Astron. Astrophys.* 275, 101.

Fitoussi C, Bourdon B, Kleine T, Oberli F, Reynolds BC (2009). Si isotope systematics of meteorites and terrestrial peridotites: implications for Mg/Si fractionation in the solar nebula and for Si in the Earth's core. *Earth Planet. Sci. Lett.* 287, 77–85.

Hewins RH, Zanda B (2012). Chondrules: Precursors and interactions with the nebular gas. *Meteoritics Planet. Sci.* 47, 1120–1138.

Lodders K (2003). Solar system abundances and condensation temperatures of the elements. *Astrophys. J.* 591, 1220–1247.

Luck JM, Ben Othman D, Albarède F (2005). Zn and Cu isotopic variations in chondrites and iron meteorites: Early solar nebula reservoirs and parent-body processes. *Geochim. Cosmochim. Acta* 69, 5351-5363.

Moynier F**,** Beck P, Jourdan F, Yin QZ, Reimold UW, Koeberl C (2009). Isotopic fractionation of Zn in tektites. *Earth Planet. Sci. Lett.* 277, 482-489.

Moynier F**,** Beck P, Yin QZ, Ferroir T, Barrat JA, Paniello R, Telouk P, Gillet P (2010). Volatilization induced by impacts recorded in Zn isotope composition of ureilites. *Chemical Geology* 276, 374-379.

Moynier F, Blichert-Toft J, Telouk P, Luck JM, Albarede F (2007). Comparative stable isotope geochemistry of Ni, Cu, Zn, and Fe in chondrites and iron meteorites. *Geochim. Cosmochim. Acta* 71, 4365–4379.

Poitrasson F, Halliday AN, Lee D-C, Levasseur S, Teutsch N (2004) Iron isotope differences between Earth, Moon, Mars and Vesta as possible records of contrasted accretion mechanisms. *Earth Planet. Sci. Lett.* 223, 253–266.

Pringle E, Savage P, Jackson M, Barrat JA, Moynier F (in press). Si isotopic homogeneity in the solar nebula. (accepted by *Astrophysical Journal*).

Savage P, Moynier F (2013). Si isotopic variations in enstatite meteorites: clues to their origin. *Earth Planet. Sci. Lett.* 361 487-496.

Scott ERD (2007). Chondrites and the protoplanetary disk. *Annu. Rev. Earth Planet. Sci.* 35, 577–620.

Teng F-Z, Wadhwa M, Helz RT (2007). Investigation of magnesium isotope fractionation during basalt differentiation: Implications for a chondritic composition of the terrestrial mantle. *Earth Planet. Sci. Lett.* 261, 84–92.

Wang K, Moynier F, Barrat JA, Zanda B, Paniello RC, Savage PS (2013). Homogeneous distribution of Fe isotopes in the early solar nebula. *Meteoritics Planet. Sci.*, 48, 354-364.

Weyer S, Anbar AD, Brey GP, Munker C, Mezger K, Woodland AB (2005) Iron isotope fractionation during planetary differentiation. *Earth Planet. Sci. Lett.* 240, 251–264.

Wombacher F, Rehkamper M, Mezger K, Bischoff A, Munker C (2008). Cadmium stable isotope cosmochemistry. *Geochim. Cosmochim. Acta* 72, 646–667.

Wulf AV, Palme H, Jochum KP (1995). Fractionation of volatile elements in the early solar system: evidence from heating experiments on primitive meteorites. *Planet. Space Sci.,* Vol. 43, 451-468.

Young ED, Galy A, Nagahara H (2002). Kinetic and equilibrium mass-dependent isotope fractionation laws in nature and their geochemical and cosmochemical significance. *Geochim. Cosmochim. Acta* 66, 1095–1104.

Young ED, Galy A (2004) The isotope geochemistry and cosmochemistry of magnesium. In: *Geochemistry of Non-Traditional Stable Isotopes*, vol. 55 (eds. C. M. Johnson, B. L. Beard and F. Albarede). Min. Soc. Am., Washington, pp. 197–230.

Zhu X. K., Guo Y., O'Nions R. K., Young E. D. and Ash R. D. (2001) Iron isotope homogeneity in the early Solar Nebula. *Nature* 412, 311–313.

2. Methodology

Meteorites were obtained from museum collections and from the Antarctic collections of the Meteorite Working Group at NASA and the National Institute of Polar Research in Japan; the specific sources are noted in the data tables. Most samples were ~1 g. They were washed in water, ground to a fine powder and homogenated, and subsamples were used for analysis. The details of the acid dissolutions are given in the respective chapters of this thesis.

Zinc was extracted from the dissolved samples using anion exchange chromatography, following the method of Moynier et al. (2006). Briefly, the AG1x8 resin is cleaned with dilute HNO_3, charged with HBr, and the dissolved sample passes over the resin by gravity. In dilute HBr, zinc forms $ZnBr_3^-$ and therefore sticks to the anionic resin, while most other elements do not form complexes with HBr and go through the column (Figure 2-1). Additional HBr is run through the column to remove elements which are not strongly bonded to the resin, leaving essentially only the zinc bound to the column. The Zn is then recovered by passing very dilute HNO_3 through the column (this changes the speciation of zinc to Zn^{2+}, and it is released from the column). The process is repeated one or two times on different columns until the remaining matrix, and particularly Ni, is minimized.

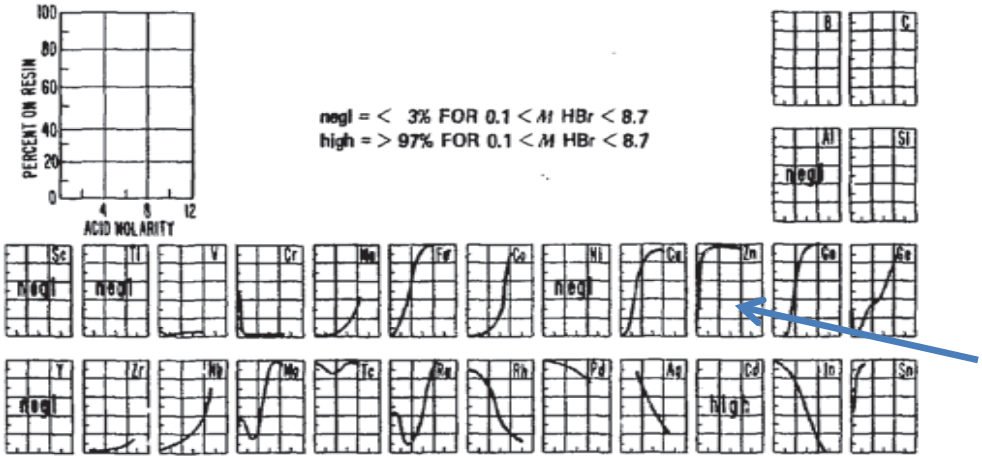

Figure 2-1. Elemental binding to AG1x8 resin as used in these experiments. It can be seen that Zn (arrow) has a very high affinity for the resin compared with other transition metals.

The possibility of isotopic fractionation on the column can be eliminated if all of the zinc is recovered. With this combination of resin (AG1x8, 200-400 mesh) and solvent (HBr), the recovery of Zn from the column is 99±1 % (Moynier et al. 2006), so column fractionation is not significant. The Zn-containing eluent is dried and re-dissolved in very dilute HNO_3 for mass spectrometry.

Inductively-coupled plasma is formed in the mass spectrometer by passing argon gas through an electrically-induced magnetic field. The sample is added by a nebulizer and is ionized by the plasma. The ionized sample is subjected to a magnetic field, and the ions are separated based on their mass-to-charge ratio, based on the equation

$(m/q)a = E + v \times b$ (Eq.3)

where m is the mass, q is the charge (usually +1), a is the acceleration, E is the electric field, and *v x b* is the vector cross-product of the ion velocity *v* and the magnetic field *b*. The availability of multiple collection cups enables simultaneous recording of ions of different masses.

The mass spectrometer counts ions strictly by mass, which means that interference from alternate species with the same atomic mass must be considered. The most abundant Zn isotope has a mass of 64, and interference from ^{64}Ni must be corrected in order to obtain accurate Zn isotopic determinations. With seven collection cups on our multi-collector, we typically count ions at each mass from 62 to 68. Mass 62 is only Ni, so it can be used to determine how much ^{64}Ni is included in the 64 cup, assuming natural abundances of Ni isotopes (^{62}Ni is 3.63% of Ni isotopes, ^{64}Ni is 0.93%).

The isotopic ratios ^{66}Zn/^{64}Zn, ^{67}Zn/^{64}Zn, and ^{68}Zn/^{64}Zn are calculated, and then compared to the JMC/Lyon standard ratio using delta notation:

$$\delta^{X}\text{Zn (‰)} = \left(\frac{\left({}^{x}\text{Zn} / {}^{64}\text{Zn} \right)_{\text{sample}}}{\left({}^{x}\text{Zn} / {}^{64}\text{Zn} \right)_{\text{standard}}} - 1 \right) \times 1000 \qquad \text{with X = 66, 67, or 68.}$$

REFERENCE

Moynier, F. , Albarède, F., Herzog, G. Isotopic composition of zinc, copper, and iron in lunar samples. *Geochim. Cosmochim. Acta* **70**, 6103-6117 (2006).

3. Martian Meteorites and Lunar Materials

Manuscript citation: Paniello RC, Day JMD, Moynier F (2012). Zinc isotopic evidence for the origin of the Moon. *Nature* 490, 376–379.

Introduction

The prevailing theory on the origin of the moon is the "giant impact" theory, in which a Mars-sized planetary body (called "Theia") collided with the proto-Earth, shattering the impactor and part of the Earth (e.g., Cameron 1997). The fragments remained in Earth's gravitational field and eventually re-accreted into the moon. Such a major impact would certainly be expected to generate substantial heat, likely melting and potentially evaporating much of the colliding material. A volatization event of this magnitude would be expected to be reflected in the zinc isotopes of lunar materials.

The historic Apollo missions returned about 380 kg of rock, soil and regolith that is available for scientific analysis (Table 3-1). In addition, a number of meteorites have been found that were ejected from the moon. We measured the Zn isotopes in these materials and used them to make inferences about the origin of the volatile depletion on the Moon.

Apollo Samples

Mission	# samples
11	67
12	68
14	207
15	415
16	730
17	702

Table 3-1. Available Apollo lunar samples by mission number.

The thermal history of Mars during and after its accretion may have been very similar to Earth's. There are a number of meteorites that have been identified as originating on Mars, based on measurements of noble gases trapped in impact-melted glasses, which are virtually identical to the martian atmosphere (Bogard and Johnson 1983, Becker and Pepin 1984, Swindle 1986). These meteorites were initially grouped into three classes, called "shergottites, nahklites and chassignites" (SNCs) based on the names of their first members. Since then, a fourth type has been found in Antarctica, simply referred to as an orthopyroxenite, and it remains the only specimen in its class. We studied Zn isotopes in martian meteorites from three of the four groups to compare with Earth and Moon values and gain information on the volatile history of Mars.

	Ant.	Non-Ant.	Falls	Total
Martian				
Shergottites	19	83	3	102
Nahklites	7	7	1	14
Chassignites	0	2	1	2
Orthopyroxenite	1	0	0	1
Lunar	33	133	0	166

Table 3-2. Available martian and lunar meteorites by type. Ant. = Antarctic.

REFERENCES

Becker RH, Pepin RO (1984). The case for a martian origin of the shergottites: nitrogen and noble gases in EETA79001. *Earth Plan. Sci. Lett.* 69: 225-242.

Bogard DD, Johnson (1983). Martian gases in an Antarctic meteorite. *Science* 221: 651-654.

Cameron, A. The origin of the moon and the single impact hypothesis V. *Icarus* **126**, 120-122 (1997).

Swindle TD, Caffee MW, Hohenburg CM (1986). Xenon and other noble gases in shergottites. *Geochim Cosmochim Acta* 50, 1001-1015.

Zinc isotopic evidence for the origin of the Moon

Randal C. Paniello[1], James M.D. Day[2], Frédéric Moynier[1,*]

[1]*Department of Earth and Planetary Sciences and McDonnell Center for Space Sciences, Washington University, St. Louis, MO 63130, USA*

[2]*Geosciences Research Division, Scripps Institution of Oceanography, La Jolla, CA 92093-0244, USA*

**Corresponding Author e-mail: moynier@levee.wustl.edu*

Volatile elements play a fundamental role in the evolution of planets. However, our understanding of how volatile budgets were set in planets, and the nature and extent to which planetary bodies became volatile-depleted during the earliest stages of Solar System formation remain poorly understood[1,2]. The Moon is considered to be volatile-depleted and consequently it has been predicted that volatile loss should have fractionated stable isotopes of moderately volatile elements[3]. One such element, zinc, exhibits strong isotopic fractionation during volatization in planetary rocks[4-5], but is hardly fractionated during terrestrial igneous processes[6], making Zn a powerful tracer of the volatile histories of planets. Here we present high-precision Zn isotopic and abundance data that show lunar magmatic rocks are enriched in the heavy isotopes of Zn and have lower Zn concentrations

than terrestrial or martian igneous rocks. Conversely, Earth and Mars have broadly chondritic Zn isotopic compositions. We show that these variations represent large-scale evaporation of Zn, most likely in the aftermath of the Moon-forming event, rather than small-scale evaporation processes during volcanic processes. These results therefore represent the first evidence for volatile depletion of the Moon through evaporation and are consistent with a giant impact origin for the Earth and Moon.

The mode-of-origin for the Earth-Moon system that is most consistent with both physical and chemical constraints is through a giant impact between the proto-Earth and a Mars-sized body[7,8]. Depending on the Hf/W values of the bulk silicate Earth and Moon, this event occurred some 10 to 150 Ma after the formation of the first Solar System solids[9,10]. This highly energetic collision is predicted to have melted the impactor, with much of its core material being sequestered into Earth, while silicate material spun into an Earth-orbiting disk that later accreted to form the Moon[11,12]. Despite this cataclysmic mode-of-origin, and silicate vapor-phase models proposed to explain non-volatile stable isotope fractionation[13], to date there have been no collateral heavy isotope enrichments found for moderately-volatile elements (e.g., potassium) in lunar or terrestrial rocks[3].

Zinc is more volatile than both K and Cl[14] under solar nebula conditions and exhibits limited isotopic fractionation during igneous processes[6,15]. On Earth, and in primitive meteorites such as chondrites, variations of δ^{66}Zn ($[(({}^{X}Zn/{}^{64}Zn)_{sample}/({}^{X}Zn/{}^{64}Zn)_{JMC\text{-}Lyon\ standard}-1) \times 1000]$, where X = ^{66}Zn or ^{68}Zn) larger than 1‰ have only been observed associated with evaporation events[4,16]. Therefore any Zn isotopic fractionation, combined with differences in Zn

concentrations between planetary igneous rocks from differentiated bodies such as Earth, the Moon and Mars, can reveal important differences in volatile depletion and replenishment events for these bodies.

Here we report high precision Zn isotopic data for lunar basalts, martian meteorites, and terrestrial igneous rocks (See Methods, Table S1 and the Supplementary Information). Combined with previously published data for lunar rocks, terrestrial basalts, and carbonaceous, ordinary and enstatite chondrites, these new data allow us to establish the nature and extent of volatile depletion in Earth, the Moon and Mars. Fractionation between δ^{66}Zn and δ^{68}Zn is mass dependent (**Figure 1**), conforming to the expected mass-dependent mass-fractionation slope of two, hence only δ^{66}Zn is discussed in the text although ^{64}Zn, ^{66}Zn, and ^{68}Zn intensities were precisely measured. Since terrestrial, martian and lunar rocks all lie on the same mass-dependent mass-fractionation line, along with all classes of chondritic meteorites[16,17], this implies that Zn from all of the analysed samples evolved from a single, isotopically homogeneous reservoir. This relationship presumably reflects Zn isotope homogeneity in the solar nebula prior to terrestrial planet formation and, thus, that all reported isotopic variations are due to mass-dependent fractionations. Spallogenic effects or secondary neutron capture would lead to non-mass-dependent behavior.

Low-Ti mare basalts, including the mare basalt meteorite LAP 02205, span a range in δ^{66}Zn of -3.13 to +1.56‰ (**Figure 2**). Sample 12018 is isotopically light (δ^{66}Zn = -3.10 ±0.03‰, n = 2) when compared with the other 11 low-Ti mare basalt samples measured. If sample 12018

is excluded from the comparison, we find a limited range in $\delta^{66}Zn$ for low-Ti mare basalts of +0.84 to +1.56‰, with a mean of +1.31 ±0.13‰. The mean $\delta^{66}Zn$ for low-Ti mare basalts is

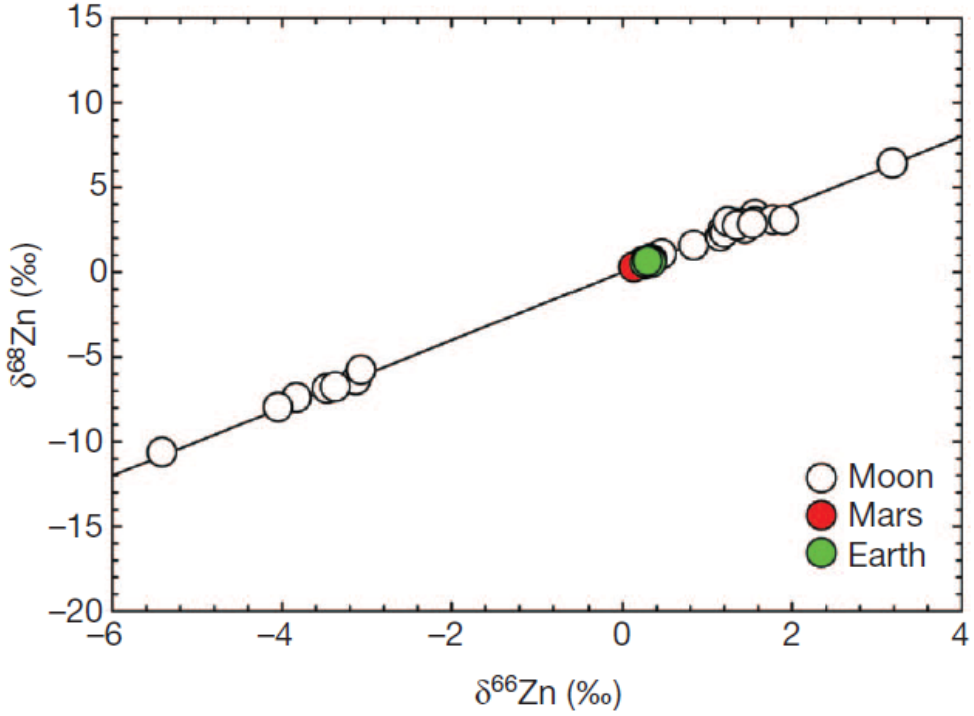

Figure 1 | $\delta^{68}Zn$ versus $\delta^{66}Zn$ for lunar, terrestrial and Martian samples. All of the samples fall on the mass-dependent mass-fractionation line of slope 2. Analytical uncertainties (2σ) are smaller than the data marker size. $\delta^{X}Zn = [(^{X}Zn/^{64}Zn)_{sample}/(^{X}Zn/^{64}Zn)_{JMC\ Lyon\ standard} - 1] \times 1{,}000$, where $X = 66$ or 68.

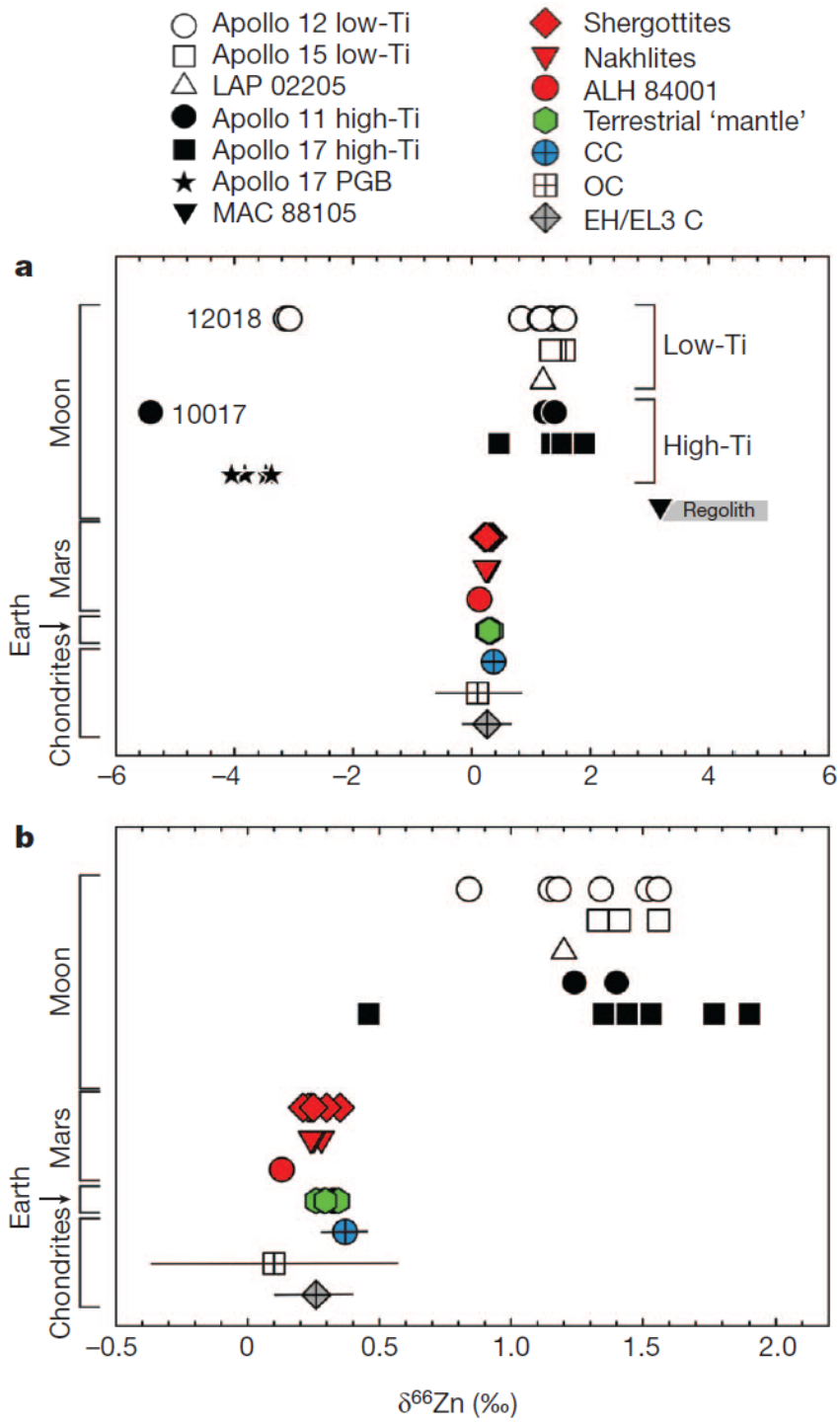

Figure 2 | Zinc isotopic composition of terrestrial, lunar, Martian and chondritic samples. CC, carbonaceous chondrite; OC, ordinary chondrite; and EH/EL3 C, enstatite chondrite. Data for chondrites and Earth represent an average of the different samples measured so far (refs 4, 6, 16, 17 and Methods); error bars, 2σ. For Martian meteorites and lunar samples, each data point represents one sample; 2σ on the δ^{66}Zn is 0.05‰.

identical, within the uncertainties, to that derived for high-Ti mare basalts (δ^{66}Zn = +1.39 ±0.31‰; n = 8), and excluding the isotopically light sample 10017 (δ^{66}Zn = -5.42‰; ref. ***18***). Zinc concentrations in mare basalts range from 0.6 to 12 ppm, and are lower than concentrations of Zn measured in lunar soils (average = 25 ppm), or in lunar pyroclastic glass beads (129 to 231 ppm).

Martian Shergotty-Nakhla-Chassigny (SNC) meteorites span a limited range in δ^{66}Zn (+0.13 to +0.35‰), with an average δ^{66}Zn of +0.25 ±0.03‰ (n = 11) (**Figure 2**). Measured values of δ^{66}Zn are slightly higher in Mg-rich shergottites (e.g., EETA 79001; ALHA 77005), than in more evolved shergottites, nakhlites, and ALH 84001, which has the lowest δ^{66}Zn composition of martian meteorites. The average Zn isotopic composition of martian meteorites (+0.25 ±0.03‰) is identical to the average measured δ^{66}Zn composition of terrestrial igneous rocks (+0.27 ±0.10‰). Zinc concentrations in shergottite meteorites are higher than for lunar mare basalts at between 41 and 130 ppm, and Zn concentrations in nakhlite meteorites lie within the range of shergottite meteorites at between 61.5 and 89 ppm (Supplementary Information); martian igneous rock Zn concentrations are therefore similar to terrestrial basaltic lavas (typically 70 to 100 ppm; GERM database http://earthref.org/GERM/).

The range of δ^{66}Zn values measured for lunar rocks are bracketed by the low δ^{66}Zn values of 12018 (-3.10 ±0.03‰), 10017 (-5.42‰), and pyroclastic glass beads (-2.9 to -4.2‰) and by the high δ^{66}Zn values of MAC 88105 (δ^{66}Zn +3.18‰) that we have measured. MAC 88105 is a lunar anorthositic regolith breccia meteorite[19], and has a δ^{66}Zn value similar to lunar regolith and soil samples from the Apollo 14, 15, 16 and 17 sites (+2.6 to +5.6‰) (**Figure 2**).

The high $\delta^{66}Zn$ of the regolith and soil samples reflect both sputtering effects and impact gardening of the lunar regolith[4,18], and do not represent primary magmatic compositions, so will not be considered further.

The isotopically light Zn values measured for 10017, 12018 and pyroclastic glass beads are not associated with petrology, mineralogy, or cosmic ray exposure ages (see Supporting Information). Previously, light Zn isotope enrichment in pyroclastic glass beads has been attributed to Zn evaporation during fire-fountaining, with condensation of isotopically light Zn on the surfaces of the ejected beads[4], as also proposed for ^{32}S enrichments[20]. These observations appear to be supported by elevated Zn concentrations on the exterior portions of the pyroclastic glass beads, relative to interior portions (e.g., *Refs. 18, 21*). Vapour loss should increase the $\delta^{66}Zn$ value of the residual magma and this process can be modeled assuming exhalative evaporation of Zn as $ZnCl_2$ on the Moon (e.g., *21*), versus for Earth, where Zn is evaporated as Zn^{2+} (e.g., *22*) with essentially no fractionation between vapour and melt ($\alpha = 1$).

For volatilization of a liquid into a vacuum, fractionation between vapour and melt (α) during Rayleigh distillation ($\delta_{final} = \delta_{initial} + [(1000 + \delta_{initial}) (F^{(\alpha-1)} -1)]$, where F is the fraction of Zn remaining in the melt) can be approximated as the square-root of the light isotopolog over the heavy isotopolog of the vapourising species. For $ZnCl_2$ the α value is 0.993. Extreme fractionations of Zn isotopes in the melt and associated vapour phase are computed for low remaining Zn in the melt fraction, and fractionations greater than those measured for lunar rocks can be calculated, possibly reflecting incomplete evaporation to low melt fractions, or the competing effect of diffusion rates being insufficient to maintain isotopic homogeneity in melts

on the Moon (effect exemplified as lower α value of 0.999, for reference; **Figure 3**). These calculations demonstrate that isotopically light vapour Zn isotope compositions conforming to those measured in 12018, 10017 and pyroclastic glass beads can also be achieved by evaporation and re-deposition of $ZnCl_2$ from lunar melts. We therefore exclude these isotopically light samples from the planetary comparisons made between Earth, the Moon and Mars.

As demonstrated above, Zn isotopes can be strongly fractionated during high-temperature evaporative processes, and an important distinction to be made is how and when Zn isotopic fractionation occurred between different planetary basalts. For example, there is a clear difference in the Zn isotopic composition of lunar mare basalts relative to martian and terrestrial rocks, but with no corresponding differences between terrestrial and martian rocks. Zinc isotopic compositions for the majority of mare basalts (0.7-1.9‰) can be attained from between 10 to >90% evaporative loss of Zn using the different α values shown in **Figure 3**, whereas terrestrial and martian samples do not require significant evaporative loss. Therefore, the conditions responsible for Zn isotopic fractionation in lunar rocks do not appear to have existed, or have been overprinted, for terrestrial and martian igneous rocks.

There is strong evidence that 'planet-scale' evaporation of Zn during the Moon-forming event, rather than 'localised-scale' evaporation processes during volcanic eruption into hard vacuum (as suggested for Cl isotopes[23]), is responsible for the Zn isotopic character of mare basalts. The limited range in Zn isotopic compositions and systematically low Zn abundances for 19 of the 21 studied mare basalts, combined with the identical $\delta^{66}Zn$ values for low- and high-Ti mare basalts, support a large-scale planetary volatile depletion process. Low-Ti mare basalts are

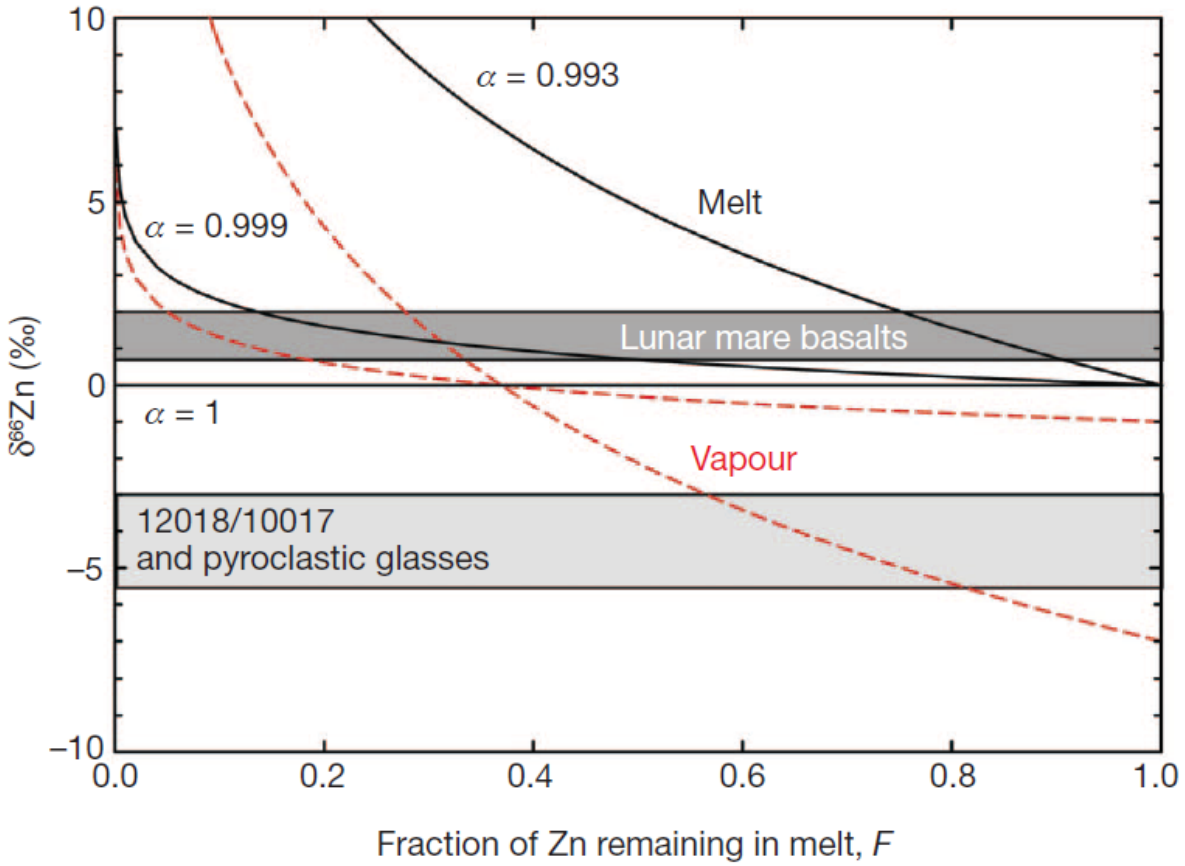

Figure 3 | Zinc isotopic fractionation as a function of the fraction of Zn remaining during open-system Rayleigh distillation. Results are shown for three different fractionation factors (α) between vapour and melt versus the range of Zn isotopic compositions measured for lunar samples. The two grey areas represent the δ^{66}Zn ranges of lunar mare basalts and the 12018/10017/ pyroclastic glasses.

the predominant form of basalt exposed on the lunar surface (~90%; ref. *24*), and their prevalence over high-Ti mare basalts is consistent with magma ocean crystallization models that indicate >78% of the lunar mantle would be dominated by olivine and orthopyroxene, whereas ilmenite-rich cumulates formed after 95% crystallisation[25]. Thus, low-Ti mare basalts are often considered more representative of lunar mantle composition than high-Ti mare basalts (e.g., *26*) and so the identical Zn isotopic composition of low- and high-Ti mare basalts points towards identical processes acting on both basalt types, despite conspicuously differing modes-of-origin and lunar mantle sources.

The evidence for extreme volatile depletion of the Moon from Zn isotopes and abundance contrasts with the more elevated Zn abundance and broadly chondritic Zn isotopic compositions of Earth and Mars. The simplest explanation for these differences is that conditions during or after formation of the Moon may have led to more extensive volatile loss and Zn isotopic fractionation than experienced by Earth or Mars. The Zn isotopic homogeneity in lunar materials suggests that this would have to result from a large-scale process rather than from small-scale processes, or by hydrodynamic escape[15]. Given these lines of evidence, the most likely large-scale event to explain evaporative Zn isotopic fractionation would be a whole-sale melting event associated with the formation of the Moon. The Zn isotope data therefore supports existing dynamical models that argue for a giant impact event at the origin the Earth-Moon system[11,12,27].

While Zn abundances and isotopic compositions for Earth, the Moon, and Mars, provide compelling evidence for evaporative loss of volatile elements during lunar formation, they also provide important insights into planetary volatile inventories. In the case of the Moon, studies

have shown that pyroclastic glass beads have elevated volatile contents, and contain water[28], suggesting a volatile-rich reservoir in the lunar interior. However, a study of Cl isotopes[23] suggests a volatile-depleted Moon, and our results for Zn isotopes suggest that the source regions of mare basalts are strongly volatile-depleted. In contrast with mare basalts, the elevated Zn abundances and light δ^{66}Zn values of lunar pyroclastic glasses are possibly consistent with derivation from a locaolized volatile-rich mantle reservoir within the Moon. For Mars, the identical Zn isotopic content of martian meteorites with terrestrial igneous rocks, combined with the elevated estimate of Zn abundance in the martian mantle[29] suggests a volatile-rich planet. Thus, Zn isotopic data for Earth, Mars and the Moon place fundamental constraints on planetary accretion, pointing to evaporative lost during the Moon forming event but that evaporative loss of volatiles in Earth and Mars did not occur, or has been over-printed by later events.

Methods Summary

500-1000 mg sample fragments were leached in double-distilled water for 300 s in an ultrasonic bath. After removal from the water and drying, sample fragments were crushed to a homogeneous fine powder in an agate mortar. Samples were dissolved in a 4:1 mixture of ultra-pure HF/HNO_3 in Teflon beakers for four days. Zinc purification was achieved using anion-exchange chromatography using procedures described previously (Ref. 4), with recovery of 99 ±1%. Zinc was purified by anion-exchange chromatography. The samples were loaded in 1.5N HBr on 0.25 ml AG-1X8 (200-400 mesh) ion-exchange columns and Zn was collected in 0.5N HNO_3. The Zn fraction was further purified by eluting the samples twice on a 100 μl column with the same eluting solutions. Blanks were <10 ng and represent less than 1 % of total measured Zn. Zinc isotopic compositions were measured on the *ThermoElectron* Neptune Plus

multi collector-inductively coupled plasma-mass spectrometer housed at the Isotope Geochemistry Laboratory, Washington University, St. Louis. The Faraday cups were positioned to collect the masses 62, 63, 64, 65, 66, 67 and 68. Possible ^{64}Ni isobaric interferences were controlled and corrected by measuring the intensity of the ^{62}Ni peak. A solution containing 500 ppb Zn in 0.1 M HNO_3 was prepared for isotopic analysis. Isotopic ratios of Zn in all samples were analysed using a spray chamber combined with a 100μl/min PFA nebulizer. 1 block of 30 ratios in which the integration time of 1 scan was 10 sec, were measured for each sample. The background was corrected by subtracting the on-peak zero intensities from a blank solution. The instrumental mass bias was corrected by bracketing each of the samples with standards. External precision based on the JMC Lyon Zn standard was 0.05 permil/amu (2σ).

REFERENCES

1. Albarède, F. Volatile accretion history of the terrestrial planets and dynamic implications. *Nature* **461**, 1227-1233 (2009).
2. Wood, B. J., Halliday, A. N. Rehkämper, M. Volatile accretion of the Earth. *Nature* **467**, E6-E7 (2011).
3. Humayun, M. & Clayton, R.N. Potassium isotope cosmochemistry: Genetic implications of volatile element depletion. *Geochim. Cosmochim. Acta* **59**, 2131-2148 (1995).
4. Moynier, F. , Albarède, F., Herzog, G. Isotopic composition of zinc, copper, and iron in lunar samples. *Geochim. Cosmochim. Acta* **70**, 6103-6117 (2006).
5. Moynier F. *et al*. Isotopic fractionation of zinc in tektites. *Earth Planet. Sci. Lett.* **277**, 482-489 (2009).
6. Ben Othman D., Luck, J.M., Bodinier, J.L., Arndt, N., Albarede, F. *Geochim. Cosmochim. Acta* **70**, 46 (2006)
7. Hartmann, W. & Davis, D. Satellite-sized planetesimals and lunar origin. *Icarus* **24**, 504-514 (1975).
8. Cameron, A. The Origin of the Moon and the Single Impact Hypothesis V. *Icarus* **126**, 120-122 (1997).
9. Yin Q. *et al.*, A short timescale for terrestrial planet formation from Hf-W chronometry of meteorites. *Nature* **418**, 949-952 (2002).
10. Touboul, M., Kleine, T., Bourdon, B., Palme, H., Wieler, R. Late formation and prolonged differentiation of the Moon inferred from W isotopes in lunar metals. *Nature* **450**, 1206-1209 (2007).

11. Canup, R., Origin of the Moon in a giant impact near the end of the Earth's formation. *Nature* **412**, 708-712 (2001).

12. Ida, S., Canup, R., Stewart, G. Lunar accretion from an impact-generated disk. *Nature* **389**, 352-357 (1997).

13. Pahlevan, K. & Stevenson, D.J. Equilibration in the aftermath of the lunar-forming giant impact *Earth Planet. Sci. Lett.* **262**, 438 (2007).

14. Lodders, K. Solar System abundances and condensation temperatures of the elements. *Astrophys. J.* **591**, 1220-1247 (2003).

15. Albarède, F. in *Rev Mineral Geochem,* C. M. Johnson, B. L. Beard, F. Albarede, Eds. (Mineralogical Society of America, 2004), vol. 55, pp. 409-427.

16. Moynier F., *et al.*, Nature of volatile depletion and genetic relations in enstatite chondrites and aubrites inferred from Zn isotopes. *Geochim. Cosmochim. Acta* **75**, 297-307 (2011).

17. Luck, J.M., Othman, D.B., Albarède, F. Zn and Cu isotopic variations in chondrites and iron meteorites: Early solar nebula reservoirs and parent-body processes. *Geochim. Cosmochim. Acta* **69**, 5351-5363 (2005).

18. Herzog, G. F. , Moynier, F., Albarède, F., Berezhnoy, A.A. Isotopic and elemental abundances of copper and zinc in lunar samples, Zagami, Pele's hairs, and a terrestrial basalt. *Geochim. Cosmochim. Acta* **73**, 5884-5904 (2009).

19. Neal, C. R., Taylor, L.A., Schmitt, R.A. Paired lunar meteorites MAC88104 and MAC88105: A new "FAN" of lunar petrology. *Geochim. Cosmochim. Acta* **55**, 3037-3049 (1991).

20. Ding, T.P., Thode, H. G., Rees, C. E. Sulphur content and sulphur isotope composition of orange and black glasses in Apollo 17 drive tube 74002/1. *Geochim. Cosmochim. Acta* **47**, 491-496 (1983).

21. Chou, C. L., Boynton, W. V., Sundberg, L. L., Wasson, J. T. Volatiles on the surface of Apollo 15 green glass and trace-element distributions among Apollo 15 soils. *Lunar and Planetary Science Conference* **6**, 1701-1727 (1975).

22. Symonds, R. B., Rose, W. I., Reed, M. H., Lichte, F. E., Finnegan, D. L. Volatilization, transport and sublimation of metallic and non-metallic elements in high temperature gazes at Merapi Volcano, Indonesia. *Geochim. Cosmochim. Acta* **51**, 2083-2101 (1987).

23. Sharp, Z., Shearer, C., McKeegan, K., Barnes, J., Wand, Y. The chlorine isotope composition of the moon and implоctions for an anhydrous mantle. *Science* **329**, 1050-1053 (2010).

24. Giguere, T., Taylor, G. J., Hawke, B., Lucey, P. G. The titanium contents of lunar mare basalts. *Meteorit. Planet. Sci.* **35**, 193-200 (2000).

25. Snyder, G. A., Taylor, L. A., Neal, C. R. A chemical model for generating the sources of mare basalts: Combined equilibrium and fractional crystallization of the Lunar magmasphere. *Geochim. Cosmochim. Acta* **56**, 3809-3824 (1992).

26. Spicuzza, M.J., Day, J.M.D., Taylor, L. A., Valley, J. W. Oxygen isotope conatraints on the origin and differentiation of the Moon. *Earth Planet. Sci. Lett.* **253**, 254-265 (2007).

27. Reufer, A., Meier, M.M.M., Benz, W., Wieler, R. A hit-and-run Giant Impact scenario. *Icarus,* http://dx.doi.org/10.1016/j.icarus.2012.07.021 (2012).

28. Hauri, E. H.,Weinreich, T., Saal, A., Rutherford, M., Van Orman, J. A. High Pre Eruptive Water Contents Preserved in Lunar Melt Inclusions. *Science* **333**, 213-215 (2011).

29. Lodders, K. & Fegley, B. An oxygen isotope model for the composition of Mars. *Icarus* **126**, 373-394 (1997).

Correspondence and requests for materials should be addressed to F.M. (moynier@levee.wustl.edu).

Acknowledgements

We thank the NASA curation staff, CAPTEM and the meteorite working group for samples. This work was supported by the NASA LASER, Cosmochemistry programs to FM (NNX09AM64G; NNX12AH70G) and JMDD (NNX11AG34G; NNX12AH75G).

Author contributions

R.C.P and F.M. performed Zn isotope and abundance measurements, J.M.D.D. and F.M. wrote the paper and all authors contributed to discussion and interpretation of results in the manuscript.

Additional information

The authors declare no competing financial interests. Supplementary information accompanies this paper at www.nature.com. Reprints and permissions information is available online at www.nature.com/reprints. Correspondence and requests for materials should be addressed to F.M.

Figure captions

Figure 1 – $\delta^{68}Zn$ versus $\delta^{66}Zn$ for lunar, terrestrial, and martian samples. All of the samples fall on the mass-dependent mass-fractionation line of slope 2. Analytical uncertainties (2σ) are smaller than the data marker size.

Figure 2 – Zinc isotopic composition of terrestrial, lunar, martian and chondritic samples. $\delta^{66}Zn$ is the permil deviation of the $^{66}Zn/^{64}Zn$ value from the JMC-Lyon standard. Abbreviations CC, OC and EH/EL3 C stand for carbonaceous, ordinary and enstatite chondrites, respectively. Data for chondrites and Earth represent and average of the different samples measured so far [ref. 4, 6, 16, 17, 31]. For martian meteorites and lunar samples each data point represents one sample. The 2σ on the $\delta^{66}Zn$ is 0.05 permil.

Figure 3 – Zinc isotopic fractionation as a function of the fraction of Zn remaining during open-system Rayleigh distillation. Results are shown for three different fractionation factors (α) between vapour and melt versus the range of Zn isotopic compositions measured for lunar samples.

Methods

We employed methods for the purification and isotopic measurement of Zn described previously (*Refs. 4, 5, 16, 18, 30-31*). Briefly, 500-1000 mg sample fragments were leached in double-distilled water for 300 s in an ultrasonic bath. After removal from the water and drying, sample fragments were crushed to a homogeneous fine powder in an agate mortar. Samples were dissolved in a 4:1 mixture of ultra-pure HF/HNO_3 in Teflon beakers for four days. Zinc purification was achieved using anion-exchange chromatography using procedures described previously (*Ref. 4*), with recovery of 99 ±1%. Zinc was purified by anion-exchange chromatography. The samples were loaded in 1.5N HBr on 0.25 ml AG-1X8 (200-400 mesh) ion-exchange columns and Zn was collected in 0.5N HNO_3. The Zn fraction was further purified by eluting the samples twice on a 100 µl column with the same eluting solutions. Blanks were <10 ng and represent less than 1 % of total measured Zn. Zinc isotopic compositions were measured on the *ThermoElectron* Neptune Plus multi collector-inductively coupled plasma-mass spectrometer housed at the Isotope Geochemistry Laboratory, Washington University, St. Louis (see Table S2 for parameters). The Faraday cups were positioned to collect the masses 62, 63, 64, 65, 66, 67 and 68. Possible ^{64}Ni isobaric interferences were controlled and corrected by measuring the intensity of the ^{62}Ni peak. A solution containing 500 ppb Zn in 0.1 M HNO_3 was prepared for isotopic analysis. Isotopic ratios of Zn in all samples were analysed using a spray chamber combined with a 100µl/min PFA nebulizer. 1 block of 30 ratios in which the integration time of 1 scan was 10 sec, were measured for each sample. The background was corrected by subtracting the on-peak zero intensities from a blank solution. The instrumental mass bias was corrected by bracketing each of the samples with standards. External precision based on the JMC Lyon Zn standard was 0.05 permil/amu (2σ).

Sample selection for this study was designed to complement and expand the existing high-precision Zn isotopic data available for the Moon (e.g., *Refs. 4, 18*), and to investigate the Zn isotopic composition of Mars. Previous Zn isotopic studies of the Moon have focused on high-Ti mare basalts, high-Ti pyroclastic glass beads, and lunar soils. We have expanded the high-precision dataset through the analysis of seven Apollo 12 and four Apollo 15 low-Ti mare basalts. We have also measured LaPaz Icefield [LAP] 02205, a low-Ti mare basalt meteorite with possible association to Apollo 12 mare basalts (e.g., *Ref. 32*), and MacAlpine Hills [MAC] 88105, an anorthositic regolith breccia paired with MAC 88104 (e.g., *Refs. 19, 33*). From the available martian Shergotty-Nakhla-Chassigny (SNC) meteorite suite, we measured Zn isotopic compositions in six shergottites (Shergotty, Zagami, Los Angeles, Elephant Morraine [EETA] 79001, Allan Hills [ALHA] 77005, Sayh al Uhaymir [SaU] 008), three nakhlites (Nakhla, Lafayette, Miller Range [MIL] 03346) and the orthopyroxenite ALHA 84001. We also prepared a terrestrial granite (G-2, a granite from Sullivan Quarry, Rhode Island, USA) and basalt (BCR-1, from the Columbia River region, Oregon, USA) for comparison with martian and lunar samples.

30. Moynier, F. *et al.,* Volatilization induced by impacts recorded in Zn isotope composition of ureilites. *Chem. Geol.* **276**, 374 (2010).
31. Barrat, J.A. *et al*., Geochemistry of CI chondrites: Major and trace elements, Cu and Zn isotopes. *Geochim. Cosmochim. Acta* **83**, 79-92 (2012)
32. Day, J.M.D. *et al.,* Comparative petrology, geochemistry and petrogenesis of evolved, low-Ti lunar mare basalt meteorites from the La Paz icefield, Antarctica. *Geochim. Cosmochim. Acta* **70**, 1581 (2006).
33. Warren, P. H., & Kallemeyn, G. W. in Proceedings of the NIPR Symposium on Antarctic Meteorites. (Nat. Inst. Polar Res., Tokyo, 1991), vol. 4, pp. 91-117.

doi:10.1038/nature11507

Supplementary Discussion

Isotopically light Zn measured in mare basalts and glass beads

The isotopically light Zn values measured for 10017 and 12018 require explanation. Because isotopically light values are measured in two samples with differing Mg and Ti contents, and contrasting mineralogy, there is no evidence that the low δ^{66}Zn values are related to sample petrology. Similarly, despite the long measured cosmic ray exposure ages of 10017 (308-510 Ma; *S1-S2*), and 12018 (170-210 Ma; *S3, S4*) compared with the majority of other mare basalts analysed in this study, the small thermal neutron capture cross-section of Zn, and long measured exposure ages of some mare basalts with isotopically heavier Zn values (e.g., the CRE age of 12021 is reported at 303 Ma by (*S5*) makes it improbable that isotopically light Zn values for 10017 and 12018 are a consequence of post-crystallisation disturbance.

For isotopically light Zn to be generated in 10017 and 12018 in the same manner as for the pyroclastic glass beads (e.g., *S6, S7)*, the Zn isotopic composition must have been inherited by trapping of light Zn in these samples during evaporative exhalation of Zn from their associated lava flows, or by contamination of 10017 and 12018 through assimilation of material on the lunar surface with isotopically light Zn. However, there is limited evidence for either process acting on the samples from their petrology, with one sample (10017) being a texturally variable, low-MgO (~7.9 wt.%) high-Ti basalt, and the other sample (12018) being a low-Ti high-MgO (~15 wt.%) basalt with accumulative mafic phases. In both scenarios, the Zn concentration of the samples would also be expected to be elevated with respect to other mare basalts with positive δ^{66}Zn values, and the positive δ^{66}Zn values measured for lunar regolith materials would be expected to yield highly variable and positive δ^{66}Zn values in 10017 and

12018. Sample 10017 does have the highest measured Zn concentration of the measured mare basalts, however, 12018 has a Zn concentration in the range of other low-Ti mare basalts. In summary, while the most likely explanation for isotopically light Zn in samples 10017 and 12018 is due to addition of isotopically light Zn from evaporation of Zn as $ZnCl_2$ during volcanic eruption, there is no clear mechanism for this process preserved in the samples, and further study of Zn isotope behavior in lunar lava flows, such as that implied as the source for some lunar meteorites (e.g., *S8*), is warranted.

Supplementary References:

S1. Marti, K., Lugmair, G. W., Urey, H. C. Solar wind gases, cosmic ray spallation products, and irradiation history *Science* **167**, 548 (1970).

S2. Turner, G. . Argon-40/argon-39 dating of lunar rock samples. *Science* **167**, 466 (1970).

S3. Eberhard, P. *et al.,* Noble gas investigation of lunar rocks 10017 and 10071. Geochim. Cosmochim. Acta **38**, 97 (1974).

S4. Stettler, A., Eberhard, P., Geiss, J., Grogler, N. Ar39-Ar40 ages of samples from Apollo 17 Station boulder and implications for its formation. *Earth Planet. Sci. Lett.* **23**, 453 (1974).

S5. Lugmair, G. W., Marti, K. Neutron-capture effects in lunar gadolinium and irradiation histories of some lunar rocks. *Earth Planet. Sci. Lett.* **13**, 32 (1971).

S6. Herzog, G. F. , Moynier, F., Albarede, F. , Berezhnoy, A. A. Isotopic and elemental abundances of copper and zinc in lunar samples, Zagami, Pele's hairs, and a terrestrial basalt. *Geochim. Cosmochim. Acta* **73**, 5884 (2009).

S7. Moynier, F., Albarede, F., Herzog, G. Isotopic composition of zinc, copper, and iron in lunar samples. *Geochim. Cosmochim. Acta* **70**, 6103 (2006).

S8. Day, J. M. D., & Taylor, L. A. On the structure of mare basalt lava flows from textural analysis of the LaPaz icefield and Northwest Africa 032 lunar meteorites. *Meteorit. Planet. Sci.* **42,** 3 (2007).

S9. Day J. M. D. *et al.*, Comparative petrology, geochemistry and petrogenesis of evolved, low-Ti lunar mare basalt meteorites from the La Paz icefield, Antarctica. *Geochim. Cosmochim. Acta* **70**, 1581 (2006).

S10. Day, J. M. D., Taylor, L. A., Floss, C., McSween, H. Y. J. Petrology and chemistry of MIL 03346 and its significance in understanding the petrogenesis of nakhlites on Mars. *Meteoritics Planet. Sci.* **41**, 581 (2006).

S11. Luck, J. M., Othman, D. B., Albarede, F., Zn and Cu isotopic variations in chondrites and iron meteorites: Early solar nebula reservoirs and parent-body processes. *Geochim. Cosmochim. Acta* **69**, 5351 (2005).

S12. Moynier *F., et al.*, Nature of volatile depletion and genetic relations in enstatite chondrites and aubrites inferred from Zn isotopes. *Geochim. Cosmochim. Acta* **75**, 297 (2011).

Table S1: Isotopic composition and concentration of Zn in lunar, Martian and terrestrial igneous rocks and in chondrites. 2σ error is 0.09‰ for δ^{66}Zn and 0.30 ‰ for δ^{68}Zn

Sample	Type	MgO wt.% (Lit)	[Zn] ppm (Lit)	[Zn] ppm (Meas.)	δ^{66}Zn ‰	δ^{68}Zn ‰	Ref.
Low-Ti bas.s							
12002	Olivine bas.	14.8	2.8	1.5	0.84	1.57	A
12018	Olivine bas.	15.0	2.3	1.3	-3.13	-6.37	A
12018 replicate					-3.07	-5.76	
12021	Pigeonite bas.	7.4	4.2	1.4	1.15	2.09	A
12052	Pigeonite bas.	8.6	9	1.1	1.34	2.76	A
12065	Pigeonite bas.	8.3	0.8	1.1	1.52	2.91	A
12063	Ilmenite bas.	9.8	3.4	1.0	1.18	2.49	A
12016	Ilmenite bas.	13.9	-	0.9	1.56	3.39	A
15557	Ol-norm bas.	9.5	1.3	0.6	1.34	2.85	A
15555	Ol-norm bas.	11.3	1.0	1.1	1.56	2.98	A
15058	Qtz-norm bas.	9.3	0.9	1.7	1.41	2.76	A
15065	Qtz-norm bas.	10.4	1.3	1.1	1.33	2.87	A
LAP 02205*	Olivine bas.	7.0	2.9		1.2	2.32	B
High-Ti bas.s							
10017,52[a]	Ilmenite bas. (high K)	7.9	48	12.1	-5.42	-10.63	A
10022,47[a]	Ilmenite bas. (high K)	7.3	2.9	2.2	1.24	2.97	A
10024, 108[a]	Ilmenite bas. (high K)	7.9	14	2.8	1.40	2.86	A
70215, 323[a]	Ilmenite bas.	8.3	4	0.8	1.44	2.55	A
71055, 234[a]	Ilmenite bas.	9.4	2.5	2.1	1.35	2.74	A

74255, 191[a]	Ilmenite bas.	10.6	5.4	1.2	1.77	3.07	A
74275[b]	Ilmenite bas.	10.2	3.6	6.0	0.46	1.06	A
75055, 118[a]	Ilmenite bas.	6.6	7	1.3	1.53	2.85	A
75075, 193[a]	Ilmenite bas.	9.6	5	2.0	1.90	3.06	A
Feldspathic regolith breccia and lunar soils							
MAC 88105*	An. Regolith Breccia				3.18	6.42	C
Lunar Soils[a,b]				25	4.35	8.64	
Lunar pyroclastic glass beads							
74220, 793[b]	Soil (Clod)	14.5	248	231	-3.47	-6.87	A
74220, 849[b]	Soil (Clod)			140	-3.83	-7.40	A
74220, 860[a]	Soil (Clod)			161	-3.37	-6.78	A
74001, 2207[a]	Soil (Clod)	15	156	129	-4.05	-7.96	A

*Lunar meteorites

Shergottite meteorites							
Zagami	bas.ic	11.2	60.3		0.24	0.62	D
Los Angeles	bas.ic	4.0	80.8		0.23	0.49	D
EETA 79001	Ultramafic	15.5	73.0		0.35	0.72	D
ALHA 77005	Ultramafic	28.0	63.3		0.30	0.65	D
SaU 008					0.21	0.47	D
Shergotty	bas.ic	9.5	71.5		0.25	0.44	D
Nakhlite meteorites							
MIL 03346 chip 1		9.3	61.5		0.28	0.60	E
MIL 03346 chip2					0.24	0.57	
Nakhla		12.1	53.7		0.25	0.56	D
Lafayette		12.9	71.5		0.24	0.53	D
Martian Orthopyroxenite							
ALH 84001		24.7	93.4		0.13	0.29	D
Terrestrial Igneous Rocks							
G-2					0.32	0.76	
BCR-1		3.6	130		0.26	0.53	F
BHVO-2[a]		7.2	103	98	0.29	0.60	F
BCR-2[a]		3.6	127	115	0.33	0.69	F
BIR-1[a]		9.7	72	70	0.26	0.54	F
Piton Des Neige[a]					0.34	0.57	
Pele's Hair[a]				36	0.30	0.64	

Chondrites		
Carbonaceous[g]	0.16 to 0.52	0.26 to 1.01
Ordinary[g]	-0.48 to 0.55	-1.05 to 0.82
EH and EL3[h]	0.26±0.16	0.53±0.35
EL6[h]	1.88±2.5	3.77±5.00

Literature MgO and Zn concentrations from (a) the lunar compendium; (b) ref. S9; (c) the lunar meteorite compendium; (d) the Mars meterotie compendium; € ref. S10; (f) GEOREM; (g) ref. S11; (h) S12

Table S2: MC-ICP-MS ThermoElectron Neptune Plus settings for the Zn isotope measurements at Washington University in St Louis.	
RF power (W)	1300
Acceleration potential (V)	10000
Gas flow rates	
Ar coolant (l/min)	18
Ar auxiliary (l/min)	0.5-0.7
Ar sample (l/min)	1-1.2
Solution uptake rate (μl/min)	100
Analysis parameters	
Number of blocks	1
Number of measurements per block	30
Integration time (s)	8.389
Typical Zn concentration of samples and standard (ppb)	500
Typical transmission efficiency V/ppm	10
RF power (W)	1300
Acceleration potential (V)	10000

4. Howardites, Eucrites and Diogenites (HEDs)

Manuscript citation: Paniello RC, Moynier F, Beck P, Barrat JA, Podosek F, Pichat S (2012). Zinc isotopes in HEDs: clues to the formation of 4-Vesta, and the unique composition of Pecora Escarpment 82502. *Geochim. Cosmochim. Acta* 86, 76-87.

Introduction

The HED meteorites are a large group of achondrites that appear to represent a range of planetary formation processes, most likely from asteroid 4-Vesta (e.g., McSween et al. 2011). Eucrites are pigeonite-plagioclase basalts that are thought to derive from the crust, diogenites are orthopyroxenites that are possibly from the outer mantle, and howardites appear to be breccias that are essentially a mix of the other two groups. Among these meteorite are cumulates, polymicts and monomicts; most are brecciated but some are unbrecciated, and some are melts or partial melts. We were able to obtain samples of all of these subtypes to include in this study (Table 4-1). In addition, this study was undertaken just prior to arrival at Vesta of NASA's Dawn mission, from which new spectroscopic data might provide support for some of our conclusions (Reddy et al. 2013).

	Ant.	Non-Ant.	Falls	Total
HEDs	553	714	61	1267
Howardites	122	132	16	254
Eucrites	276	446	34	722
Diogenites	155	136	11	291

Table 4-1. Available HED meteorites by subtype. (Ant. = Antarctic.)

REFERENCES

McSween HY, Mittlefehldt DW, Beck AW, Mayne RG, McCoy TJ (2011). HED meteorites and their relationship to the geology of Vesta and the Dawn mission. *Space Sci. Rev.* 163, 141-174.

Reddy V, Li J-Y, LeCorre L, and 10 co-authors (2013). Comparing Dawn, Hubble Space Telescope, and ground-based interpretations of (4) Vesta. *Icarus* 226, 1103-1114.

Zinc isotopes in HEDs: clues to the formation of 4-Vesta, and the unique composition of Pecora Escarpment 82502

Randal C. Paniello[1]

Frédéric Moynier[1]

Pierre Beck [2]

Jean-Alix Barrat[3]

Frank A. Podosek[1]

Sylvain Pichat[4]

[1]Department of Earth and Planetary Sciences and McDonnell Center for Space Sciences, Washington University in St Louis, One Brookings Drive, St Louis, MO 63130
[2]Laboratoire de Planetologie, Université Joseph Fourier, Grenoble, France
[3]Université Européenne de Bretagne et Université de Brest, I.U.E.M., CNRS UMR 6538 (Domaines Océaniques), Place Nicolas Copernic, 29280 Plouzané Cedex, France

[4]Ecole Normale Superieure de Lyon, France

ABSTRACT

The $\delta^{66}Zn$ (permil deviation of the $^{66}Zn/^{64}Zn$ ratio from a terrestrial standard) values for a suite of 20 non-Antarctic HED (howardite – eucrite – diogenite) meteorites and one mesosiderite, and for 8 Antarctic eucrites and diogenites, were measured in order to determine the role of volatization in the formation of their presumed parent body, the asteroid 4-Vesta. The 20 non-Antarctic HEDs had $\delta^{66}Zn$ values that ranged from -2.0 ‰ to +1.67 ‰, with a mean value of -0.01 ± 0.39 ‰ (2se); this range likely represents a small-scale heterogeneity due to brecciation induced by multiple impacts. The non-Antarctic eucrites ($\delta^{66}Zn$ = +0.00 ± 0.58 ‰ (2se), n=12) were isotopically the same as the diogenites ($\delta^{66}Zn$ = -0.31 ± 0.80 ‰ (2se), n=4), and the howardites ($\delta^{66}Zn$ = +0.26 ± 0.37 ‰ (2se), n=4). On average, non-Antarctic eucrite falls were isotopically heavier (+0.50 ‰) than non-Antarctic finds (-1.00 ‰). The Antarctic finds studied were all unbrecciated samples, and they were significantly heavier than the non-Antarctic samples with a $\delta^{66}Zn$ range of +1.63 to +6.22‰ for 4 eucrites (mean, +4.32‰) and +0.94 to +1.60‰ for 3 diogenites (mean +1.23‰), excluding one anomalous sample, while their Zn concentration is significantly lower than the brecciated samples. These data suggest that the unbrecciated eucrites probably represent the eucritic crust shortly after differentiation and cooling of the parent asteroid, at which time volatization of lighter zinc isotopes led to an isotopically heavy crust. Early impact events caused the ejection of these unbrecciated meteorites, which were subsequently spared from brecciation caused by multiple additional impacts on the much larger Vesta. The range of $\delta^{66}Zn$ values and Zn concentration for the brecciated HEDs in this study supports a major contribution to the Vestan surface by chondritic impactors ($-1.30 < \delta^{66}Zn < +0.76$ ‰ for ordinary and carbonaceous chondrites). The anomalous eucrite PCA 82502 ($\delta^{66}Zn$= -7.75 ‰) is significantly isotopically lighter than the other HEDs

and is the natural sample with the lightest Zn isotopic composition reported in the solar system to date. This meteorite most likely originated from a distinct parent body.

INTRODUCTION

The HED meteorites (howardites, eucrites, and diogenites) comprise the largest group of achondrites, and are generally agreed to have originated from asteroid 4 Vesta based on visible and near-infrared reflectance spectrographic similarities (e.g., McCord et al., 1970; Binzel and Xu, 1993; Burbine et al., 2001). With a few exceptions (Scott et al., 2009), they share the same $\Delta^{17}O$ ratios that distinguish them from the Earth or the Moon (Clayton and Mayeda, 1996; Greenwood et al., 2005). Most eucrites are pigeonite-plagioclase basalts, most diogenites are orthopyroxenites, and howardites are mechanical mixtures of these (with some exceptions; see Warren et al 2009). Almost all of the HED meteorites are breccias, implying significant "gardening" occurred after their initial formation due to multiple impacts on the parent body. Mesosiderites are stony-iron meteorites with about equal parts metal (nickel-iron) and silicates that are similar in composition to HEDs. They have an oxygen isotope composition that is indistinguishable from the HEDs and may also have originated from Vesta (Greenwood et al., 2006).

Studies of major elements and rare earth elements in HED meteorites have led to different theories of formation and differentiation of 4 Vesta. In one model (Takeda 1979), the asteroid is initially totally melted; then, differentiation led to a metallic core surrounded by a magma ocean. A fractional crystallization sequence then proceeded to form orthopyroxenites (diogenites), followed by increasing plagioclase content to form basalts (eucrites). Since the eucrites formed last in this model from the remaining melt, it is sometimes called the "residual liquid" model of

eucrite petrogenesis (e.g., Warren, 1997). Alternatively, the original parent body formed and cooled, then underwent heating events that caused primary partial melts (Stolper 1977). In this model, total melting would not be expected. Over the last 30 years a number of additional models have been proposed that are basically variants of these **(**e.g., Warren and Jerde, 1987; Hewins and Newsom, 1988; Righter and Drake, 1997; Ruzicka et al., 1997; Warren 1997; Mittlefehldt and Lindstrom, 2003; Greenwood et al., 2005**),** however, consensus on a single model of HED petrogenesis has been elusive**.**

Recent petrological studies suggest that the magmatic history of Vesta was certainly much more complex than previously thought. Firstly, a magma ocean model cannot account for the diversity of the REE patterns displayed by the diogenites and their pyroxenes (e.g., Mittlefehldt, 1994; Shearer et al., 1997), and diogenites could have formed from melts produced by the remelting of magma ocean cumulates (Barrat, 2004; Barrat et al., 2008). Secondly, the eucritic crust was probably remelted, producing new melts able to contaminate not only normal eucrites (e.g., Barrat et al., 2007; Yamaguchi et al., 2009) but also some of the parental melts of diogenites (Barrat et al., 2010). Finally, K-rich impact spherules in howardites indicate that the lithologies exposed on the surface of Vesta are not restricted to eucrites and diogenites, and point to some distinct K-rich areas (Barrat et al., 2009).

Vesta shows spectroscopic evidence of differentiation by igneous processes (Binzel and Xu, 1993), which most likely led to a layered structure with a crust chiefly eucritic, an ultramafic mantle, and a metallic core (e.g., Righter and Drake, 1997). Most eucrites show evidence of metamorphism with reheating to >800^{o}C, as evidenced by altered pyroxene compositions from subsolidus diffusion of Mg, Fe and Ca (Takeda and Graham, 1991; Yamaguchi et al., 1996, 1997, 2009). The source of this additional heat may have been from large impacts (Nyquist et

al., 1986), heating at depth after burial of surface basalts (Yamaguchi et al., 1996, 1997), or the differentiation into layers (Takeda 1997). A large impact crater of 460 km diameter, 13 km depth with a large central peak, has been identified on Vesta (Thomas et al., 1997) which may have extended beyond the crust into the mantle layer and ejected many Vestoids and HEDs (McSween et al. 2010). The age of this impact crater is controversial, with some evidence suggesting it occurred during the Late Heavy Bombardment period of 3.5-4.0 billion years ago (Scott et al., 2009), and other evidence supporting an age of only 1 billion years (Asphaug 1997). Ejecta from this large impact, possibly including samples of the deep asteroidal crust and mantle, may now be present on the surface of 4-Vesta.

Compared with chondritic meteorites, HEDs show large depletions in moderately volatile elements, Zn being one of the best examples. Zinc is present in very low concentrations ([Zn]<7 ppm) in all three HED groups (e.g., Barrat et al 2000, 2007, Kitts and Lodders 1998) with most diogenites less than 1 ppm (Barrat et al., 2008); this is lower than the zinc level found on larger planetary bodies such as the Moon, the Earth, or Mars (5-20 ppm, 50 ppm and 90 ppm, respectively; Lodders and Fegley, 1998; Wolf et al, 2009) and chondrite meteorites (40-300 ppm, Lodders and Fegley, 1998). The mechanism by which the moderately volatile elements were depleted from HEDs is still debated. Volatilization is known to fractionate isotopes, thus comparing the isotope compositions of volatile elements between HEDs and other meteorites may help to understand the physical and chemical conditions involved in the loss of volatile elements.

Zinc is a moderately volatile element with a 50% condensation temperature, T_c(Zn), of ~730K (Lodders, 2003) and seems to be even more volatile under conditions relevant to the metamorphism of ordinary chondrites (Schaefer and Fegley, 2010). Measurements of Zn

isotopes in a variety of terrestrial magmatic materials show a remarkably homogeneous distribution, with $^{66}Zn/^{64}Zn$ ratios consistently within 0.2 permil of each other (Ben Othman et al., 2006). This suggests that within the Earth's mantle, Zn isotopes are well mixed and homogeneously distributed, and that igneous processes do not result in significant Zn isotopic fractionation (Ben Othman et al., 2006).

In this study, we used Zn isotopic measurements to investigate possible formation mechanisms of the HED parent body 4-Vesta. Previous studies have demonstrated the utility of Zn isotopes for this purpose. Zn isotopic determinations in chondrites and iron meteorites show significantly more variation than is found in terrestrial materials (Luck et al. 2005, Moynier et al. 2007), suggesting volatilization processes and core/mantle segregation in their formation. On the Earth and on the Moon, volatization from impact events is the primary cause of Zn isotopic fractionation (Moynier et al 2006, 2009; 2010; Albarède 2007; Herzog et al. 2009). We have previously used Zn isotope ratios to determine the role of impact-induced volatization in the formation of tektites (Moynier et al. 2009) and ureilites (Moynier et al. 2010). Thus, the study of Zn isotopes in extraterrestrial samples can provide clues to their mechanisms of formation (Luck et al., 2005), especially as they relate to evaporation/condensation processes (Moynier et al. 2006). Here, we used zinc isotopic composition in HEDs to assess the role of volatization processes in the formation of 4-Vesta.

Due to its very low abundance in HEDs, the analysis of zinc isotopic composition requires a highly sensitive technique. In this study, HED meteorites were analyzed for Zn isotopic composition using Multi Collector-Inductively Coupled Plasma-Mass Spectrometry (MC-ICP-MS).

1. SAMPLES AND ANALYTICAL METHODS:

1.1 Sample Description:

The Zn isotopic compositions of 43 samples from 28 HED meteorites, and one mesosiderite, were measured. There were 23 chips from 17 eucrites, 6 chips from 4 howardites, and 8 chips from 7 diogenites analyzed. In five cases, multiple chips were created from a single museum sample by fracturing it into two or more smaller chips, which were then processed separately (dissolution-chemical separation of Zn and mass-spectrometry analysis) on different dates. Among the eucrite samples, Pasamonte and PCA 82502 are unusual samples with $\Delta^{17}O$ plotting outside the HED range (Greenwood et al. 2009). In addition, to study the sample heterogeneity, 3 clasts and 2 matrix samples prepared from 'large' aliquots (> 2 g each time, Barrat et al., 2003) of the eucrite Juvinas were analyzed.

Seventeen of the meteorites were falls, twelve were finds. Most of the eucrites were monomict breccias. The Antarctic finds (5 eucrites and 3 diogenites) were all unbrecciated, as was one diogenite fall (Tatahouine). The sample descriptions are summarized in Table 1.

To better constrain the terrestrial isotopic composition of Zn, the isotopic composition of two terrestrial igneous geostandards GIT-IWG BE-N (a terrestrial basalt from Essey-la-Côte, France) and USGS G-2 (a terrestrial granite) were analyzed as well.

1.2 Methods:

All sample processing was performed in a "clean room" in order to minimize any possible contamination. Each meteorite chip was 75-500mg in order to extract enough zinc for analysis,

the mass chosen was based on anticipated Zn concentrations from published studies. Fusion crust, if present, was gently removed; the chip was fractured into multiple small pieces, and then those with fusion crust were hand-picked and separated. Chips were cleansed in water in an ultrasonic bath, then crushed in an agate mortar into a homogenous powder. The powder was dissolved in HNO_3/HF in closed Teflon beakers at ~120 °C for 2 days. A final step of dissolution in 6N HCl was done in order to re-dissolve the fluorides formed by the HF. All reagents used were of the highest available purity.

The procedure described by Moynier et al. (2006) was used to extract and purify the zinc from the samples. The dissolved solute was evaporated under a heating lamp, and the residue was re-dissolved in 1.5N HBr. Teflon columns were prepared for anion-exchange chromatography by loading with AG-1X8 (200-400 mesh), cleaning with 0.5N HNO_3, and then pre-loading with 1.5N HBr. Each sample was loaded onto a column, and the Zn bound to the mesh while the remaining non-Zn components passed through the column with additional 1.5N HBr. The Zn was then recovered from the column with 0.5N HNO_3. The entire process was repeated twice more on smaller columns to further purify Zn from impurities. Column fractionation of Zn was avoided by near-complete (>99%) recovery of the Zn. The final Zn eluent was evaporated, then redissolved in 0.05N HNO_3 for isotopic compositional analysis by MC-ICP-MS.

Zinc isotopic compositions were measured on a Nu Plasma High Resolution MC-ICP-MS at the Ecole Normale Superieure de Lyon, France, or on a Thermo-Finnigan Neptune Plus MC-ICP-MS at Washington University, St. Louis, following the procedure described in Marechal et al. (1999). Both instruments are high-resolution MC-ICP-MS and routinely provide similar quality Zn stable isotopic data. For both machines, the yield was found to be greater than 99%

and the blank was ~10 ng. Isotope ratios are expressed as parts per 1,000 deviations relative to a standard:

$$\delta^{X}\mathrm{Zn}\ (‰) = \left(\frac{\left({}^{x}\mathrm{Zn}/{}^{64}\mathrm{Zn} \right)_{\mathrm{sample}}}{\left({}^{x}\mathrm{Zn}/{}^{64}\mathrm{Zn} \right)_{\mathrm{standard}}} - 1 \right) \times 1000$$

with x = 66 or 68. The reference material used is the Zn "Lyon" standard JMC 3-0749 L (Marechal et al. 1999). The "Lyon" standard is the most broadly used reference material to normalize Zn isotope data (reviewed in Albarède, 2004). At least 2 replicate analyses were performed for 80% of the samples; 3-6 replicates were performed for the more extreme samples such as PCA 82502. The replicate analyses of the same samples carried out during different analytical sessions define an external reproducibility (±2SD) of ± 0.09 ‰ for δ^{66}Zn and ± 0.27 ‰ for δ^{68}Zn (see Moynier et al. (2006) and Herzog et al. (2009) for extensive discussion of our analytical precision). With respect to the total amount of Zn in the samples, the blank of about 10 ng introduces an error of 0.10‰ or less, based on a "worst case" contaminant of δ^{66}Zn= -2.0‰ added to the smallest Zn content sample (Zn = 290 ng) at a presumed +1.0‰ (thus the blank is 3.4% or less of the sample). We note that there are no known potential terrestrial contaminants with a δ^{66}Zn below zero, so this is a highly conservative estimate.

Elemental concentrations of Zn were calculated by comparing the voltage peak heights of ^{64}Zn with peak heights for known standards. In most cases the unknown concentrations were adjusted so as to be within ±10% of the standard concentrations. No systematic dependence of isotopic abundances on solution concentration was observed. Uncertainties in concentrations were about ±10%.

2. RESULTS

The measurements of $\delta^{66}Zn$ and $\delta^{68}Zn$ for all of the samples are given in Table 1, and plotted in Figure 1. All data plot on the mass-dependent fractionation line of slope 1.978 (R^2=0.9993) on the three-isotope plot. All of the non-Antarctic HED $\delta^{66}Zn$ values lie within 0 ± 2‰, The HED subgroup ranges overlap significantly: non-Antarctic eucrites from -1.76 to +1.67 ‰, with a mean of $\delta^{66}Zn$ = 0.00 ± 0.58 ‰ (2 standard error, se); howardites from -0.43 to + 1.38 ‰, with a mean of $\delta^{66}Zn$ = +0.26 ± 0.62 ‰ (2se); non-Antarctic diogenites from -2.00 to +0.58 ‰, with a mean of $\delta^{66}Zn$ = -0.31 ± 0.80 ‰ (2se). The mean $\delta^{66}Zn$ for all of the non-Antarctic HEDs studied is -0.01 ± 0.39 ‰ (2se). The Antarctic values are significantly heavier, with one notable exception (PCA 82502, discussed below): the Antarctic eucrites (excluding PCA 82502) have $\delta^{66}Zn$ from +1.63 to +6.22 ‰, with a mean of 4.31 ± 2.23 ‰ (2se), while the Antarctic diogenites have $\delta^{66}Zn$ from +0.94 to +1.60 ‰, with a mean of 1.23 ± 0.39 ‰ (2se). The 3 separated clasts and 2 separated matrix samples of Juvinas show some limited isotopic variability with $0.30 < \delta^{66}Zn < 0.57$. The mesosiderite Estherville is isotopically light with $\delta^{66}Zn$ = -1.66 ± 0.09 ‰. Figure 1 also gives the results for $\delta^{68}Zn$, which are consistent with the $\delta^{66}Zn$ values as the results of mass-dependent fractionation.

The two terrestrial geostandards analyzed in the present study, the basalt BE-N ($\delta^{66}Zn$=0.32) and the granite G-2 ($\delta^{66}Zn$=0.30) show typical terrestrial isotopic composition ($\delta^{66}Zn$=0.20-0.60) reported by Albarède (2004), Ben Othman et al. (2006), and Cloquet et al. (2008).

In Figure 2, the $\delta^{66}Zn$ ranges for the HEDs in this study and literature values for other groups of meteorites, terrestrial samples and lunar samples are shown for comparison. The non-Antarctic HED mean is similar and the range only slightly broader than corresponding values for ordinary and carbonaceous chondrites. The unbrecciated Antarctic HEDs are heavier and range

from $\delta^{66}Zn$ = +0.94 to +6.22 ‰. By contrast, the range for terrestrial igneous rocks is quite narrow, with $\delta^{66}Zn$ = +0.2 to +0.6 ‰ (Ben Othman et al. 2006, Cloquet et al., 2008, and this study); while the range for enstatite meteorites is very broad, from -7.08 ‰ for aubrites to + 7.35 ‰ for EL chondrites (Paniello et al. 2009, Moynier et al. 2011). Nevertheless, with $\delta^{66}Zn$ = -7.75 ‰, PCA 82502 lies outside this range as the most extreme Zn fractionation reported to date.

Figure 3 shows the $\delta^{66}Zn$ values as a function of zinc concentration. In general there is no clear relationship among these samples, although the plot does highlight the very low zinc concentrations in most of the samples. Considering only the Antarctic meteorites, there is a definite trend of higher $\delta^{66}Zn$ with lower concentration (R^2=0.8271). This would be consistent with mass-dependent evaporation with preferential loss of lighter isotopes.

3. DISCUSSION

3.1 Isotopic variation within an individual meteorite

Some of the samples showed significant Zn isotopic heterogeneity within the same small chip from the meteorite. For example, two analyses on different fragments of the chip of howardite Kapoeta gave $\delta^{66}Zn$ values of -0.43 and +0.38 ‰. Two analyses on different fragments of the eucrite Pasamonte chip from ASU gave $\delta^{66}Zn$ values of -0.81 and +0.05 ‰. These variations occur in fragments of the rock that are physically separated by only a few millimeters. Variations were also seen in different chips from the same meteorite. Chips obtained from two different museums gave significantly different values for the eucrites Pasamonte (+1.35 (New Mexico) vs. +0.05 and -0.81 ‰ (ASU)) and Sioux County (-0.73 (ASU) vs. + ~1.0 ‰ (NHM)), and for the diogenite Aioun el Atrouss (-2.0 (FMNH) vs. +0.36 ‰ (ASU)). It is not known how

far apart these chips were on the original meteorite, but it was likely on the order of centimeters based on the sizes of the meteorites at the time of recovery.

This small-scale heterogeneity is best explained by the brecciation process present in almost all of these samples. Some of the samples are polymict and contain multiple lithologies; further, the single-lithology monomict samples may or may not represent the bulk. The chips prepared for analysis contain variable amounts of matrix, clast, and inclusion contaminants; thus, small-scale variability should be expected in these measurements.

Less small-scale variability would be expected if larger samples were analyzed, since the homogenized powder essentially gives the average of the total mass. This concept was tested using larger (~2 g) samples from the monomict eucrite fall Juvinas. Two matrix samples had the same δ^{66}Zn, within error (0.30 and 0.37), while three large clasts showed small heterogeneity (0.39, 0.57 and 0.31). This resembles a chondritic Zn isotopic composition (see below).

Zinc isotopic heterogeneity has been previously reported in chondrites and in iron meteorites by Luck et al (2005) and by Ghidan and Loss (2011). Ghosh and McSween (1995) proposed a model for Vesta of a melted center with an unmelted outer shell which would be expected to retain some isotopic heterogeneity. This idea was further supported by Wiechert et al (2004), who reported heterogeneous oxygen isotope measurements in HEDs consistent with a very rapid early history of large-scale, incomplete mixing on Vesta. The Zn isotopic heterogeneity found in our study fits with both of these models if the Zn was initially isotopically heterogeneous in Vesta or if some isotopic fractionation occurred early in Vesta history.

The low zinc concentration in these rocks (about 1 ppm for most HEDs) also contributes to the measured heterogeneity. Very small inclusions rich in light or heavy isotopes of zinc could significantly alter the isotopic composition of these small chips. For example, carbonaceous

chondrite xenoliths have been reported in Kapoeta (Wilkening, 1973) and Pasamonte (Metzler et.al. 1995) and could alter the measured Zn ratios; these may have been introduced by an impactor. CM- and CR- like clasts, ranging in size from 25 μm to 5 mm, have been reported in HEDs by Buchanan et al. (2009); their wide distribution in the breccias suggested efficient energetic mixing of impactors as the most likely source. Since the HEDs are almost all monomict or polymict breccias, there is also a possibility that the measured fractionation is influenced by the isotopic makeup of the matrix, which contains higher levels of contaminant debris than the clast minerals, rather than the primary minerals themselves.

By contrast, terrestrial basalts from a variety of magmatic settings show a very narrow range of $+0.2\ 0 < \delta^{66}Zn < +0.60$ (Albarède 2004; Ben Othman et al. 2003, 2006; Cloquet et al. 2008; Herzog et al. 2009; this study) which suggest that Zn isotopes are homogeneously well distributed within the Earth's mantle, and that igneous processes do not lead to subsequent Zn isotopic fractionation. This may be related to the higher zinc concentrations in terrestrial igneous rocks ([Zn] = 50-100 ppm; Lodders and Fegley, 1998), or a greater homogenation of kilogram-sized terrestrial samples used as standards, but it may also indicate a significant difference in the formation history of the two planetary bodies. Earth is substantially larger than Vesta, and would have required a much longer cooling time, with a corresponding greater degree of convection and equilibration than Vesta. Thus, Earth would also be expected to have greater isotopic homogeneity than Vesta, as described above for Zn isotopes.

3.2 Unbrecciated Antarctic samples & weathering

Of the nearly 600 eucrites currently recognised with official names, there are 30 meteorites (about 5%) that are classified as unbrecciated eucrites, and all of these are Antarctic finds. Our $\delta^{66}Zn$ measurements in five of these meteorites were striking; four were isotopically quite heavy

(mean, +4.31‰), while one was anomalously light (PCA 82502, discussed below). These unbrecciated specimens are most likely samples of the original, early Vestan crust, which were expelled by early impacts and thus spared from further impacts that would have led to their brecciation. The three unbrecciated Antarctic diogenites studied were also isotopically heavier than the other diogenites, but to a lesser degree. These likely formed deeper in the crust or upper mantle, where volatization of Zn would occur to a lesser extent, making them isotopically heavy but not as extreme as the eucrites.

The role of weathering on the measured Zn fractionation is unclear, but is likely limited. Biswas et al. (1980) studied trace elements in four Antarctic meteorites, and found that there was limited contamination or leaching of trace elements at the periphery of the meteorites, but interior samples gave reasonably normal values for their respective subgroups. Kallemeyn et al (1993) compared chondrite Antarctic finds with falls, and found "concentration ranges and median values of two chalcophile elements, Se and Zn, are nearly identical between the Antarctic H chondrites and H falls." Wang et al. (1992) studied a large suite of chondrites, HEDs and lunar meteorites, and found that although REE composition may have been altered in some eucrites, there was no evidence for labile trace element transport into or out of eucrites of weathering grade A to B (our 5 eucrites include four A and one B; our 3 diogenites are all A/B). Carbonaceous chondrites and lunar meteorites were also essentially unaltered. Wang and Lipshutz (1995) also found no weathering effects in Zn and other trace elements for Antarctic ureilites. Mittlefehldt and Lindstrom (1991) found significant REE depletion in a group of abnormal Antarctic eucrites, but trace elements such as Zn were not reported.

We note that there are no known terrestrial materials with the extreme fractionations seen in these Antarctic meteorites (either very heavy, like four in this study, or very light, like PCA

82502), so this degree of Zn fractionation cannot be explained by local contamination.We conclude that weathering effects in our Antarctic meteorites, if any, are likely small (< 1‰) and thus cannot possibly explain the large differences in Zn fractionation seen between the unbrecciated Antarctic samples and the brecciated falls and finds.

3.3 Falls vs. finds

There was a small difference in δ^{66}Zn values based on the mechanism of recovery of the meteorite. For the eucrites, the δ^{66}Zn for the 8 observed falls averaged +0.50 ± 0.51 ‰ (2se), while the 4 non-Antarctic finds averaged -1.00 ± 1.01 ‰. This finding may simply be a result of sampling, as all of the HEDs seem to be scattered between δ^{66}Zn = 0 ± 2‰. This observation could also suggest that the terrestrial non-Antarctic weathering process preferentially removes heavy isotopes from the meteorite. This direction of isotopic fractionation during weathering was also reported by Luck et al. (2005) for Zn isotopes in undifferentiated ordinary chondrites: an H3.7 find was 0.40 ‰ lighter (for δ^{66}Zn) than an H3.8 fall, while an L3.6 find was 1.27 ‰ lighter than an L3.6 fall . All of the howardites and diogenites in the present study were falls.

3.4 Chondritic origin for Vesta and the origin of the elemental depletion of HEDs

The range of δ^{66}Zn observed in the 3 large clasts and 2 matrix samples from Juvinas (0.30 to 0.57‰) and the average value close to zero (-0.01 ± 0.39 (2se) for all non-Antarctic HED samples) suggest a chondritic Zn isotopic composition for Vesta. Individual fragments of brecciated HEDs exhibit a small scale isotopic heterogeneity. The isotopic variation measured in lunar soils (Moynier et al. 2006) suggests that the heterogeneity observed in brecciated eucrites is the result of the brecciation processes. Zinc isotopes are redistributed at the surface of 4-Vesta, presumably by evaporative processes. Under this scenario, the volatilized isotopically light zinc may have left the molten body's surface, then remained in a primordial atmosphere and

was later recondensed back into the asteroid, initially at the surface. The result would be a heterogeneous Vesta surface with some isotopically light and isotopically heavy regions. Subsequent impacts would pulverize these rocks to varying degrees, and result in brecciation such as seen in the meteorites that reach the Earth. The depletion of moderately volatile elements such as Zn would have to have occurred prior to this process.

The average Zn fractionation for this group of HED meteorites was approximately zero, similar to ordinary chondrites (Luck et al. 2005, Moynier et al. 2007, Ghidan and Loss 2011). Considering only the eucrite falls, the average δ^{66}Zn value of +0.50 ± 0.51 ‰ was identical to the CI chondrites reported by Luck et al (2005), who found mean δ^{66}Zn = +0.49 ‰ and +0.47 ‰ for Orgueil and Ivuna, respectively. In addition, large clasts and matrix samples from Juvinas show a fairly homogeneous Zn isotopic composition of 0.33 ± 0.13 ‰, similar to chondritic values.

Thus, Vesta may have originally accreted from chondritic material. However, the typical chondrite Zn abundance is about 50 ppm (e.g., Luck et al. 2005), while the range of Zn in HEDs is about 1-7 ppm, so the HEDs must have lost 86-98% of their Zn without any isotopic fractionation. The unbrecciated samples allow us to propose an explanation for these findings. The data fit with a model in which Vesta originally accreted from material with a chondritic Zn content; Vesta then lost by evaporation most (> 90%) of its volatiles (e.g. Zn) early in its history as it slowly cooled. This left a surface comprised of unbrecciated, isotopically heavy eucritic material, with a layer of diogenites below that was also heavy, but less so. Early impacts ejected the unbrecciated meteorites that were found in this study to be enriched in heavy Zn isotopes, before they could become brecciated. Additional impacts, likely from largely chondritic material, led to the brecciation of the surface as well as the addition of Zn with a chondritic

isotopic composition. This hypothesis is consistent with Scott et al. (2009), who note that unbrecciated eucrites show no shock features, unlike most brecciated ones.

A Rayleigh evaporation model can be used to further test this hypothesis, using the equation

$$\delta^{66}Zn = (\delta^{66}Zn_0 + 1000)\, f^{(\alpha-1)} - 10^3 \qquad (1)$$

where $f = [Zn]/[Zn]_0$ and $\alpha = (64/66)^{0.5}$ based on the masses of the species. Starting with chondritic values from Luck et al. (2005) of $[Zn]_0 = 50$ ppm and $\delta^{66}Zn_0 = +0.50$ ‰, using (1), we find that the expected Zn fractionation for pure Rayleigh evaporation to a final [Zn] of 1 ppm gives $\delta^{66}Zn = +62.1$ ‰. The measured $\delta^{66}Zn$ values reported in this study are all substantially lower than this, implying that significant mixing must have occurred after evaporation. This supports the model for evaporative volatile loss proposed above.

A comparison may also be made with the surface of the Moon. Like Vesta, the lunar surface has been largely depleted of its Zn, with [Zn] of 5-20 ppm in most samples. The lunar basalts show Zn fractionation that is largely chondritic, while the soil, which has been substantially gardened by impacts, is isotopically heavy (Moynier et al. 2006, Herzog et al. 2009)(Figure 2). Micrometeorite vaporization and sputtering were proposed as mechanisms by which the regolith might become isotopically heavier; but evaporation of light isotopes and Zn contributions from chondritic impactors, as proposed for Vesta herein, may also have played a role on the Moon.

Schönbächler et al. (2008) found a similar depletion without fractionation of another moderately volatile element, cadmium, in three eucrites, Béréba, Bouvante, and Juvinas. The cadmium isotopic composition of these eucrites was chondritic, within error (~0.4 ‰), and the concentration was depleted by a factor of ~600 to the ~1 ppb level compared to CI chondrites. Wombacher et al. (2008) had similar results for $^{114}Cd/^{110}Cd$ ratios in two monomict eucritic

breccias. They also concluded that the primary volatile element depletion of the inner solar system did not involve kinetic Rayleigh evaporation or condensation. Moynier et al. (2011) also reported Zn depletion without fractionation in enstatite chondrites and aubrites, again concluding that the findings were not due to evaporative/condensation processes. It is possible that Vesta's original depletion in Zn may have also been non-evaporative, but the heavy unbrecciated Antarctic samples support a mass-dependent fractionation process such as volatization.

If we assume that 4-Vesta accreted from chondritic material, then most of the Zn was subsequently removed or stored in phases not sampled by HEDs, with no associated isotopic fractionation, early in 4-Vesta history. One possibility includes the sequestration of Zn into spinel, as suggested by Chikami et al. (1997), which would have happened at high temperature with little or no associated isotopic fractionation and is consistent with the depletion of Cu, Zn, and Cd in these meteorites. Another proposed phase is the sulfides (troilite), but studies have found little or no troilite in the HEDs, and little or no Zn in the troilite that is found (Chikami et al. 1997, Nishimura and Sandell 1964). Another alternative would be that the chondritic material that formed Vesta lost most of its Zn in a non-fractionating process prior to or during accretion. These speculations regarding zinc-containing phases cannot be resolved with the data collected in this study.

3.5 PCA 82502

The Antarctic eucrite Pecora Escarpment (PCA) 82502 was extremely light in Zn isotopes compared with the other HEDs, with δ^{66}Zn of – 7.75 ‰, a value that represents the most extreme Zn fractionation in the solar system reported to date. It is an unbrecciated eucrite (Grossman 1994, Scott et al. 2009), although Bermingham et al. (2008) describe it as consisting of rounded basaltic clasts surrounded by a fine-grained matrix. These authors suggest this meteorite is

unequilibrated, and probably erupted as a surface flow. Bermingham et al. (2008) report that PCA 82502 has a light REE-depleted pattern with a positive europium anomaly, as well as other incompatible trace element depletions, and they suggest that this meteorite (and three others in their study) should be considered a "new variety of non-cumulate basaltic eucrite." It has a weathering grade of "A," and its initial write-up indicated that essentially no weathering was observed. This suggests that the extreme Zn isotopic fractionation measured was not significantly affected by its Antarctic exposure.

PCA 82502 is unusual in other ways. Jovanovic and Reed (1988) found that it had a higher Hg equilibration temperature than the other eucrites tested, and proposed that it could be a rapidly chilled magma representing the original crust that has not undergone impact melting and burial. Greenwood et al. (2009) noted that PCA 82502 has a $\Delta^{17}O$ value enough outside the expected range that its origin on Vesta can be regarded as uncertain (along with Pasamonte and 4 others). Herpers et al. (1995) found this meteorite to have an extremely low ^{10}Be activity, implying, at minimum, a "complex exposure history." These peculiarities, and especially the extremely negative Zn isotopic fractionation, lead us to conclude that PCA 82502 most likely originated from a different parent body, and not from 4-Vesta.

4. CONCLUSION

The isotopic composition of 20 non-Antarctic HEDs show an average $\delta^{66}Zn = -0.01 \pm 0.39$ ‰ (2se), with a range of about 0 ± 2 ‰. This isotopic variation among and within HED meteorites is much larger than anything observed in terrestrial igneous rocks from various magmatic settings and suggest that the HED parent body (4 Vesta) retained an initial heterogeneity that has been lost on Earth, or acquired heterogeneity later from impact contributions. This is probably

due to a weaker and much shorter geological activity on Vesta than on Earth. The unbrecciated Antarctic HEDs are isotopically heavy, suggesting that Vesta may have lost most of its zinc (and other volatiles) early in its accretion history, and impacts led to the creation of isotopically heavy Vestoids. Additional impacts led to impact gardening and brecciation, with major contributions to the surface zinc delivered by chondritic impactors.

The unbrecciated eucrite PCA 82502 is an unique sample which has the lightest Zn isotopic composition measured so far in any solar system materials (δ^{66}Zn=-7.75 ‰). This dramatic enrichment in light isotopes of PCA 82502 together with its unusual oxygen isotopic composition suggest that this sample has a very different history than the other HED meteorites. PCA 82502 is most likely derived from a completely different parent body.

REFERENCES

Albarède, F. (2004). The stable isotope geochemistry of copper and zinc. *Rev. Mineral. Geochem.* 55, 409–427.

Albarède, F., et al. (2007). Isotope fractionation during impact: Earth versus the moon. *Meteor. Planet. Sci.* 42, A11.

Asphaug E. (1997). Impact origin of the Vesta family. *Meteor. Planet. Sci.* 32, 965-980.

Barrat J. A. (2004). Determination of the parental magmas of HED cumulates: the effects of interstitial melts. *Meteor. Planet. Sci.* 39, 1767–1779.

Barrat J.A., Blichert-Toft J., Gillet P., Keller F. (2000). The differentiation of eucrites: the role of *in situ* crystallization. *Meteor. Planet. Sci.* 35, 1087-1100.

Barrat J. A., Yamaguchi A., Greenwood R. C., Bohn M., Cotten J., Benoit M., Franchi A. (2007). The Stannern trend eucrites: contamination of Main-Group eucritic magmas by crustal partial melts. *Geochim. Cosmochim. Acta* 71, 4108–4124.

Barrat J.A., Yamaguchi A., Greenwood R.C., Benoit M., Cotten J., Bohn M., Franchi I. A. (2008). Geochemistry of diogenites: still more diversity in their parental melts. *Meteor. Planet. Sci.* 43, 1759–1775.

Barrat J.A., Jambon A., Bohn M., Blichert-Toft J., Sautter V., Gopel C., Boudouma O., Keller F. (2003). Petrology and geochemistry of the unbrecciated eucrite North West Africa 1240 (NWA 1240) : an HED parent body impact melt. *Geochim. Cosmochim. Acta* 67, 3959–3970.

Barrat JA, Yamaguchi A, Greenwood RC, Bollinger C, Bohn M, Cotten J, Franchi IA (2009). Geochemistry of HED Cumulates: A Synthesis. 72nd MetSoc meeting, abstract #5151.

Barrat JA, Bohn M, Gillet P, Yamaguchi A. (2009). Evidence for K-rich terranes on Vesta from impact spherules. *Meteor. Planet. Sci.* 44, 359–374.

Barrat JA, Yamaguchi A, Zanda B, Bollinger C, Bohn M (2010). Relative chronology of crust formation on asteroid Vesta: Insights from the geochemistry of diogenites. *Geochim. Cosmochim. Acta* 74, 6218-6231.

Ben Othman D., Luck J.M., Tchalikian A., Albarède F. (2003). Cu-Zn isotope systematics in terrestrial basalts. Geophys. Res. Abs. 5, # 09669.

Ben Othman D., Luck J.M., Bodinier J.L., Arndt N.T., Albarède F. (2006). Cu-Zn isotopic variations in the Earth's mantle. *Geochim. Cosmochim. Acta Supp.* 70, A46.

Bermingham K.R., Norman M.D., Christy A.G., Arculus R.J. (2008) A new variety of eucrite? Clues to early differentiation of igneous asteroids. LPSC 39, abstract #1225.

Binzel R. P., Xu S. (1993). Chips off asteroid 4 Vesta: evidence for the parent body of basaltic achondrite meteorites. *Science* 260, 186–191.

Biswas, S.; Ngo, H. T.; Lipschutz, M. E. (1980). Trace element contents of selected Antarctic meteorites. I - Weathering effects and ALH A77005, A77257, A77278 and A 77299. *Zeitschrift fuer Naturforschung*, Teil 35, 191-196.

Bogard D.D., Garrison D.H. (2003). ^{39}Ar-^{40}Ar ages of eucrites and thermal history of asteroid 4 Vesta. *Meteor. Planet. Sci*. 38, 669–710.

Buchanan P.C., Zolensky M.E., Greenwood R.C., Franchi I.A. (2009). Foreign materials in polymict breccias from Vesta. 72nd MetSoc meeting, abstract #5180.

Burbine T.H., Buchanan P.C., Binzel R.P., Bus S.J., Hiroi T., Hinrichs J.L., Meibom A., McCoy T. J. (2001). Vesta, Vestoids, and the howardite, eucrite, diogenite group: Relationships and the origin of spectral differences. *Meteor. Plan. Sci.* 36, 761–781.

Chikami J., Takeda H., Yugami K., Mikouchi T., Miyamoto M. (1997). Zn abundance in coexisting troilite and spinel in achondrites: remnant indicative of the primitive source materials. LPS 28, abstract #1490.

Clayton R.N., Mayeda T. K. (1996). Oxygen isotope studies of achondrites. *Geochim. Cosmochim. Acta* 60, 1999–2017.

Cloquet C., Carignan J., Lehmann M.F., Vanhaecke F. (2008). Variation in the isotopic composition in the natural environment and the use of zinc isotopes in the biosciences: a review. *Anal. Bioanal. Chem.* 390, 451-463.

Ghidan O.Y., Loss R.D. (2011). Isotope fractrionation and concentration measurements of Zn in meteorites determined by the double spike, IDMS-TIMS techniques. *Meteor. Plan. Sci.* 46, 830-842.

Ghosh A., McSween H.Y. (1998), A thermal model for the differentiation of asteroid 4 Vesta, based on radiogenic heating. *Icarus* 134, 187-206.

Greenwood R.C., Franchi I.A., Jambon A., Buchanan P.C. (2005). Widespread magma oceans on asteroidal bodies in the early Solar System. *Nature* 435, 916-918.

Greenwood R.C., Franchi I.A., Jambon A., Barrat J.A., Burbine T.H. (2006). Oxygen isotope variation in stony-iron meteorites. *Science* 313, 1763-1765.

Greenwood R.C., Franchi I.A., Scott E.R.D., Barrat J.A., Norman M. (2009). Oxygen isotope variation in the HEDs: how homogenous is Vesta? 72nd Met.Soc. meeting, abstract #5436.

Grossman J.N. (1994), Meteoritical Bulletin, No. 76, *Meteoritics* 29, 100-143.

Herpers U., Vogt S., Bremer K., Hofmann H.J., Suter M., Wieler R., Lange H.-J.,Miche R. (1995). Cosmogenic nuclides in differentiated Antarctic meteorites: measurements and model calculations. *Planet. Space Sci.* 43, 545-556.

Herzog G. F., Moynier F., Albarède F. Berezhnoy A. (2009). Isotopic and elemental abundances of copper and zinc in lunar samples, Zagami, Pele's hairs, and a terrestrial basalt. *Geochim. Cosmochim. Acta* 73**,** 5884-5904.

Hewins R.H., Newsom H.E. (1988). Igneous activity in the early solar system. In: *Meteorites and the early solar system*, Kerridge J.F. and Matthews M.S., eds. Univ. Arizona Press, Tuscon, AZ, pp 73-101.

Jovanovic S., Reed G.W. (1988). Thermometry of eucritic achondrites. Met.Soc. abstracts, 278.

Kallemeyn, G. W.; Krot, A. N.; Rubin, A. E. (1993). Preliminary compositional comparisons of H-chondrite falls to Antarctic H-chondrite populations. *Meteoritics* 28: 377.

Kitts K, Lodders K (1998). Survey and evaluation of eucrite bulk compositions. *Meteor. Plan. Sci.* 33: A197-A213.

Lodders K., Fegley B. (1998). *The planetary scientist's companion.* Oxford U. Press, New York.

Luck, J. M., Ben Othman D., Albarède F. (2005). Zn and Cu isotopic variations in chondrites and iron meteorites: Early solar nebula reservoirs and parent-body processes. *Geochim. Cosmochim. Acta* 69**,** 5351-5363.

Mayne R.G., McSween Jr. H.Y., McCoy T.J., Gale A. (2009). Petrology of the unbrecciated eucrites. *Geochim. Cosmochim. Acta* 73, 794–819

McCord TB, Adams JB, Johnson TV (1970). Asteroid Vesta: Spectral reflectivity and compositional implications. *Science* 168, 1445–1447.

McSween Jr. H.J., Mittlefehldt D.W., Beck A.W., Mayne R.G., McCoy T.J. (2010). HED meteorites and their relationship to the geology of vesta and the Dawn mission. *Space Sci. Rev.*, DOI 10.1007/s11214-010-9637-z.

Metzler K., Bobe K.D., Palme H., Spettel B., Stoffler D. (1995). Thermal and impact metamorphism on the HED parent asteroid. *Planet. Space Sci.* 43, 499-525.

Misawa K., Yamaguchi A., Kaiden H. (2006). U–Pb and ^{207}Pb–^{206}Pb ages of zircons from basaltic eucrites: implications for early basaltic volcanism on the eucrite parent body. *Geochim. Cosmochim. Acta* 69, 5847–5861.

Mittlefehldt D.W. (1994). The genesis of diogenites and HED parent body petrogenesis. *Geochim. Cosmochim. Acta* 58, 1537–1552.

Mittlefehldt, D. W., Lindstrom, M. M. (1991). Generation of abnormal trace element abundances in Antarctic eucrites by weathering processes. (Workshop on Differences between Antarctic and non-Antarctic Meteorites, Vienna, Austria, July 27, 28, 1989). *Geochim. Cosmochim. Acta* 55, 77-87.

Mittlefehldt D.W., Lindstrom M.M. (2003). Geochemistry of basaltic eucrites, and Hf and Ta as petrogenetic indicators for altered Antarctic meteorites. *Geochim. Cosmochim. Acta* 67, 1911–1935.

Moynier, F., Albarède F., Herzog G.F. (2006). Isotopic composition of zinc, copper, and iron in lunar samples. *Geochim. Cosmochim. Acta* 70, 6103-6117.

Moynier, F., Blichert-Toft, J., Telouk, P., Luck, J.M., Albarède, F., (2007). Comparative stable isotope geochemistry of Ni, Cu, Zn, and Fe in chondrites and iron meteorites. *Geochim. Cosmochim. Acta*, 71: 4365-4379.

Moynier F., Beck P., Jourdan F., Yin Q.-Z., Reimold U., Koeberl C. (2009). Isotopic fractionation of zinc in tektites. *Earth Planet. Sci. Lett.* 277**,** 482-489.

Moynier F., Beck P., Barrat J-A., Ferroir T., Paniello R., Telouk P., Gillet P. (2010). Volatilization induced by impacts recorded in Zn isotope composition of ureilites. *Chem. Geol.* 276, 374-379.

Moynier F., Paniello, R., Gounelle, M., Albarède, F., Beck, P., Podosek, F., and Zanda, B. (2011). Nature of volatile depletion and genetic relationships in enstatite chondrites and aubrites inferred from Zn isotopes. *Geochim. Cosmochim. Acta, 75: 297-397.*

Nishimura M. and Sandell E. B. (1964). Zinc in meteorites. *Geochim Cosmochim Acta* 28: 1055-79.

Nyquist L. E., Takeda H., Bansal B., Shih C. Y., Wiesmann H., Wooden J. L. (1986). Rb-Sr and Sm-Nd internal isochron ages of a subophitic basalt clast and a matrix sample from the Y75011 eucrite. *J. Geophys. Res.* 91:8137–8150.

Paniello R.C., Moynier F., Podosek F.A., Beck P. (2009). Zn isotopic composition of achondrites and enstatite chondrites. 72nd Met.Soc. meeting, abstract #3153.

Righter K., Drake M. J. (1997) A magma ocean on Vesta: core formation and petrogenesis of eucrites and diogenites. *Meteor. Planet. Sci.* 32, 929–944.

Rudnick R.L., Gao S. (2003). Composition of the continental crust. In: Holland H.D., Turekian K.K. (Eds.), *Treatise on Geochemistry*, Elsevier, Amsterdam, pp. 1-64.

Ruzicka A., Snyder GA, Taylor LA (1997). Vesta as the howardite, eucrite, and diogenite parent body: implications for the size of the core and for large-scale differentiation. *Meteor. Planet. Sci*. 32, 825-840.

Schönbächler M, Baker RGA,Williams H, Halliday AN, Rehkämper M. (2008). The cadmium isotope composition of chondrites and eucrites. 71st Met.Soc. meeting, abstract #5268.

Scott ERD, Greenwood RC, Franchi IA, Sanders IA (2009). Oxygen isotopic constraints on the origin and parent bodies of eucrites, diogenites, and howardites. *Geochim. Cosmochim. Acta* 73, 5835–5853.

Scott ERD, Bogard DD, Bottke WF, Taylor GJ, Greenwood RC, Franchi IA, Keil K, Moskovitz NA, Nesvorny D (2009). Impact histories of Vesta and Vestoids inferred from howardites, eucrites, and diogenites. LPSC 40, abstract #2295.

Shearer CK, Fowler GW, Papike JJ (1997). Petrogenic models for magmatism on the eucrite parent body: Evidence for orthopyroxene in diogenites. *Meteor. Planet. Sci.* 32, 877-889.

Stolper E. (1977). Experimental petrology of eucrite meteorites. *Geochim. Cosmochim. Acta* 41, 587-611.

Takeda H (1979). A layered-crust model of a howardite parent body. *Icarus* 40, 455-470.

Takeda H (1997). Mineralogical records of early planetary processes on the howardite, eucrite, diogenite parent body with reference to Vesta. *Meteor. Planet. Sci.* 32, 841–853.

Takeda H, Graham AL (1991). Degree of equilibration of eucritic pyroxenes and thermal metamorphism of the earliest planetary crust. *Meteoritics* 26, 129-134.

Thomas PC, Binzel RP, Gaffey MJ, Storrs AD, Wells EN, Zellner BH (1997). Impact excavation on asteroid 4 Vesta: Hubble space telescope results. *Science* 277, 1492-1495.

Wang, M.-S.; Xiao, X.; Lipschutz, M. E. (1992). Alteration of Labile Trace Element Concentrations in Antarctic Meteorites by Weathering: A Five-Year Assessment. *Meteoritics* 27, 303.

Wang, M.-S.; Lipschutz, M. E. (1995). Volatile trace elements in Antarctic ureilites. *Meteoritics* 30, 319-24.

Wang J, Davis AM, Clayton RN, Mayeda TK, Hashimoto A (2001) Chemical and isotopic fractionation during the evaporation of the FeO-MgO-SiO2-CaO-Al2O3-TiO2 rare earth element melt system. *Geochim. Cosmochim. Acta* 65, 479–494.

Warren PH (1997). Magnesium oxide-iron oxide mass balance constraints and a more detailed model for the relationship between eucrites and diogenites. *Meteor. Planet Sci.* 32, 945-963.

Warren PH, Jerde EA (1987). Composition and origin of Nuevo Laredo trend eucrites. *Geochim. Cosmochim. Acta* 51, 713-725.

Warren PH, Kallemeyn GW, Huber H, Ulff-Møller F, Choe W (2009). Siderophile and other geochemical constraints on mixing relationships among HED-meteoritic breccias. *Geochim. Cosmochim. Acta* 73, 5918–5943.

Wiechert UA, Halliday AN, Palme H, Rumble D (2004). Oxygen isotope evidence for rapid mixing of the HED meteorite parent body. *Earth Planet. Sci. Lett.* 221, 373-382.

Wilkening LL (1973). Foreign inclusions in stony meteorites-I. Carbonaceous chondrite xenoliths in the Kapoeta howardite. *Geochim. Cosmochim. Acta* 37, 1985-1989.

Wolf SF, Wang M-S, Lipschutz ME (2009). Labile trace elements in basaltic achondrites: Can they distinguish between meteorites from the Moon, Mars, and V-type asteroids? *Meteor. Planet. Sci.* 44, 891–903.

Wombacher F, Rehkamper M, Mezger K, Bischoff A, Munker C (2008). Cadmium stable isotope cosmochemistry. *Geochim. Cosmochim. Acta* 72, 646–667.

Yamaguchi A, Taylor GJ, Keil K (1996). Global crustal metamorphism of the eucrite parent body. *Icarus* 124, 97–112.

Yamaguchi A, Taylor GJ, Keil K (1997). Metamorphic history of the eucritic crust of 4 Vesta. J. *Geophys. Res.* 102, 13381–13386.

Yamaguchi A, Barrat JA, Greenwood RC, Shirai N, Okamoto C, Setoyanagi T, Ebihara M, Franchi IA, Bohn M (2009). Crustal partial melting on Vesta: evidence from highly metamorphosed eucrites. *Geochim. Cosmochim. Acta* 73, 7162–7182.

Yu Y, Hewins RH, Alexander CM O'D, Wang J (2003). Experimental study of evaporation and isotopic mass fractionation of potassium in silicate melts. *Geochim. Cosmochim. Acta* 67, 773–786.

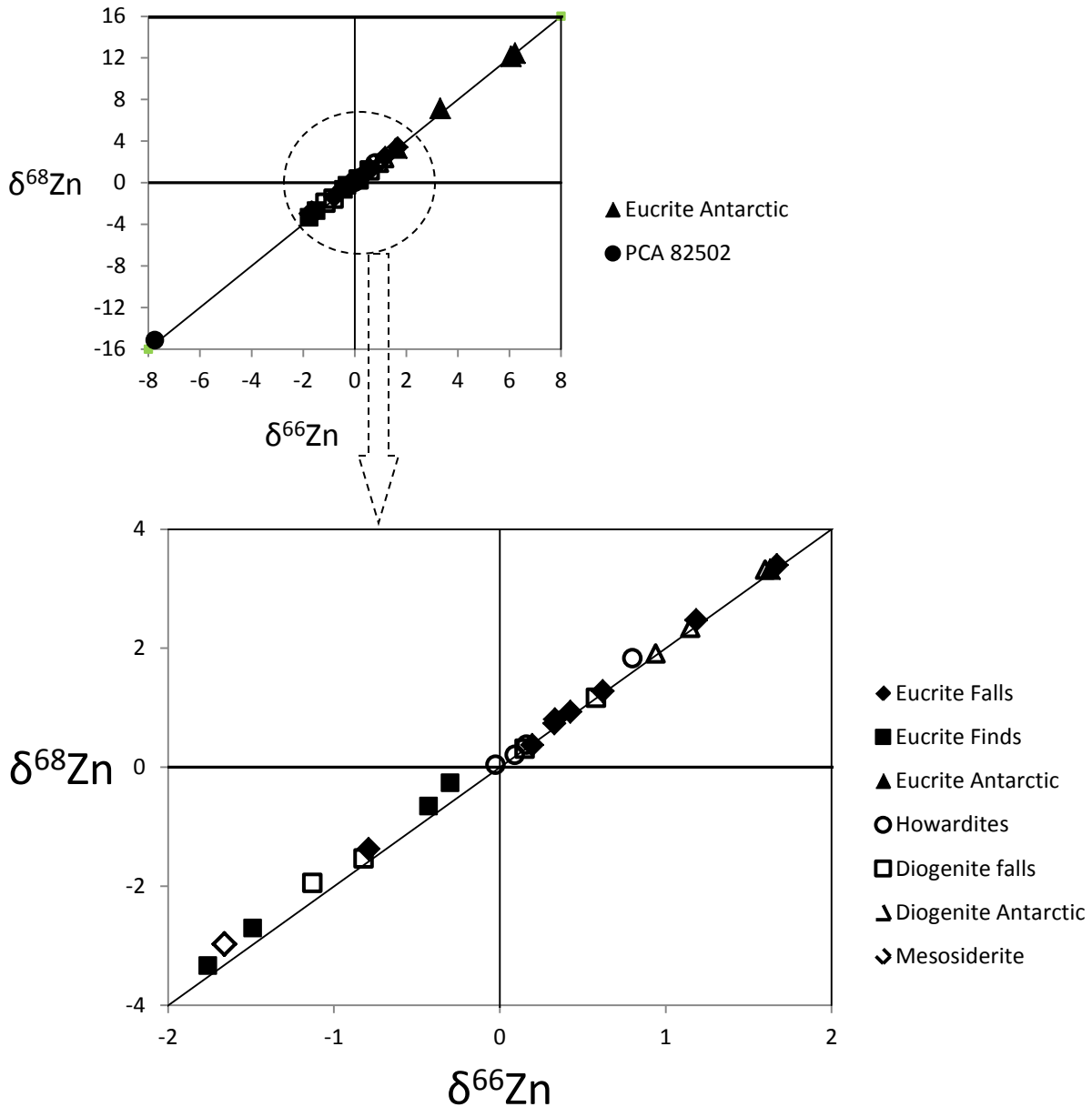

Figure 1. Three-isotope plot of Zn isotopic measurements in HED meteorites and one mesosiderite. With the exception of the eucrite PCA 82502, all $\delta^{66}Zn$ values fall between 0 ± 2 ‰. All data plot on the mass-dependent fractionation line of slope 1.978.

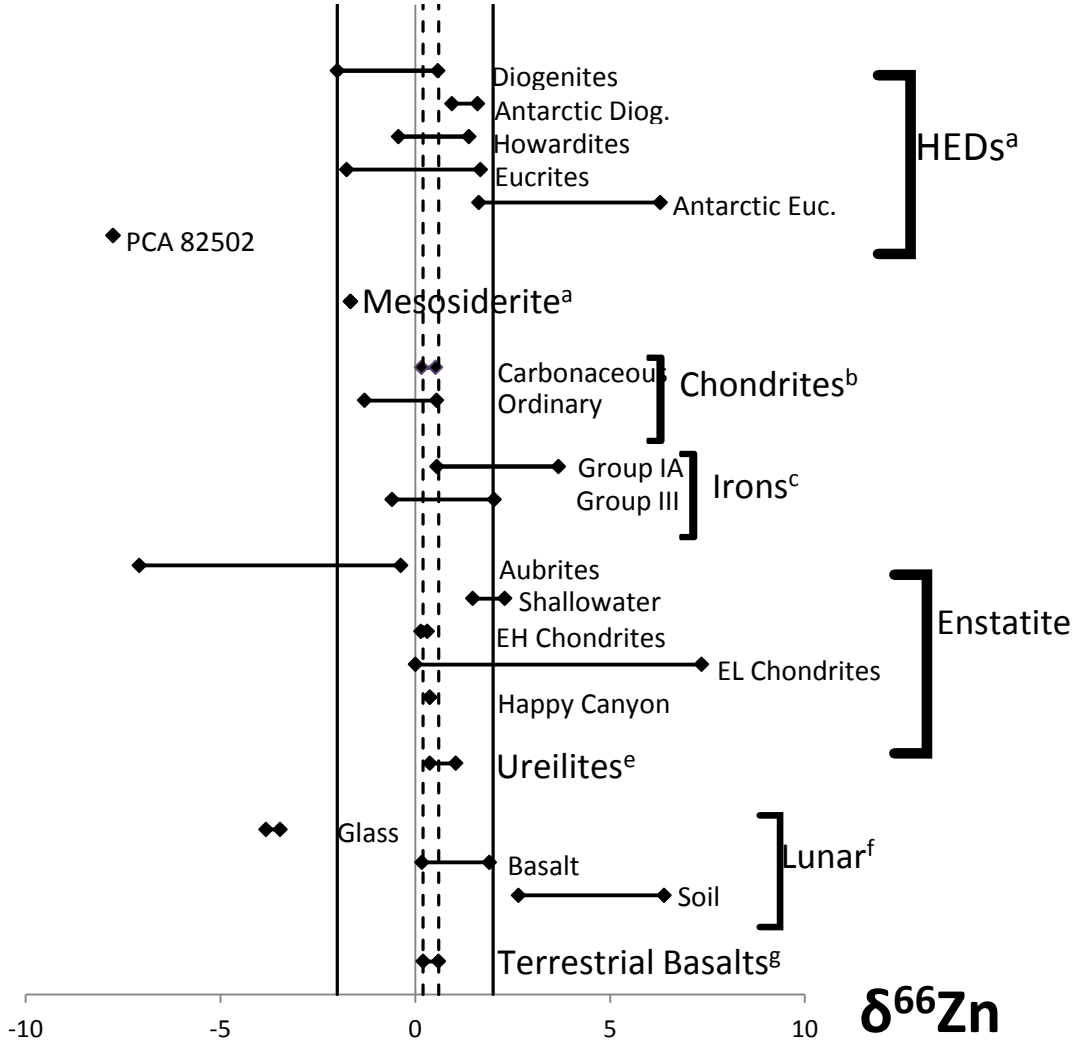

Figure 2. δ^{66}Zn ranges for different group of meteorites, lunar samples and terrestrial igneous rocks. Vertical broken lines show the range for terrestrial basalts, +0.2 to +0.6 ‰; solid lines represent the heterogeneity range of non-Antarctic HEDs, 0 ± 2 ‰.

References: a – this work; b– Luck et al. 2005; Moynier et al. 2007; c – Luck et al. 2005 ; d – Paniello et al. 2009, Moynier et al. 2010; e – Moynier et al. 2010; f – Moynier et al. 2006, Herzog et al. 2009; g – Ben Othman et al. 2003, 2006; Cloquet et al. 2008; this study.

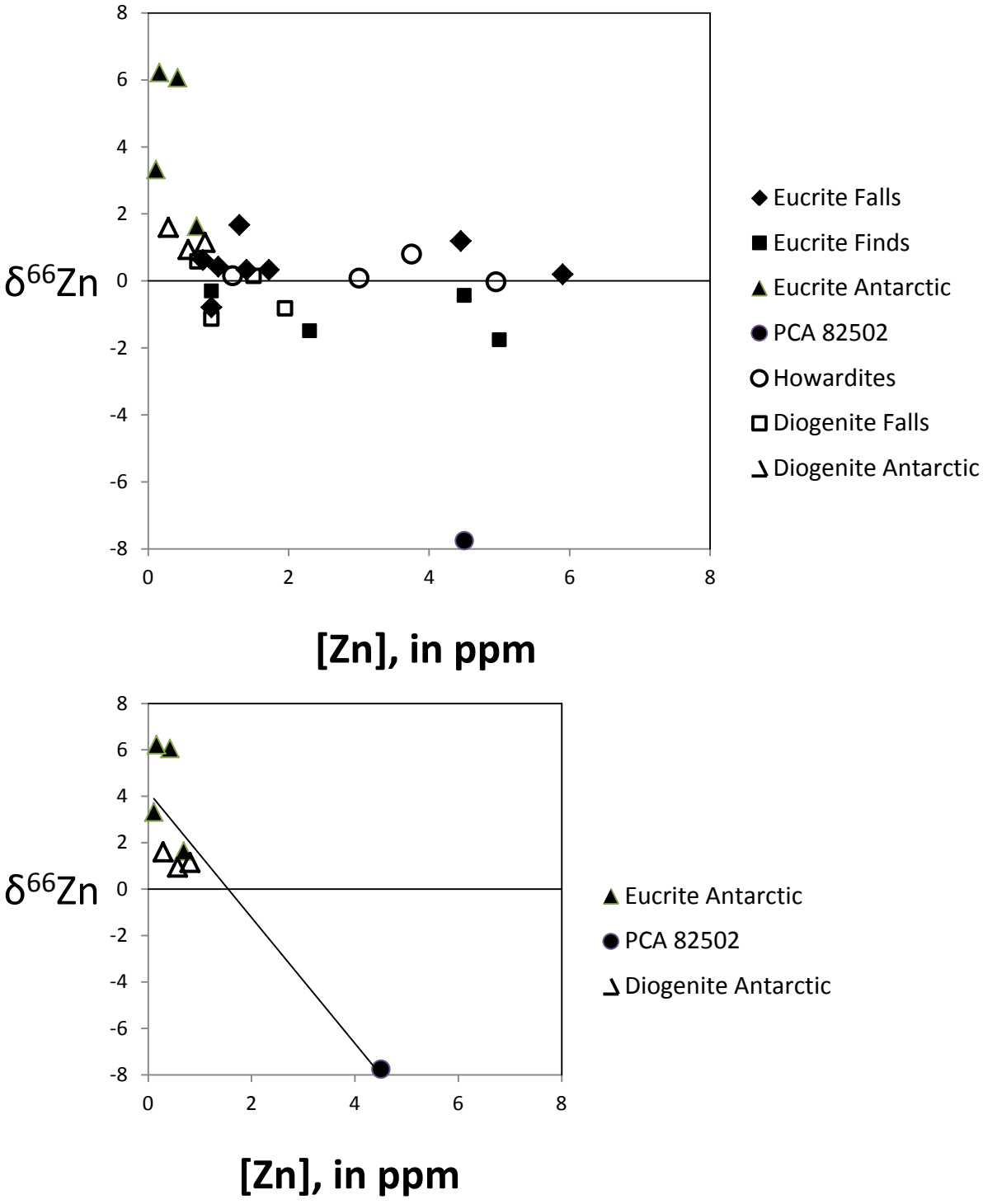

Figure 3. $\delta^{66}Zn$ values as a function of Zn concentration. Overall, no correlation was found (upper plot); but a loose correlation (R^2=0.8271) was seen among the Antarctic meteorite samples (lower plot).

Table 1. Zinc isotope measurements for HED meteorites and terrestrial standards.

Class	Name	Split	type	f/f	δ^{66}Zn	δ^{68}Zn	[Zn]	mass
Eucrites					‰	‰	ppm	mg
Falls	Béréba	MNHN 1297CPE	mm	Fall	1.67	3.40	1.30	242
	Jonzac	NMV A419	mm	Fall	0.33	0.74	1.40	460
	Juvinas	MNHN 40PE2	mm	Fall	0.06	0.17	2.50	300
	Matrix 1	MNHN	mm	Fall	0.30	0.72	2.30	~2000
	Matrix 2	MNHN	mm	Fall	0.37	0.86	0.70	~2000
	Clast 1	MNHN	mm	Fall	0.39	1.02	1.50	~2000
	Clast 2	MNHN	mm	Fall	0.57	1.22	2.90	~2000
	Clast 3	MNHN	mm	Fall	0.31	0.85	1.20	~2000
	Mean - Juvinas				0.33	0.81		
	Millbillillie	WAM 13357.3	mm	Fall	-0.79	-1.37	0.90	323
	Pasamonte chip 1	ASU 197g	pm	Fall	0.05	0.14	6.70	813
	Pasamonte chip 2	ASU 197g	pm	Fall	-0.81	-1.58	8.90	320
	Pasamonte chip 3	USNM 897	pm	Fall	1.35	2.57	2.10	975
	Mean - Pasamonte				0.20	0.38		
	Serra de Magé	MNHN 1560PE	cm	Fall	0.62	1.28	0.78	296
	Sioux County chip 1	NHM BM.1959,1029	mm	Fall	1.11	2.41	1.30	249
	Sioux County chip 2	NHM BM.1959,1029	mm	Fall	0.90	1.88	0.80	437
	Sioux County chip 3	ASU 198.3	mm	Fall	-0.73	-1.49	0.90	346
	Mean - Sioux County				0.43	0.93		
	Stannern chip 1	NMV	mm	Fall	1.42	2.90	1.00	334
	Stannern chip 2	MNHN 4027PE1	mm	Fall	0.95	2.05	7.80	290
	Mean - Stannern				1.19	2.48		
	Mean - Eucrite falls (n=8)				0.50	1.08		
Finds Non-Antarctic	Bouvante	MNHN 3223PE	mm	Find	-1.76	-3.33	5.00	235

	Camel Donga	WAM 13715	mm	Find	-0.30	-0.26	0.90	356
	Palo Blanco Creek	UNM	mm	Find	-1.49	-2.70	2.30	396
	Pomozdino		mm	Find	-0.43	-0.65	4.50	72
	Mean - Non-Antarctic Eucrite finds (n=4)				-1.00	-1.74		
Antarctic	PCA 82502	NASA, .97	unbr	Find	-7.75	-15.14	4.50	414
	GRA 98098 chip 1	NASA, .55	unbr	Find	5.84	11.75	0.46	530
	GRA 98098 chip 2	NASA, .55	unbr	Find	6.29	12.54	0.39	470
	Mean - GRA 98098				6.06	12.15	0.42	
	QUE 97014	NASA, .31	unbr	Find	1.63	3.33	0.69	557
	BTN 00300	NASA, .13	unbr	Find	3.32	7.12	0.11	575
	EET 90020	NASA, .51	unbr	Find	6.22	12.45	0.16	611
	*Mean - Antarctic Eucrite finds (n=4)**				4.31	8.76		
	*Mean - All Eucrite finds (n=8)**				1.66	3.51		
	*Mean - All non-Antarctic Eucrites (n=12)**				*0.00*	*0.14*		
Mean - All Eucrites (n=16)*					***1.08***	***2.30***		
± 2 SE					***1.17***	***2.32***		
Howardites	Kapoeta chip 1	NHM BM.1946,141	pm	Fall	-0.43	-0.68	1.90	169
	Kapoeta chip 2	NHM BM.1946,141	pm	Fall	0.38	0.77	8.00	546
	Mean - Kapoeta				-0.03	0.05		
	LeTeilleul	MNHN 711PE	pm	Fall	0.09	0.21	3.00	218
	Pavlovka chip 1	MNHN 2698PE	pm	Fall	0.22	0.63	3.00	261
	Pavlovka chip 2	MNHN 2698PE	pm	Fall	1.38	3.04	4.50	77
	Mean - Pavlovka				0.80	1.84		
	Petersburg		pm	Fall	0.16	0.38	1.20	511
Mean - All Howardites (n=4)					***0.26***	***0.62***		
± 2 SE					***0.37***	***0.82***		
Diogenites								
Falls	Aioun el Atrouss chip 1	FMNH Me2778#3	pm	Fall	-2.00	-3.81	0.80	396
	Aioun el Atrouss chip 2	ASU 1058f	pm	Fall	0.36	0.75	3.10	824

	Mean - Aioun el Atrouss				-0.82	-1.53		
	Johnstown	AMNH	mm	Fall	0.58	1.17	0.70	491
	Shalka	NMV	mm	Fall	0.15	0.31	1.50	529
	Tatahouine	FMNH Me2651#10	unbr	Fall	-1.13	-1.94	0.90	839
	Mean - Diogenite falls (n=4)				*-0.31*	*-0.50*		
Antarctic	ALHA 77256	NASA, .167	unbr	Find	1.15	2.34	0.81	586
(an)	GRO 95555	NASA, .43	unbr	Find	1.60	3.32	0.29	524
(oliv)	MIL 07001	NASA, .29	unbr	Find	0.94	1.91	0.57	590
	Mean - Antarctic Diogenite finds (n=3)				1.23	2.52		
	Mean - All Diogenites (n=7)				**0.35**	**0.80**		
	± 2 SE				***0.77***	***1.49***		
HEDs	***Mean - All HEDs (n=27)****				***0.77***	***1.66***		
	± 2 SE				***0.72***	***1.44***		
	Mean - non-Antarctic HEDs (n=20)				***-0.01***	***0.11***		
	± 2 SE				***0.39***	***0.75***		
	Mean - Antarctic HEDs* (n=7)				***2.99***	***6.09***		
	± 2 SE				***1.73***	***3.45***		
Mesosiderite	Estherville	UNM		Fall	-1.66	-2.97	0.80	405
Geostandards	GIT-IWG BE-N		Basalt		0.32	0.79		100
	USGS G-2		Granite		0.30	0.57		101

$\delta^{66}Zn$ and $\delta^{68}Zn$ measurements in per mil (‰). Zn concentrations in ppm.

*PCA 82502 excluded from Eucrite means.

Samples were generously provided by the following collections: Meteorite Working Group, NASA, Houston (8); Museum National D'Histoire Naturelle, Paris (MNHN, 7 samples including the powders prepared by Barrat); Arizona State University (ASU, 3); Naturhistorisches Museum, Vienna (NMV, 3); Natural History Museum, London (NHM)(BM, 2); Field Museum of Natural History, Chicago (FMNH, 2); Western Australian Museum, Perth (WAM, 2); University of New Mexico (UNM, 2); Smithsonian Institution, Washington D.C. (USNM, 1); American Museum of Natural History, New York (AMNH, 1).

5. Ordinary Chondrites (OCs)

Manuscript citation: Paniello RC, Moynier F. Zinc isotopic variations in ordinary chondrites. (submitted to *Geochimica et Cosmochimica Acta*, under review. The final published version may differ subject to the editorial and revision process.)

Introduction

The OCs comprise the vast majority of meteorites in the worldwide collection, accounting for more that 87% of all specimens. The parent bodies of these meteorites are not known with certainty, but it is highly likely that there are many. The Hayabusa spacecraft collected dust particles and spectra from near-earth S-type asteroid 25143 Itokawa, and found it was chemically, mineralogically, and spectrally identical to LL5 or LL6 ordinary chondrites (Nakamura 2011). Gaffey and Gilbert (1998) found spectral evidence supporting S-type asteroid 6 Hebe as the parent body for the H chondrites. Nesvorny et al. (2009) identified a link between L chondrites and a group of asteroid fragments called the Gefion family. The compositional differences among the three major subtypes (H, L, and LL) suggest that there must be at least three parent bodies, but the large number of meteorites would imply many more.

OCs have been found to exhibit a range of metamorphic changes likely induced by thermal or shock exposures. A rating scale was first proposed by Van Schmus and Wood (1967) and remains in common use. By this scale, a grade of 3 is considered the least metamorphosed sample; such specimens are frequently called “unequilibrated” ordinary chondrites (UOCs). Within grade 3, a series of subgrades (3.0 through 3.9) have also been defined. Grades of 4 through 6 (or maybe 7) represent increasing degrees of structural change of olivines and pyroxenes, and are sometimes refered to as equilibrated (EOCs). All of these grades preserve the

original structure of the chondrules; if heating was intense enough to cause a melt, the chondrule structure is lost and the meteorite cannot be classified as a chondrite (Scott 2007). Grades 2 and 1 are used for samples that have undergone aqueous alteration. Table 5-1 shows that there are many more EOCs than UOCs.

	Ant.	Non-Ant.	Falls	Total
OCs	28864	11935	857	40799
H chondrites	12691	5606	358	18297
H3.x	472	406	18	878
H4	3432	1420	61	4852
H5	5237	2402	172	7639
H6	3460	1151	92	4611
Other H	90	227	15	317
L chondrites	11216	5073	403	16289
L3.x	556	374	11	930
L4	698	701	23	1399
L5	3855	1195	82	5050
L6	6038	2479	263	8517
Other L	69	324	24	393
LL chondrites	4957	1256	96	6213
LL3.x	154	205	13	359
LL4	151	176	8	327
LL5	2708	265	19	2973
LL6	1636	478	42	2114
Other LL	308	132	14	440

Table 5-1. Available ordinary chondrites by subtype. Ant. = Antarctic.

REFERENCES

Gaffey MJ, Gilbert SL (1998). Asteroid 6 Hebe: The probable parent body of the H-Type ordinary chondrites and the IIE iron meteorites. *Meteoritics Planet. Sci.* 33, 1281-1295.

Nakamura T, Noguchi T, Tanaka M, and 19 coauthors (2011). Itokawa dust particles: a direct link between S-type asteroids and ordinary chondrites. *Science* 333, 1113-16.

Nesvorný D, Vokrouhlický D, Morbidelli A, Bottke WF (2009). Asteroidal source of L chondrite meteorites. *Icarus* 200, 698–701.

Scott ERD (2007). Chondrites and the protoplanetary disk. *Annu. Rev. Earth Planet. Sci.* 35, 577–620.

Van Schmus WR, Wood JA (1967). A chemical-petrologic classification for the chondritic meteorites. *Geochimica et Cosmochimica Acta* 31: 747–765.

Zinc isotopic variations among ordinary chondrites

Randal C. Paniello

Frederic Moynier

Department of Earth and Planetary Sciences and McDonnell Center for Space Sciences, Washington University in St Louis, One Brookings Drive, St Louis, MO 63130

ABSTRACT

Zinc is a moderately volatile element that may be capable of movement among minerals or even volatization during thermal metamorphism. We obtained high-precision isotopic measurements of zinc by MC-ICP-MS from a suite of 86 ordinary chondrites (OCs), in order to study their variation across the metamorphic range. The samples included 27 LL-, 28 L-, and 31 H-chondrites; 31 of the 86 were non-Antarctic falls, 10 were non-Antarctic finds, and 45 were Antarctic finds. Serial leachates were obtained from the LL3.0 Semarkona, and magnetic (metal), silicate and sulfide fractions were separated in three other samples in order to determine the contributions of each phase to the total zinc budget. Three larger OC samples were broken into several smaller chips and each was measured in order to determine the small-scale homogeneity of the zinc isotopes.

The $\delta^{66/64}$Zn (permil deviation of the ^{66}Zn/^{64}Zn ratio reported against the JMC-Lyon standard) for the entire suite fell within a broad range of ±2.5‰, with a mean of 0.00±0.15‰ (2se, n=86). The range of isotopic ratios for the entire suite of OCs and for each subtype followed a normal distribution curve. There was no significant difference measured between Antarctic and Non-Antarctic samples. Isotopic ratios had a slight trend across subtypes, with LL~L<H. For each subtype, higher metamorphic grade was associated with a small but resolvable increase in Zn isotopic ratios; averaging +0.05‰ per grade for $\delta^{66/64}$Zn for LL, +0.11‰ per grade for L, and +0.22‰ per grade for H. Isotopic ratio trended heavier with decreasing zinc abundance, indicating preferential loss of light isotopes, possibly by volatization, but fractionated significantly less than would be predicted by pure Rayleigh distillation. However, zinc concentration varied only slightly with metamorphic grade and averaged 43-52ppm for all grades. Leachates and phase separates showed that the silicate phases are generally higher in

zinc concentration than the sulfide phases, and are isotopically lighter. This suggests that zinc loss may occur more readily from the sulfide phase than from the silicate phase by volatization, or that the lighter isotopes may preferentially move from the sulfide into the silicate phase during metamorphism or other secondary alteration. On a small (sub-centimeter) scale, these OCs exhibited a high degree of homogeneity. Samples of Tieschitz (H/L3.6) bulk and isolated chondrules were studied, and showed that the chondrules are lower in [Zn] and isotopically lighter than the matrix. An unusual H/L5 Antarctic sample, LAP 031047, was analyzed to determine its volatization history, and the low [Zn] (~1 ppm) and heavy fractionation ($\delta^{66/64}$Zn = +1.26‰) findings support prolonged or repeated heating as proposed by Wittmann et al. (2011).

These data suggest volatization played only a small role in determining the final zinc content of OCs; the similar [Zn] of all OCs rules out major volatization with increasing metamorphism, while the isotopic ratios show a definite small effect. Variations in zinc isotopic ratios probably also reflect pre-accretion nebular processes, and may undergo subsequent further modification by closed-system metamorphic changes in which the zinc moves between phases (from sulfide to silicate) in a mass-dependent process.

1. INTRODUCTION

Among the many classes of meteorites, ordinary chondrites (OCs) are by far the most common, with over 40,000 names in the Meteoritical Society's database of about 47,000. Less than 1,000 of these are observed falls, with the rest finds, largely from the deserts of Antarctica and North Africa. The three subtypes of OCs include H-, L-, and LL- chondrites, indicating relatively high iron, low iron, or low iron and low total metal content, respectively. Within each class, OCs have been further characterized by a metamorphic grading system from 3-6 based on qualitative petrologic properties, with type 3 showing the least and type 6 showing the most metamorphism (Van Schmus and Wood, 1967). (Types 1 and 2 are used to indicate significant aqueous alteration has occurred.) The assignment of grade 7 to some meteorites has been reported but has not been universally accepted.

Zinc is a moderately volatile element (50% condensation temperature = 726K or 453^{o}C, Lodders 2003) that occurs in most rock at concentrations of 20-100 ppm. Processes that produce enough heat to create a melt (accretion, volcanism, impacts) can cause loss of zinc by volatization, resulting in reduced zinc concentration in the residual; and due to preferential loss of isotopically lighter material in the vapor, the residual is isotopically heavier while magmatic processes have not been found to significantly fractionate zinc on Earth (Chen et al. 2013). Rather, zinc fractionation on the order of 1 ‰ or more has been associated only with evaporation events (Paniello et al. 2012, Moynier et al. 2011). And isotopic fractionation during evaporation occurs only from a melt, not during sublimation from a solid (Davis et al. 1990).

Metamorphism in OCs is thought to occur mainly as a secondary, post-accretion, thermal process (e.g., Brearley and Jones, 1998). At temperatures above ~950^{o}C, the Fe-Ni-S structure begins to break down and form a partial melt, at which point individual chondrules can no longer be recognized; thus, chondrites must not have been reheated to this level after their accretion. The source of heat is probably short-lived radioisotope decay (e.g., ^{26}Al). Prolonged heating led to increasing chemical and textural equilibration, which is manifested by changes in olivine and pyroxene crystal structure (Van Schmus and Wood, 1967). Thus, chondrites that spent significant time at temperatures between 450^{o}C and 950^{o}C were hot enough to undergo thermal metamorphosis, to possibly lose some Zn by volatization, but not hot enough to melt.

We have previously used high-precision multi-collector inductively-coupled plasma mass spectrometry (MC-ICP-MS) measurements of the stable isotopes of zinc to investigate the volatization history of several meteorites and other planetary materials (Moynier et al. 2007, 2009; Herzog et al. 2009). A study of ureilites (Moynier et al. 2010) found Zn isotopic fractionation consistent with volatization losses, but at a lower magnitude than predicted by simple Rayleigh distillation, suggesting it occurred in a diffusion-limited regime; it was also seen that shock grade correlated with fractionation, supporting impact heating as a major contributor to the isotopic shifts. Zn isotopic determination in a suite of enstatite chondrites and aubrites (Moynier et al. 2011) showed that the more highly metamorphosed EL6 chondrites were significantly isotopically heavier than EL3, suggesting that volatization during thermal metamorphism was responsible for this difference; however, enstatite achondrites (aubrites) were extremely depleted in Zn and extremely isotopically light, suggesting that aubrites lost most of their Zn and that traces of isotopically light Zn were subsequently added. A study of HED

meteorites (howardites, eucrites and diogenites; Paniello et al. 2012a), presumed to be from 4-Vesta, demonstrated the early crust was isotopically heavy in zinc, but chondritic impactors were likely lighter in zinc, causing the brecciated surface to become lighter despite some Zn loss during the process. Analysis of lunar samples and Martian meteorites (Paniello et al. 2012b) showed the zinc isotopic ratios to be nearly identical on Earth and Mars, but the Moon to be largely depleted of zinc and significantly heavier, providing isotopic evidence in support of a global scale event at the origin of the volatile loss of the Moon, most probably associated with the giant impact theory of the origin of the Moon.

The petrologic variations among OCs are thought to be caused by thermal metamorphism (e.g., Ikramuddin et al. 1977). It stands to reason that moderately volatile elements, such as zinc, might be lost during an open-system thermal process that leads to metamorphic change, and that such a trend might be observed comparing zinc isotopic ratios across the metamorphic range. Zinc might also evaporate differentially from various phases, such as sulfide, silicate, and metal. Alternately, if the metamorphism occurs in a closed system, zinc might be observed to move between phases but stay within the whole rock. These hypotheses were tested in the present study.

Luck et al. (2005) reported Zn isotopic measures in 14 ordinary chondrites (4H, 6L, 4LL). The Zn elemental abundance for all samples ranged from 35-65ppm. The 7 undifferentiated OCs (UOCs, grade 3.x) had $-1.30‰ < \delta^{66/64}Zn < +0.76‰$, while the 6 equilibrated OCs (EOCs) of petrologic grade 6 had $-0.48‰ < \delta^{66/64}Zn < +0.55‰$. There was only one sample of grade 4

($\delta^{66/64}$Zn = +0.26‰) and there were no samples of grade 5. Five of the UOCs were grade 3.6 or higher. The present study was carried out to include a complete representation of all metamorphic grades for H, L and LL.

To address possible phase differences, serial leaching was performed on several samples and zinc isotopes measured from isolated phases. Differences in the metal phases between H, L and LL could potentially result in varying degrees of zinc fractionation despite similar thermal histories. This was evaluated in this project by comparing zinc isotopic ratios among OC subtypes of the same metamorphic grades. We also measured Zn isotopes in whole rock and isolated chondrules from the same meteorite (Tieschitz, H/L3.6); the matrix composition was then determined by mass balance. It was expected that the chondrules would be isotopically lighter than the matrix (e.g., Luck et al. 2005).

Most OCs are thought to be unbrecciated (Binns 1967), although some brecciated OCs have been identified (Welzenbach et al. 2005, Corrigan et al. 2012). It would be expected that samples from unbrecciated meteorites would exhibit a high degree of homogeneity, so that small (< 0.5g) samples could be expected to represent the entire meteorite. The availability of some larger OCs enabled us to test this hypothesis by comparing multiple small chips from larger (3-5g) samples.

2. SAMPLES AND ANALYTICAL METHODS

2.1 Sample Description & Preparation

Small (0.5-1.0 g) meteorite chips were generously provided by several museum collections (NASA-JSC 42; Musee Nationale Histoire Naturele, Paris 15; Smithsonian Institution 5; American Museum of Natural History, New York 4; Arizona State University 4; National Institute of Polar Research, Tokyo 4; Natural History Museum, Vienna 1). Chips were requested from the center of the meteorite whenever possible. ~ One gram chips were washed in water to remove contaminants. Fusion crusts, when present, were carefully removed, and the one gram chip was finely ground with an agate mortar and pestle.

The chemical purification is based on the method used in Moynier et al. (2006). Aliquots of ~200mg of the homogeneous powder were digested with HF/HNO_3 4:1 v/v under a heating lamp (~ 120^{o}C) for 48-72 hours. The dissolved samples were dried and then re-dissolved in 6N HCl for 24 hours, and dried again; this removes the fluorides formed from the HF. All reagents used were of the highest available purity (sub boiled distilled 3 times).

For the isotopic heterogeneity tests, larger chips (~3g) were fractured with a single strike of the pestle against the rock, yielding 4-7 smaller fragments of about 0.5-1.0g each. Each fragment was analyzed for Zn following the method below, in order to determine the Zn homogeneity of the original chip

For the phase separation analysis, the magnetic (metal) fractions of the powdered samples were isolated using a hand magnet. The non-magnetic (silicate + sulfide) fraction was then dissolved in 3N HCl for 6 hours at room temperature to remove the most soluble components (primarily sulfides). The liquid phase was decanted, and the remaining solid was treated with in HF/HNO_3

followed by 6N HCl as described above to dissolve the remaining mass (primarily silicates). The minimal remaining solid (primarily spinel) was removed by centrifuge.

A sample of Semarkona (LL3.0) was previously leached and dissolved in a series of progressively stronger acids for a study of chromium isotopes (Dougherty et al., 1999), aliquots of leftover material from that study were generously provided by its senior author (FAP). Their method was based on a previously reported leaching/dissolution procedure (Rotaru et al. 1992, Podosek et al. 1997).

2.2 Extraction of Zinc

Samples were then re-dissolved in 1.5N HBr. Teflon columns were prepared for anion exchange chromatography, loaded with AG1x8 200-400 mesh, cleaned with 0.5N HNO_3, and pre-loaded with 1.5N HBr. The prepared samples were then loaded onto the column, where the Zn was bound. Non-Zn components were removed from the column with additional 1.5N HBr. The Zn was then recovered from the column with 0.5N HNO_3. The recovered solution was dried under a heat lamp. This sequence was repeated two more times on smaller columns to further purify the Zn. The recovery yield of Zn with this method is >99%, which eliminates the possibility of column fractionation.

2.3 Determination of Zn Isotopic ratios

The final eluent was dissolved in 0.05 HNO_3 for isotopic compositional determination, which was carried out on a Thermo-Finnegan Neptune Plus MC-ICP-MS at Washington University in St Louis. The blank is ~<10 ng. Zn isotopic ratios were expressed as deviations from a standard in part per mil (‰):

$$\delta^{X/64}\text{Zn (‰)} = \left(\frac{\left({}^{x}\text{Zn}/{}^{64}\text{Zn} \right)_{\text{sample}}}{\left({}^{x}\text{Zn}/{}^{64}\text{Zn} \right)_{\text{standard}}} - 1 \right) \times 1000$$

with x = 66, 67 or 68, using the JMC-Lyon Zn standard. The typical analytical uncertainty (2 standard deviations) of our method was discussed in Chen et al. (2013) and is 0.04‰ for $\delta^{66/64}$Zn and 0.05‰ for $\delta^{67/64}$Zn and $\delta^{68/64}$Zn.

The zinc concentration [Zn] for each sample was determined by comparing the voltage on the mass spectrometer at mass 64 with that of a standard of known concentration. The accuracy of this method is estimated at ±10%.

3. RESULTS

The analyses for $\delta^{66/64}$Zn, $\delta^{67/64}$Zn, and $\delta^{68/64}$Zn, and the calculated Zn concentrations [Zn], are listed for all samples in Table 1, along with available literature values for comparison. The $\delta^{66/64}$Zn values ranged from -2.42‰ (Clovis, H3.6) to +2.37‰ (Allegan, H5), with 55/86 (64%) of values falling between ±0.50‰ and 73/86 (85%) of values between ±1.0‰. The range was wider for the H-chondrites than for the other two groups.

The $\delta^{66/64}$Zn and $\delta^{68/64}$Zn results are shown in three-isotope plots in Figure 1. All of the data plot on a line of slope 1.97 (R^2=0.998), consistent with mass-dependent fractionation with no non-mass dependent behavior. Data for each subgroup follow a normal distribution, as shown in the histogram of Figure 2. The Kolmogorov-Smirnov statistic confirms a normal distribution for the entire data set, as well as for each of the six subgroups individually (Antarctic and non-Antarctic groups for each of LL, L and H chondrite classes).

The average values for each meteorite class and the metamorphic subgroups are summarized in Table 2. The mean $\delta^{66/64}$Zn for all samples, excluding the four grade 7s and including the twelve literature values, was exactly 0.00‰, ±0.15‰. The LL and L classes were both significantly lighter than H chondrites, but not different from each other. There also were no significant differences between results for Antarctic and non-Antarctic samples (within 2se).

Comparing petrologic grades in Table 2, in general the undifferentiated OCs (grade 3.x) were isotopically lighter than the differentiated OCs (grades 4-6) for all three classes, with a few exceptions, notably the L4s. Within the undifferentiated group (subgrades 3.0 through 3.9), there was no identifiable trend of isotopic ratios with grade (Figure 3). But if the group means

Table 1. Zinc isotopic measurements and abundances for LL, L, and H chondrites.

Type	Name	Split	Source	f/f	$\delta^{66/64}$Zn ‰	$\delta^{67/64}$Zn ‰	$\delta^{68/64}$Zn ‰	[Zn] ppm	*[Zn] lit. ppm*
	LL Chondrites								
	Non-Antarctic								
3.0	Semarkona*		SI	Fall	-0.33	-0.46	-0.60	81	*75*
3.15	*Bishunpur*[a]			*Fall*	*0.25*	*0.40*	*0.45*		
3.15	*Bishunpur*[b]			*Fall*	*0.26*	*0.39*	*0.44*		
3.2	Krymka			Fall	0.04	0.17	0.13	50	*52*
3.2	*Krymka*[a]			*Fall*	*0.09*	*0.11*	*0.18*		
3.3	Wells	4928	NY	Find	-0.13	-0.17	-0.19	44	
3.6	Parnallee			Fall	-0.32	-0.41	-0.59	59	*60*
3.6	Ngawi			Fall	-0.11	0.03	-0.01	39	*46*
3.8	Beyrout	1510	P	Fall	0.10	0.29	0.33	43	
4	Soko-Banja	712	P	Fall	0.10	0.19	0.26	28	*60*
4	Hamlet		SI	Fall	0.02	0.03	0.06	48	*48*
5	Tuxtuac	3210		Fall	0.14	0.24	0.31	37	
5	Olivenza		P	Fall	-0.18	-0.26	-0.30	50	*50*
5	*Olivenza*[b]			*Fall*	*-0.12*	*-0.18*	*-0.16*		
6	Cherokee Springs		SI	Fall	0.61	1.00	1.29	35	
6	St. Severin	2397	P	Fall	-0.38	-0.54	-0.73	45	*47*
6	*St. Severin*[a]			*Fall*	*-0.40*	*-0.62*	*-0.85*		
7	Uden			Fall	0.59	0.89	1.14		
	Antarctic								
3.2	Y790448	,116	NIPR	Find	0.06	0.09	0.13	50	
3.3	ALH 83010	,38	NASA	Find	-0.37	-0.41	-0.62	105	
3.4	ALH 84126	,19	NASA	Find	0.53	1.02	1.19	102	
3.5	ALHA 78119	,33	NASA	Find	-0.63	-0.82	-1.17	48	

3.6	DAV 92302	,8	NASA	Find	-0.67	-0.92	-1.24	108	
3.7	EET 83213	,74	NASA	Find	-0.37	-0.45	-0.61	36	
3.8	LAR 06301	,6	NASA	Find	-0.50	-0.68	-0.90	77	
4	WIS 91618	,20	NASA	Find	0.00	0.11	0.08	56	
4	LAP 02266	,9	NASA	Find	-0.38	-0.56	-0.71	50	
5	RBT 04127	,5	NASA	Find	0.98	1.62	2.06	125	
5	DOM 03194	,5	NASA	Find	0.21	0.39	0.46	44	
6	PRA 04422	,6	NASA	Find	0.11	0.28	0.34	64	
6	LAR 06250	,5	NASA	Find	0.26	0.48	0.60	39	
7	Y791067	,85	NIPR	Find	-2.06	-3.01	-4.02	47	
	L Chondrites								
	Non-Antarctic								
3.2	Gunlock	4620	NY	Find	0.64	1.00	1.28	51	
3.4	Hallingeberg			Fall	-0.21	-0.20	-0.31	49	*57*
3.5	Ioka		SI	Find	-0.26	-0.29	-0.36	44	
3.6	Khohar	1274	P	Fall	-0.30	-0.43	-0.58	41	*46*
3.6	*Khohar*[a]			*Fall*	*-0.03*	*-0.05*	*0.08*		
3.6	*Julesburg*[a]			*Find*	*0.74*	*1.05*	*1.41*		
3.7	Mezo-Madaras			Fall	-0.17	-0.23	-0.29	58	*52*
3.8-an	*Moorabie*[a]			*Find*	*-1.30*	*-1.94*	*-2.63*		
4	Barratta			Find	-1.03	-1.43	-1.93	55	
4	Saratov	4414	NY	Fall	-1.14	-1.72	-2.23	51	*62*
4	*Bjurbole*[a]			*Find*	*0.26*	*0.38*	*0.49*		
5	Tadjera	561	P	Fall	0.75	1.20	1.57	45	*83*
5	*Ausson*[b]			*Fall*	*-0.42*	*-0.60*	*-0.80*		
5-6	*Mocs*[a]			*Fall*	*0.10*	*0.18*	*0.21*		
6	L'Aigle	9	P	Fall	0.41	0.68	0.88	14	*46*

6	Voille	148	P	Fall	-0.10	-0.12	-0.16	31	*53*
6	Air	2025	P	Fall	0.64	1.01	1.34	27	*54*
6	*Granes*[a]			*Fall*	*-0.47*	*-0.72*	*-1.03*		
6	*Tiberrhamine*[a]			*Find*	*0.15*	*0.22*	*0.35*		
	Antarctic								
3.0	QUE 97008	,45	NASA	Find	0.24	0.43	0.52	40	
3.05	MET 00452	,20	NASA	Find	0.01	0.05	0.08	42	
3.1	LEW 86018	,69	NASA	Find	0.01	0.09	0.10	95	
3.2	GRO 95502	,28	NASA	Find	-0.94	-1.35	-1.77	81	
3.3	GRO 95536	,13	NASA	Find	-0.37	-0.46	-0.64	64	
3.4	ALHA 81030	,46	NASA	Find	-0.10	-0.13	-0.19	42	
3.5	MET 96515	,11	NASA	Find	0.05	0.21	0.21	108	
3.6	GRO 06054	,9	NASA	Find	-0.16	-0.16	-0.22	43	
3.7	ALH 90411	,34	NASA	Find	-0.75	-1.05	-1.41	53	
3.8	ALHA 77215	,39	NASA	Find	-0.28	-0.33	-0.49	43	
4	LAP 03554	,8	NASA	Find	-0.62	-0.81	-1.15	109	
4	ALH 85033	,41	NASA	Find	-1.31	-1.91	-2.55	43	
5	LAP 03687	,4	NASA	Find	-0.79	-0.94	-1.40	54	
5	GRO 95540	,8	NASA	Find	0.71	1.15	1.43	63	
6	ALHA 76001	,22	NASA	Find	0.17	0.44	0.45	89	
6	GRA 98118	,7	NASA	Find	0.31	0.33	0.68	53	
7	PAT 91501	,119	NASA	Find	0.43	0.64	0.88	43	
	H Chondrites								
	Non-Antarctic								
3.4	Sharps			Fall	-0.07	0.00	-0.03	50	*38*
3.4	Roosevelt	1027	ASU	Find	-0.40	-0.58	-0.75	35	
3.5	Frenchman Bay		SI	Find	-0.10	-0.11	-0.16	45	

3.6	Clovis 1			Fall	-2.42	-3.52	-4.65	53	
3.7	Grady (1937)	373	ASU	Find	0.98	1.59	1.99	35	
3.7	*Brownfield 1937*[a]			*Find*	*-0.30*	*-0.49*	*-0.57*		
3.7	*Brownfield 1937*[c]			*Find*	*-0.31*			*63*	
3.8	Flagler	1549	ASU	Find	0.48	0.77	0.97	49	
3.8	NWA 096	1429	ASU	Find	-0.05	-0.05	-0.08	86	
3.8	Dhajala*	3146		Fall	-0.36	-0.52	-0.71	40	*44*
3.8	*Dhajala*[a]			*Fall*	*0.10*	*0.31*	*0.14*		
3.8	*Dhajala*[b]			*Fall*	*0.10*	*0.30*	*0.16*		
4	Phum Sambo*		P	Fall	-0.10	-0.09	-0.12	36	
4	Ste. Margueritte	2396	P	Fall	2.24	3.42	4.48	32	
4	*Ochansk*[b]			*Fall*	*0.42*	*0.63*	*0.80*		
5	Allegan			Fall	2.37	3.52	4.68	17	*38*
5	Pultusk	1436	P	Fall	1.09	1.68	2.18	40	*69*
5	Agen	139	P	Fall	0.70	1.11	1.48	32	
5	Forest City	2421	NY	Fall	-0.03	-0.05	-0.06	33	
5	*Plainview*[c]			*Find*	*0.62*			*26*	
6	Kernouve	602B	P	Fall	0.23	0.34	0.52	49	*47*
6	Lancon	1108	P	Fall	0.33	0.57	0.70	37	
6	*Charsonville*[a]			*Fall*	*0.53*	*0.81*	*0.98*		
6	*Kernouve*[a]			*Fall*	*0.52*	*0.83*	*0.94*		
6	*Kernouve*[b]			*Fall*	*0.52*	*0.84*	*0.96*		
	Antarctic								
3.0	A881258	NIPR	,81	Find	-0.17	-0.24	-0.32	37	
3.3	WSG 95300	NASA	,59	Find	0.27	0.52	0.64	102	
3.4	QUE 97030	NASA	,11	Find	-0.56	-0.72	-1.04	31	
3.6	QUE 93030	NASA	,37	Find	-1.09	-1.46	-2.01	94	
3.7	GRA 95208	NASA	,18	Find	-0.04	0.24	0.07	158	
3.8	GRA 98050	NASA	,13	Find	0.59	0.96	1.23	75	

4	QUE 99018	NASA	,13	Find	-0.03	0.13	0.06	81
4	ALH 84103*	NASA	,11	Find	-0.43	-0.59	-0.79	43
4	DOM 03206	NASA	,7	Find	-0.86	-1.26	-1.64	37
5	LAR 06392	NASA	,4	Find	-0.72	-1.11	-1.36	44
5	LEW 85320*	NASA	,45	Find	1.75	2.69	3.51	49
6	LAP 02341	NASA	,8	Find	-0.27	-0.35	-0.48	38
6	MIL 07163	NASA	,5	Find	1.60	2.50	3.33	45
7	A880844*	NIPR	,46	Find	-1.19	-1.69	-2.29	23
	Others							
H/L3.6	Tieschitz Chondrules			Fall	-0.58	-0.65	-1.03	29
H/L3.6	Tieschitz Bulk	MNHV		Fall	-0.24	-0.36	-0.47	31
H/L 5	LAP 031047	NASA	,12	Find	1.26	2.23	2.80	1

References

a. Luck et al 2005

b. Moynier et al 2007

c. Ghidan and Loss 2011

* Isotope results shown are averages of 2 or more chips separately analyzed.

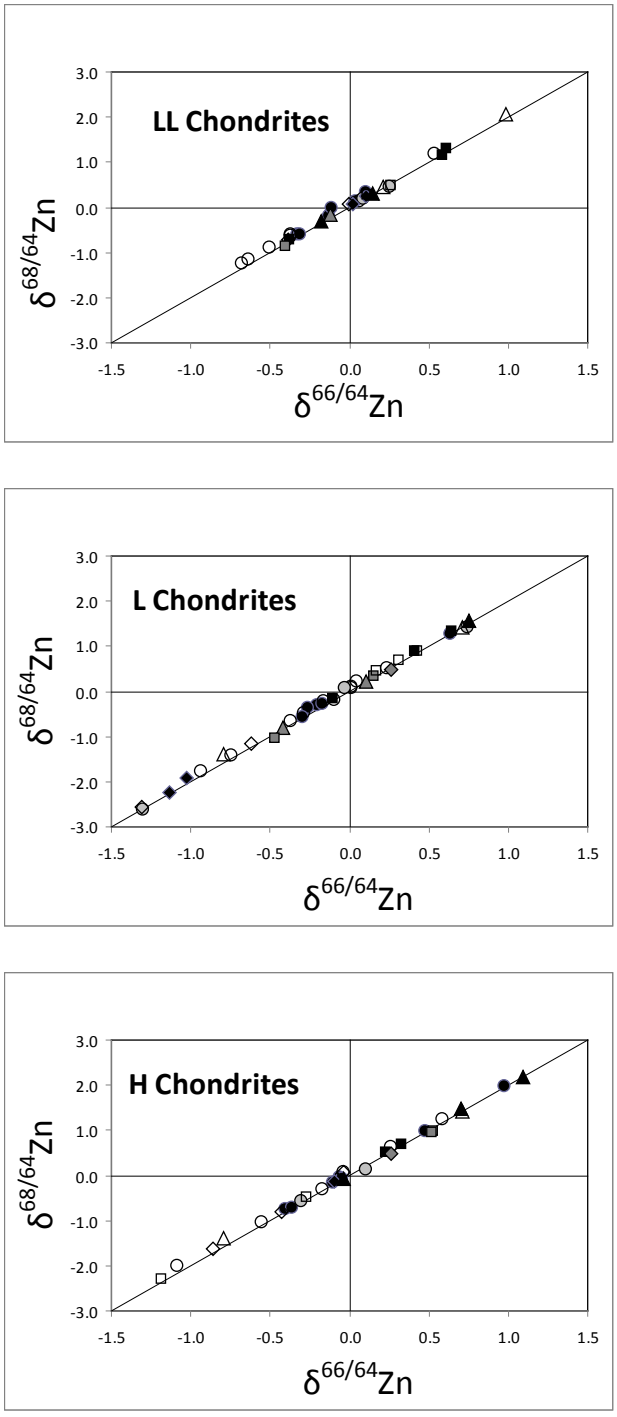

Figure 1. Three-isotope plots of Zn isotope ratios for LL, L and H chondrites.

All values plot on a line of slope ~2, indicating mass-dependent fractionation.

Black symbols, non-Antarctic samples; open symbols, Antarctic samples; grey symbols, reference samples (all non-antarctic). Circles, metamorphic grade 3.x (undifferentiated); diamonds, grade 4; triangles, grade 5; squares, grades 6-7.

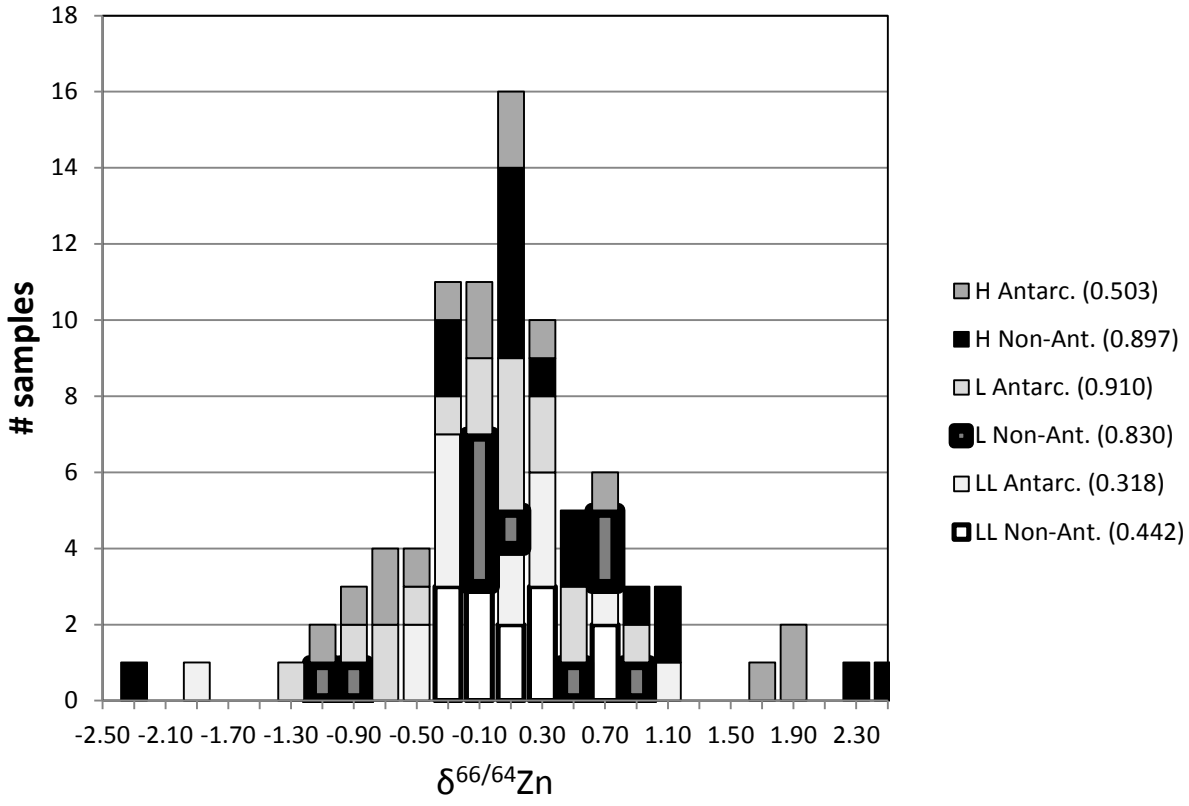

Figure 2. Histogram of $\delta^{66/64}$Zn values for all ordinary chondrites studied. Shown in parentheses are the Kolmogorov-Smirnov significance statistics for each subgroup. The K-S significance statistic for the entire suite of data is 0.346, indicating a normal distribution.

Table 2. Summary of group mean $\delta^{66/64}$Zn values.

	Non-Antarctic			Antarctic			Total		
	N	$\delta^{66/64}$Zn	± 2 SE	n	$\delta^{66/64}$Zn	± 2 SE	n	$\delta^{66/64}$Zn	± 2 SE
LL Chondrites[a]									
LL3.x	7	-0.07	0.16	7	-0.28	0.17	14	-0.17	0.18
LL4	2	0.06	0.08	2	-0.19	0.38	4	-0.07	0.19
LL5	2	-0.02	0.32	2	0.60	0.77	4	0.29	0.49
LL6	2	0.11	0.99	2	0.19	0.15	4	0.15	0.82
LL4-6	6	0.05	0.27	6	0.20	0.37	12	0.12	0.22
LL falls	12	0.00	0.28						
All LL	13	-0.01	0.15	13	-0.06	0.27	26	-0.04	0.15
L Chondrites[b]									
L3.x	7	-0.12	0.51	10	-0.23	0.23	17	-0.18	0.50
L4	3	-0.63	0.90	2	-0.96	0.69	5	-0.77	0.56
L5	3	0.14	0.68	2	-0.04	1.50	5	0.07	0.61
L6	5	0.13	0.39	2	0.24	0.14	7	0.16	0.27
L4-6	11	-0.08	0.38	6	-0.25	0.63	17	-0.14	0.32
L falls	11	-0.08	0.54						
All L	18	-0.09	0.30	16	-0.24	0.26	34	-0.16	0.20
H Chondrites[c]									
H3.x	9	-0.25	0.62	6	-0.17	0.49	15	-0.22	0.79
H4	3	0.86	1.42	3	-0.44	0.48	6	0.21	0.89
H5	5	0.95	0.80	2	0.51	2.46	7	0.83	0.79
H6	3	0.36	0.18	2	0.66	1.87	5	0.48	0.69
H4-6	11	0.76	0.50	7	0.15	0.81	18	0.52	0.96
H falls	12	0.38	1.19						
All H	20	0.31	0.45	13	0.00	0.48	33	0.19	0.33

All Ordinary Chondrites	93	0.00	0.15

All LL-, L-, and H- 7's excluded (4 total samples).

a. Includes 1 literature value.

b. Includes 7 literature values.

c. Includes 4 literature values.

Each meteorite is represented only once in group means. Data from this study used when available.

Where multiple literature values are listed in Table 1, only the first value was used.

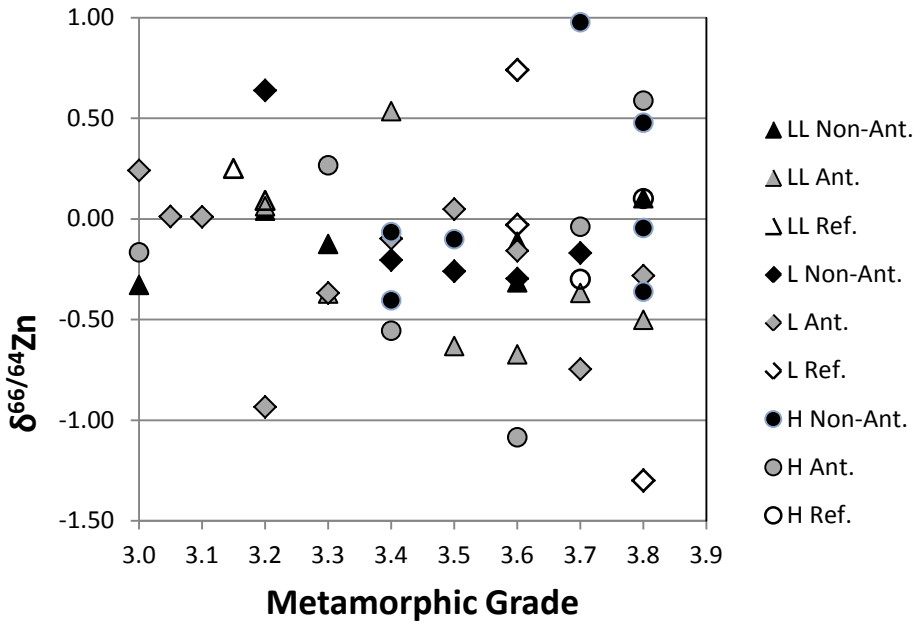

Figure 3. Isotopic ratio ($\delta^{66/64}$Zn) variability with metamorphic grade for undifferentiated OCs (grade 3.x), including non-Antarctic (black), Antarctic (gray), and reference (open) values. There was no significant trend identified for isotopic ratio across metamorphic grades (R^2<0.5). (Datum for Clovis, H3.6, $\delta^{66/64}$Zn = -2.42, is off-scale).

of the isotopic ratios are plotted against metamorphic grade (Figure 4), there is a small but resolvable increase in $\delta^{66/64}$Zn with good correlation coefficients (R^2~0.9 for LL, L and H, with one mean value omitted for each regression line). The slopes of these lines (in ‰ units per grade) are +0.05, +0.11, and +0.22 for LL, L and H, respectively. These findings are consistent with preferential loss of light isotopes with increasing metamorphism. Calculating similar slopes from data in Luck et al. (2005) for grades 3 and 6 (only) gives values of -0.20, +0.11, and +0.21 ‰ per grade for LL, L and H, respectively, providing good agreement for L and H but not for LL.

Zinc concentration in the meteorite samples is shown in Table 1, and plotted in Figure 5. There were no significant differences in [Zn] among the three OC classes. There was a general correlation of heavier isotope ratios with lower [Zn] (see trendlines in Figure 5), but the correlation coefficient R^2 was < 0.5 for all three classes. This trend is consistent with Zn loss by volatization. Zinc concentration did not differ across petrologic grade (Figure 6), with [Zn] petrologic grade averages of 46-55 ppm for LL, 49-66 ppm for L, and 45-51 ppm for H chondrites.

For samples that had major element concentrations available in the literature, the measured [Zn] was normalized to these values for [Al] and [Cr] and plotted against $\delta^{66/64}$Zn in Figure 7. It can be seen that the undifferentiated OCs are clustered in a small region of the plot, while the higher grade samples are spread out over a wider range of variability. This may indicate more variable thermal and chemical histories as the parent bodies undergo differentiation and metamorphism. Among the meteorite classes, the H chondrites seem to trend slightly lighter,

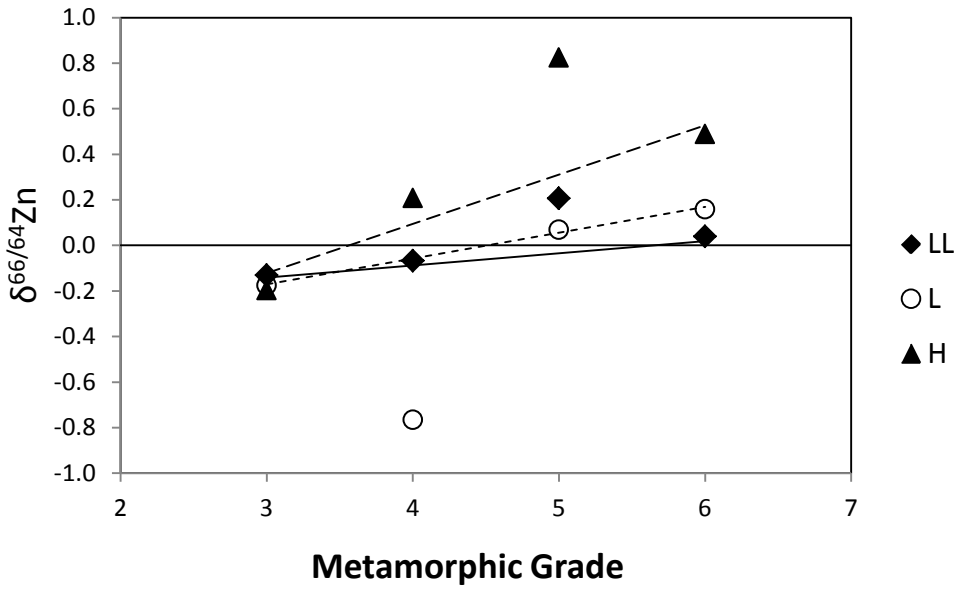

Figure 4. Mean isotopic ratios ($\delta^{66/64}$Zn) for LL, L and H chondrites by metamorphic grade. There is a small but resolvable increase in isotope ratio with increasing grade. For LL (solid line), the slope is +0.05‰/grade (R^2=0.893); for L (small dashes), the slope is +0.11‰/grade (R^2=0.995); for H (large dashes), the slope is +0.11‰/grade (R^2=0.916). (One datum is omitted from each regression line.)

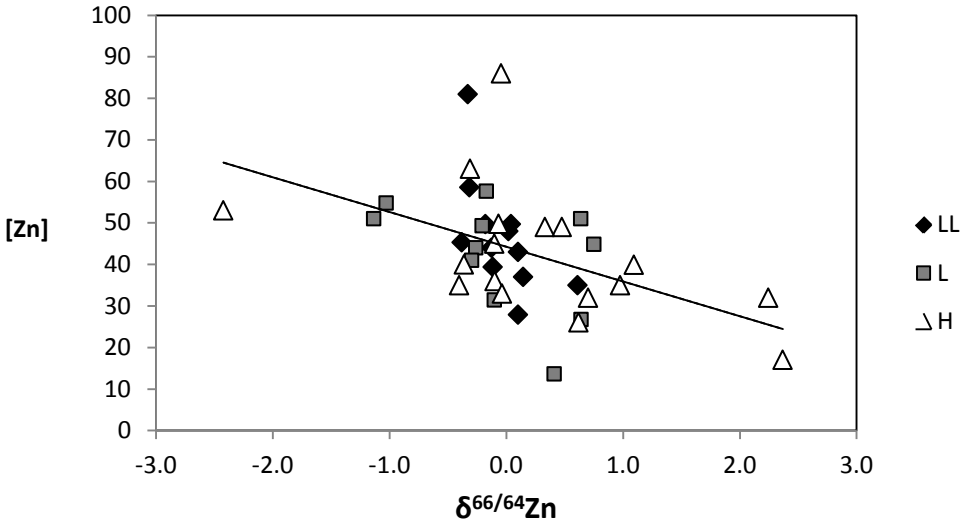

Figure 5. Zinc concentration correlated with isotopic fractionation. There is a general trend of lower [Zn] with heavier isotopic ratio (R^2 <0.5).

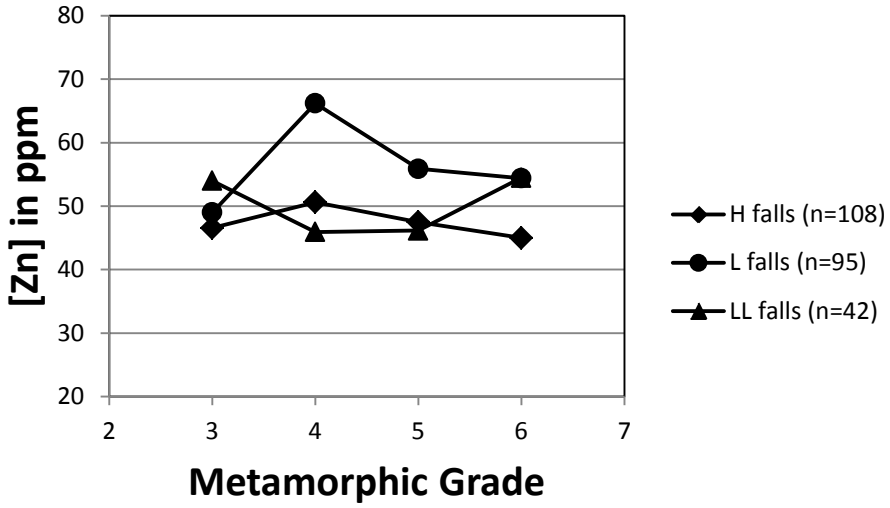

Figure 6. [Zn] compared across metamorphic grade. Results shown include data for OC falls (only) from this study (n=11, 8, and 12 for H, L and LL) and literature values from Metbase 7.3 (n=97, 87 and 30).

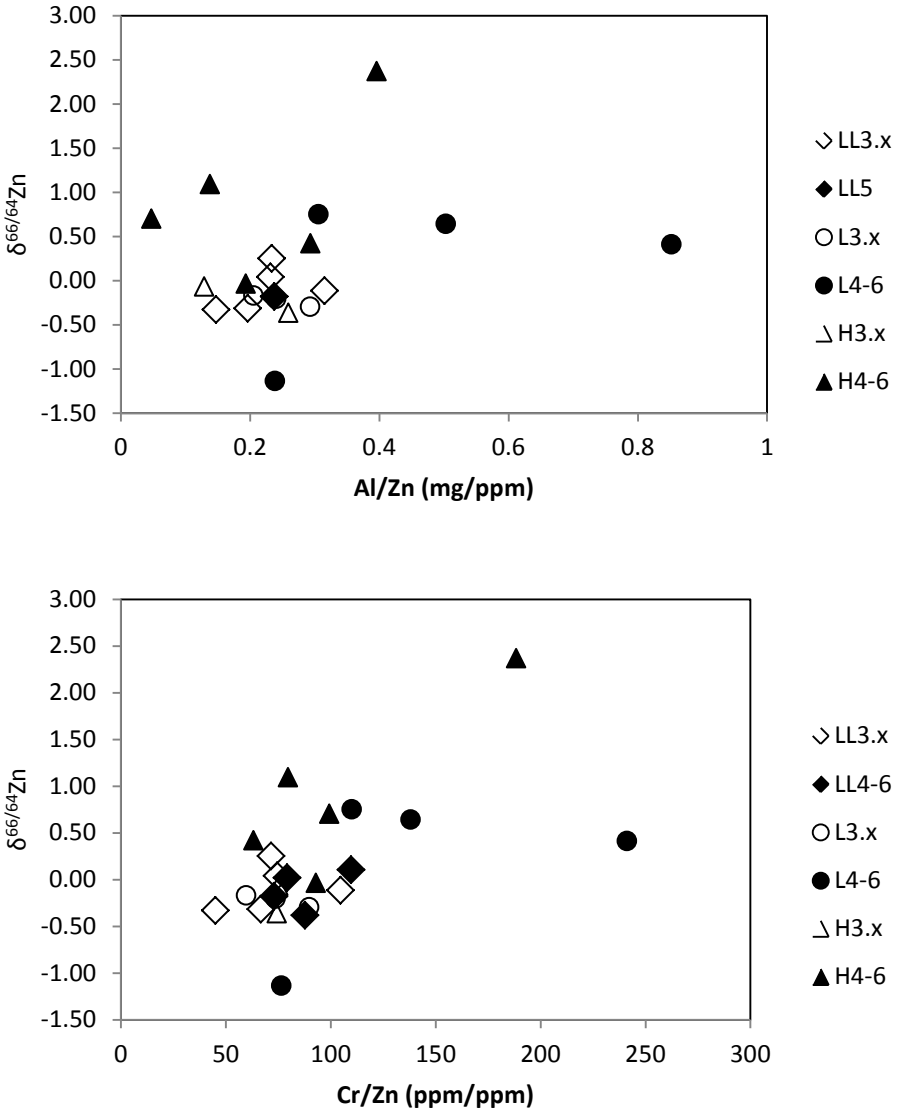

Figure 7. Zn isotopic ratio as a function of [Zn], normalized to major elements Al (top) and Cr (bottom). Open symbols are undifferentiated OCs, solid symbols are petrologic grades 4-6. The $\delta^{66/64}$Zn and [Zn] measurements are from this study; the [Al] and [Cr] are literature values.

with slightly lower [Zn], than L or LL chondrites. These correlations agree well with data from Luck et al. (2005), except that the present data encompass a wider range of values.

The meteorite's isotopic homogeneity was evaluated by determining the fractionation of several smaller chips freshly fractured from larger (1.6 – 3.1 g) samples (Table 3). One sample each of LL5, L5, and H5 was analyzed. The resulting chips measured several millimeters in each dimension, thus providing an estimate of the small-scale (sub-centimeter) zinc isotopic variability. As seen in Table 3 and Figure 8, all three sample chips exhibited a high degree of homogeneity in both zinc concentration and isotopic fractionation.

Six samples were separated into metal (magnetic), sulfide and silicate phases. The results are shown in Table 4. It was found that in each of these meteorite chips (except Clovis), the silicate portion comprised a higher mass fraction than the sulfide portion, and also had a higher [Zn]; thus, the major fraction of the Zn was hosted in the silicate. Metal comprised a small portion of the mass and was generally much lower in zinc content than the silicate or sulfide. Five of the six chips showed the sulfide component to be isotopically heavier than the silicate; this was most pronounced in the LL5 sample (RBT 04127). The mass balance isotope calculation, in which the measured fractionations of the metal, silicate and sulfide phases were combined using a weighted average based on their [Zn], compared favorably with the actual whole rock (WR) isotope measurements, suggesting the high-precision ICP-MS values and mass determinations were reasonably accurate and self-consistent. The finding that the sulfide phase has lower [Zn] and is isotopically heavier than the silicate phase suggests that zinc may be lost preferentially from the sulfide phase by volatization, or that the lighter isotopes may move from the sulfide

Table 3. Heterogeneity of three Antarctic OC samples.

	mass	d66/64	d67/64	d68/64	[Zn]
	mg	‰	‰	‰	ppm
LEW 85320 (H5)					
original	3095				
L1	513	1.77	2.69	3.54	66
L2	584	1.61	2.52	3.32	42
L3	267	1.78	2.73	3.54	66
L4	307	1.83	2.78	3.64	67
L5	410	1.81	2.74	3.59	67
L6	516	1.87	2.85	3.73	69
L7	498	1.79	2.70	3.56	61
mean		1.78	2.72	3.56	62.6
± 2 SE		0.08	0.10	0.13	9.4
GRO 95540 (L5)					
original	3149				
G1	657	0.59	0.91	1.20	54
G2	387	0.51	0.79	1.06	65
G3	652	0.40	0.58	0.89	51
G4	961	0.43	0.69	0.90	54
G5	492	0.54	0.88	1.13	46
mean		0.49	0.77	1.03	54.0
± 2 SE		0.08	0.14	0.14	7.0
DOM 03194 (LL5)					
original	1682				
D1	392	0.14	0.21	0.30	38
D2	563	-0.10	-0.08	-0.12	58
D3	277	-0.02	0.04	0.02	58
D4	450	0.02	0.07	0.13	57
mean		0.01	0.06	0.08	52.8
± 2 SE		0.10	0.12	0.18	9.8

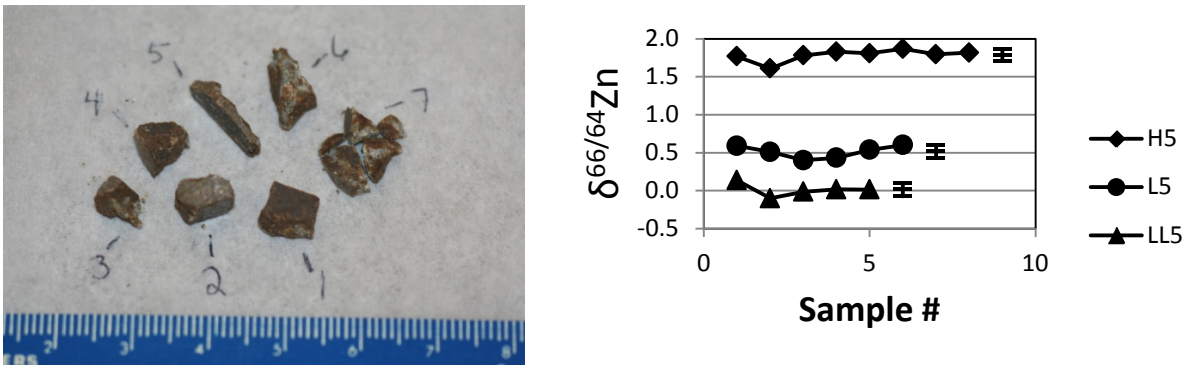

Figure 8. Heterogeneity results. Left, original 3.1 gm chip of LEW 85320 (H5) fractured into seven smaller fragments with masses of 267 mg (#3) to 584 mg (#2). Right, results of three chips fractured and analyzed for isotopic fractionation. Mean value with one SD error bars shown.

Table 4. Phase separation data for six samples. WR, whole rock. nd, not determined.

	mass mg	% mass	$\delta^{66/64}$Zn ‰	$\delta^{67/64}$Zn ‰	$\delta^{68/64}$Zn ‰	[Zn] Ppm
Clovis 1 H3.6						
start	90.9					
magnetic	11.3	12.4%	-1.64	-2.29	-2.92	28
non-mag	79.6					
silicate	39.5	43.5%	-2.57	-3.79	-4.98	68
sulfide	40.1	44.1%	-1.93	-2.84	-3.73	62
mass bal			-2.23	-3.27	-4.29	
WR			-2.42	-3.52	-4.65	
GRA 95208 H3.7						
start	99.8					
magnetic	14.1	14.1%	nd	nd	nd	41
non-mag	85.7					
silicate	45.8	45.9%	-0.42	-0.61	-0.79	58
sulfide	39.9	40.0%	0.37	0.55	0.75	44
mass bal			-0.09	-0.13	-0.16	
WR			-0.04	0.24	0.07	
LEW 85320 H5						
start	89.5					
magnetic	16.8	18.8%	1.17	1.71	2.53	25
non-mag	72.7					
silicate	41.1	45.9%	1.79	2.66	3.51	70
sulfide	31.6	35.3%	1.64	2.40	3.27	47
mass bal			1.69	2.50	3.35	
WR			1.70	2.66	3.45	
ALH 90411 L3.7						
start	228.0					
magnetic	19.2	8.4%	-1.07	-1.47	-1.94	20
non-mag	113.0					
silicate	57.7	46.8%	-0.91	-1.33	-1.74	72
sulfide	55.3	44.8%	-0.41	-0.56	-0.75	33
mass bal			-0.78	-1.12	-1.47	
WR			-0.75	-1.05	-1.41	
GRO 95540 L5						
start	242.9					
magnetic	29.5	12.1%	0.20	0.36	0.48	17
non-mag	111.7					
silicate	69.9	55.0%	0.59	0.90	1.20	51

sulfide	41.8	32.9%	0.73	1.11	1.45	39
mass bal			0.59	0.91	1.21	
WR			0.71	1.15	1.43	
RBT 04127 LL5						
start	259.0					
magnetic	17.1	6.6%	0.45	0.70	0.92	16
non-mag	104.4					
silicate	59.4	53.1%	0.52	0.82	1.02	48
sulfide	45.0	40.3%	1.30	1.95	2.55	36
mass bal			0.78	1.20	1.54	
WR			0.98	1.62	2.06	

Table 5. Leachate results for Semarkona (LL3.0). RT, room temp.

Step / Treatment	Expected Phase(s)	Total MS Zn peak height	fraction of total zinc	$\delta^{66/64}Zn$	$\delta^{68/64}Zn$
		Volts	%	‰	‰
2 RT Acetic	Sulfide, metal, easily soluble	1.9	57.14	-0.07	-0.09
3 RT HNO3	Silicates +	1.2	36.09	-0.27	-0.52
4 RT HCl	Silicates	0.09	2.71	0.13	0.30
3 + 4	*Silicates*	*1.29*	*38.8*	*-0.25*	*-0.46*
5 36C HCl	Refractory / spinels	0.025	0.75	0.04	0.25
6 80C HCl		0.04	1.20	0.03	0.11
7 80C HF/HCl		0.02	0.60	-0.78	-1.21
8 RT HF/HNO3		0.05	1.50	-2.01	-3.83

into the silicate phase during metamorphism or other alteration. In all six samples, the metal phase had lower [Zn] and was isotopically lighter than both the silicate and sulfide phases. This may reflect the original composition of the meteorite, prior to any thermal or metamorphic change, as zinc would likely fractionate preferentially into the silicate and sulfide phases rather than metal during initial accretion.

An additional meteorite, Semarkona (LL3.0), was obtained in liquid aliquots that had already been separated by a different leaching algorithm. The relative zinc content of each separate was determined based on the total voltage for all zinc isotopes obtained by the mass spectrometer; however, [Zn] could not be determined without the original masses of each fraction. The results are given in Table 5. This leaching sequence did not separate the metal from the sulfides, and may not have separated the sulfides from the silicates to the same extent as the method used for the samples in Table 4. Nevertheless, the same trend was seen, with sulfide fraction having heavier Zn isotopic ratios than the silicate fraction.

The unusual H/L5 meteorite LAP 031047, an impact melt, was very low in [Zn], at about 1ppm, similar to that reported by Wittmann et al. (2011). It was isotopically heavy, with $\delta^{66/64}$Zn of 1.26‰. Together these measurements indicate a loss of light isotopes, most likely by volatization during prolonged or repeated heating above the condensation temperature of zinc (about 726K).

Some chondrules that had been separated from the H/L3.6 chondrite Tieschitz were also analysed, and found to have a [Zn] of 29 ppm and a $\delta^{66/64}$Zn of -0.58‰. A separate sample of whole rock (chondrules plus matrix) Tieschitz had [Zn] = 31ppm and $\delta^{66/64}$Zn of -0.24‰. By

mass balance, assuming the chondrules comprise a typical 70% of the bulk mass, the matrix would have [Zn] = 36ppm and $\delta^{66/64}$Zn of +0.40‰.

Shocks grades, following the method of Stoffler et al. (1991), were available from published sources for 35 of the ordinary chondrites included in this study, and plotted against the $\delta^{66/64}$Zn values (27 new values, 8 literature values; 7 LL-, 15 L-, 13 H-chondrites) in Figure 9. There was no clear trend of heavier Zn isotopes with higher shock grade.

Weathering grades were available for 41 of the Antarctic meteorites, plotted in Figure 10. The more highly weathered samples were primarily in the H chondrite group, but these did not exhibit any shift in isotopic ratios compared with L and LL groups.

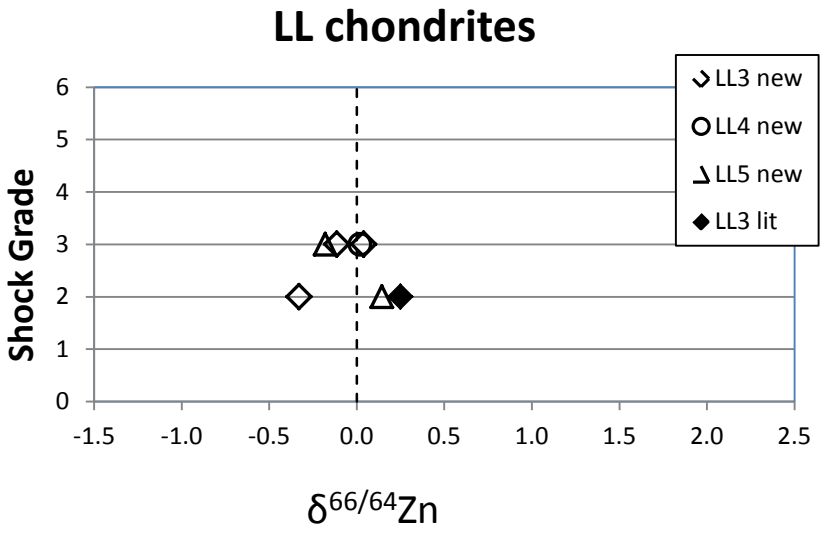
LL chondrites
LL3 new
LL4 new
LL5 new
LL3 lit
Shock Grade
0
1
2
3
4
5
6
-1.5
-1.0
-0.5
0.0
0.5
1.0
1.5
2.0
2.5
δ66/64Zn

a

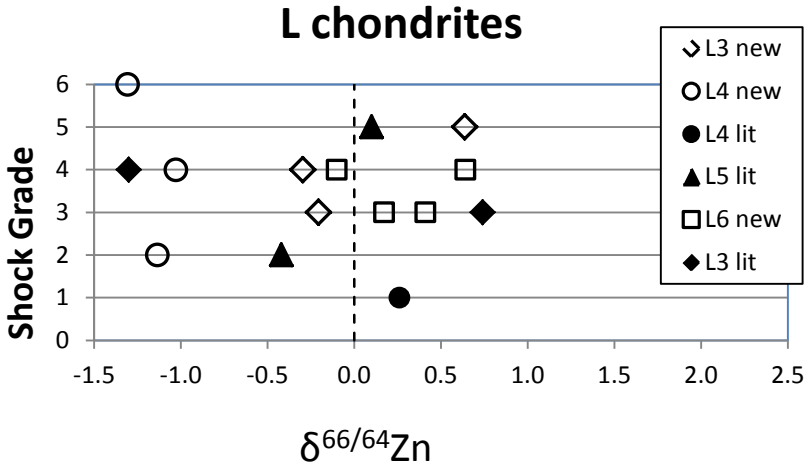
L chondrites
L3 new
L4 new
L4 lit
L5 lit
L6 new
L3 lit
Shock Grade
0
1
2
3
4
5
6
-1.5
-1.0
-0.5
0.0
0.5
1.0
1.5
2.0
2.5
δ66/64Zn

b

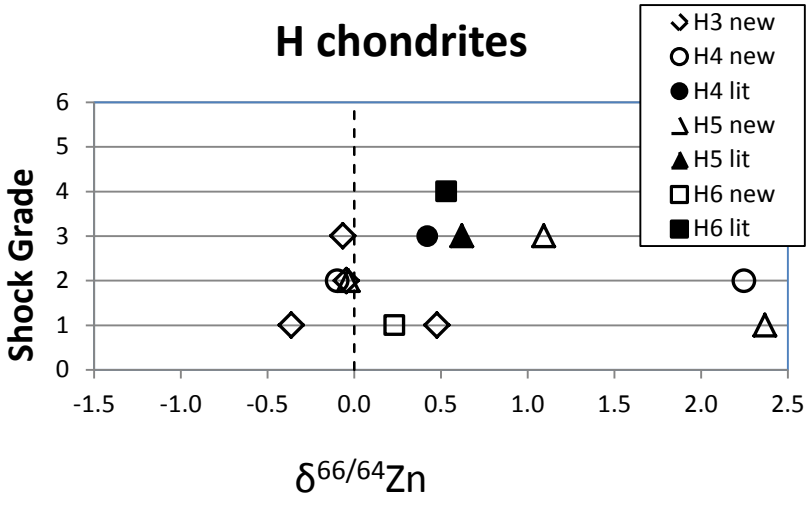
H chondrites
H3 new
H4 new
H4 lit
H5 new
H5 lit
H6 new
H6 lit
Shock Grade
0
1
2
3
4
5
6
-1.5
-1.0
-0.5
0.0
0.5
1.0
1.5
2.0
2.5
δ66/64Zn

c

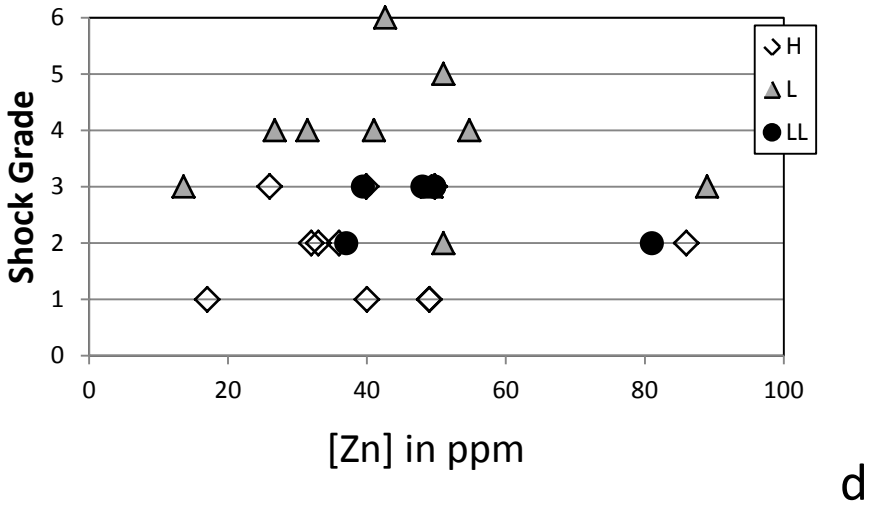

d

Figure 9. a-c, Zn fractionation as a function of shock grade for LL, L and H chondrites. Open symbols = new data (this study); solid symbols = literature values. There is no clear trend of heavier isotopes with higher shock grade. d, Zn concentration also does not follow a clear trend with shock grade for H, L or LL. (Shock grades from Stoffler et al 1991, Bennet & McSween 1996, Rubin 1993, and MetBase 7.3.).

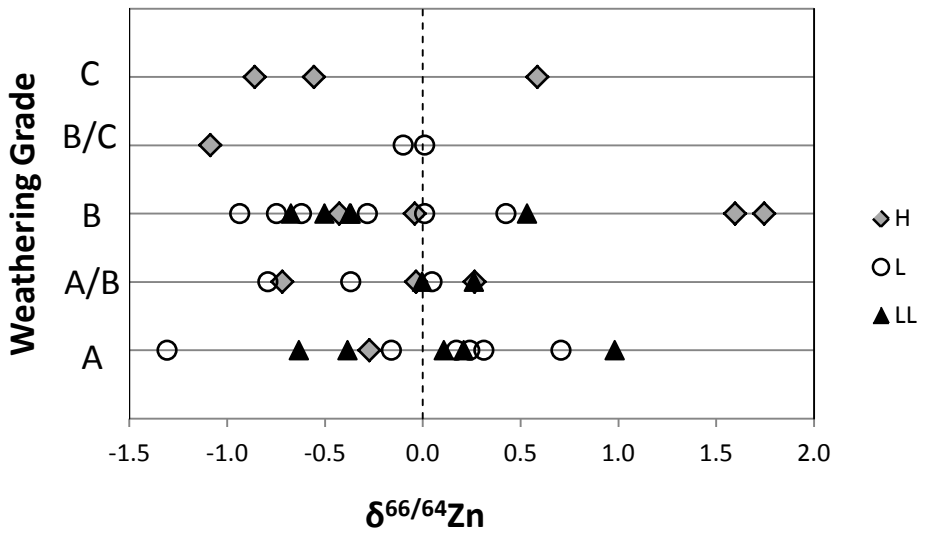

Figure 10. Zn isotopic fractionation as a function of weathering grade for Antarctic meteorites.

4. DISCUSSION

4.1 Antarctic vs Non-Antarctic samples

This study includes a large number of Antarctic meteorites, which are exclusively finds. We requested chips with the least weathering where possible, and 35 of the 41 rated Antarctic meteorites were grades A or B. We found no differences in Zn isotopic ratios based on weathering grade (Figure 9). We also requested the chips come from the center of the meteorite, where possible, and very few of the samples had any fusion crust on them. Biswas et al. (1991) found that specimens taken more than 5mm from the meteorite surface showed no evidence of weathering. In this study, the isotopic findings between the two groups were very similar. There was no systematic isotopic shift or Zn depletion comparing Antarctic to non-Antarctic samples. We also found that there was good small-scale homogeneity in three larger chips (Table 3, Figure 7). This adds confidence that these findings are representative of the whole meteorite and not a sampling error. Finally, there was no difference in Zn isotopes between the Antarctic and non-Antarctic samples (Tables 1-2, Figures 1-2). Data from the Antarctic meteorites appears to be valid, and they are invaluable as source material for meteoritic research.

4.2 Zn host phases

Zinc had higher abundance and lighter isotopic ratios in the silicates than in the sulfide phases in these OCs (Table 4). Shaefer and Fegley (2010), using thermodynamic calculations, showed that Zn most likely formed ZnS or $ZnCr_2O_4$ in pre-accretionary nebular processes. In an ideal solid solution (post-accretion, perhaps), Zn would dissolve into sulfides (primarily ZnS) at higher temperatures but into silicates ($ZnSi_2O_4$ in olivine, $ZnSiO_3$ in enstatite) at low temperatures. These findings suggest that chondrules may have formed initially with Zn as ZnS, and that the

Zn mostly moved into the silicate phase in the parent bodies after accretion. The isotopic findings in our data suggest this phase movement was a mass-dependent process. Shaefer and Fegley (2010) also report that at lower temperatures, the silicate phase is more stable than the sulfide; thus, after the parent body cooled, movement of Zn from silicate back to sulfide is unlikely.

4.3 Shock effects

Shock effects were not major factors in the zinc isotopic variations (Figure 8). Most of the meteorites included in this study, for which published shock grades were available, were not highly shocked (grades 1-3). Some of the L chondrites had shock grades 4-6, but these were not highly depleted in zinc and did not show consistent isotopic shifts. This differs from the findings of Walsh and Lipshutz (1982), which studied L4-6 chondrites; they found lower-shocked (grades a-c) samples had a mean [Zn] of 65ppm, while the higher-shocked (grades d-f) samples had a mean [Zn] of 48ppm. Statistical analysis of our data was unable to duplicate that trend.

4.4 Isotopic and abundance variation with metamorphic grade

These ordinary chondrites have clearly been exposed to one or more major heating events, leading to a variety of metamorphic grades. Based on the zinc isotopes, volatization was not a major feature of these events. Based on a pure Rayleigh distillation model, significant evaporation of zinc would have resulted in much more isotopic fractionation than was actually

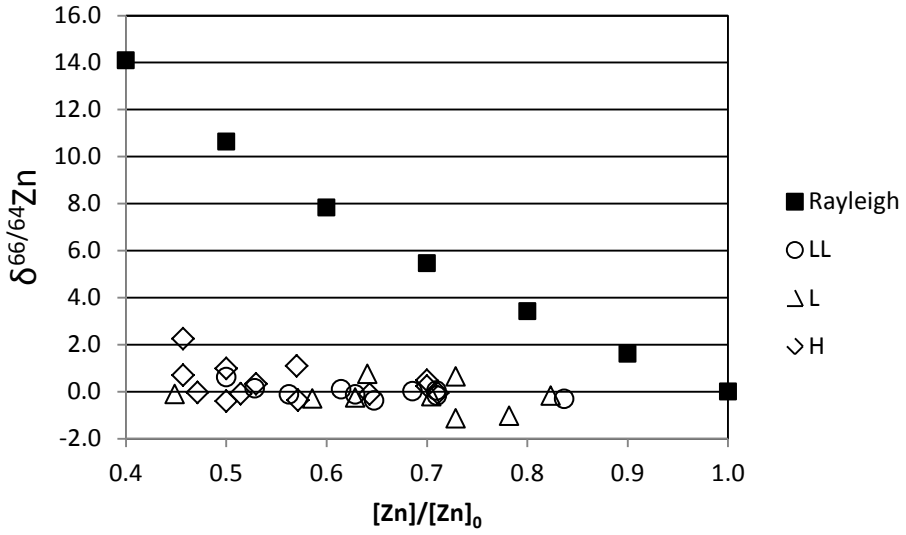

Figure 11. Measured Zn isotopic fractionation in H, L and LL falls from this study (with $[Zn]_0$=70 ppm) compared with expected fractionation determined by a pure Rayleigh distillation law.

measured in these meteorites (Figure 11). One possible explanation is a diffusion-limited regime, which has been proposed previously in tektites (Moynier et al. 2009) and ureilites (Moynier et al. 2010). The Rayleigh equation assumes that the evaporated material is immediately removed from the system, but this assumption is likely not valid. It also requires that the source is homogeneous, which would require the zinc to be free-flowing and instantly equilibrated; this is very unlikely as the OCs were never melted. The diffusion of zinc within the parent body was thus limited.

The prolonged heating may have been accretionary, or may have followed a major impact, such as occurs when two large asteroids collide with one another. Magmatic processes were probably not involved, because 1) most asteroids are not fully differentiated bodies and show no evidence of magmatism, and 2) magmatic processes on Earth have not been found to cause significant isotopic fractionation. Chen et al. (2013) found terrestrial magmatic fractionation to be no more than 0.07‰ for $\delta^{66/64}$Zn and suggest a bulk Earth isotopic composition of 0.28+/- 0.05. Thus, magmatic processes cannot account for the almost 5‰ range in our data for $\delta^{66/64}$Zn in OCs.

Davis (1990) demonstrated, measuring major element abundances, that evaporation occurs much more readily from a melt than from a solid, although the effects of a geologic time scale were not considered. Our data shows a trend of small but measurable increases in zinc isotope ratios with increasing metamorphic grade (Table 2, Figure 4) and a trend toward lower abundance with increasing grade (Figure 5). Thus, volatization probably did play a small role in these meteorites' histories. By contrast, the unusual meteorite LAP 031047 was probably an impact melt, and the large depletion of Zn and the heavy isotopic residual are consistent with major losses by volatization.

Our data do not show significant differences in abundances or isotopic ratios between the OC subtypes, although H chondrites were slightly heavier than both LL and L. Kallemeyn et al. (1989) also noted that all three groups have similar [Zn] (in the 40s-50s ppm), and concluded that the Zn in OCs formed as "fine, ZnS aerosols that inefficiently settled to the midplane." The abundance data added in the present study support this conclusion.

Clayton et al. (1991) found that O isotope composition of H3-H6 and L3-L6 chondrites were best explained by closed-system metamorphism, but noted a small degree of open-system behavior comparing LL3 with LL4-6. The similar Zn content among OC subgroups in the present study supports closed-system metamorphism; an open-system process, allowing loss of Zn by volatization, would lead to lower [Zn] with higher metamorphic grade, but this trend was weak in our data. This further suggests that isotopic variations were created in pre-accretion nebular processes. Ebihara et al. (1993) also found little variation in abundances of Zn in OCs, and concluded that [Zn] in OCs was most likely controlled by nebular fractionation, "possibly at the condensation stage." Wang and Lipshutz (2007) also found limited variability in [Zn] among Antarctic UOCs, and concluded that L, LL, and probably H exhibited closed-system behavior.

Schaefer and Fegley (2010) modeled volatile mobilization during thermal metamorphism in ordinary chondrite parent bodies using chemical equilibrium calculations. Twenty trace element abundances were determined by petrologic grades for H, L and LL OCs. Their data support open-system thermal metamorphism for all of the trace elements except Ag and Zn, whose abundance patterns "remain difficult to explain." The Zn data were most consistent with closed-system behavior.

Luck et al. (2005) studied Zn isotopes in 14 ordinary chondrites and concluded that light isotopes must be carried by OCs in the refractory materials (spinels), perhaps by reaction with a gas phase enriched in light Zn isotopes, or in the rims of chondrules; either would be a pre-accretion process. Alexander (1995) and others proposed that material lost by volatization during chondrule formation could re-condense onto chondrule rims, which would make them isotopically lighter. Our data for Tieschitz agrees with the latter, that the chondrules are lighter than the matrix in Zn isotopes.

The range of zinc fractionation found in this large group of meteorite samples ($-2.42 < \delta^{66/64}Zn < +2.24$) was significantly greater than that reported by Luck et al. (2005) ($-1.30 < \delta^{66/64}Zn < +0.76$), although their overall mean value of +0.10‰ is within error of our overall mean of +0.00‰. The plot of $\delta^{66/64}Zn$ against [Zn] normalized to major elements Al and Cr (Figure 6) is similar to Luck et al. (2005), except for our wider range of Zn isotopic values. Our sample set is significantly larger and includes representatives from all metamorphic grades for all three OC subtypes. It is likely that the more extreme values (>2σ outside the mean) were simply found by chance owing to the large number of samples tested. The data follow a normal distribution (Figure 2), suggesting that a broad and representative sample of the total population of OCs was probably included in our sample set. This large range of isotopic values also implicates nebular (pre-accretion) processes; if Zn was originally homogenous in OCs, secondary processes have not been shown capable of producing this much fractionation.

CONCLUSION

The zinc abundance and isotopic findings from a large suite of ordinary chondrites suggest that although volatization played a small role in their Zn determination, it was primarily controlled by

pre-accretionary nebular processes, during which significant variability of isotopic ratios was established. Some mass-dependent shift of zinc from sulfide to silicate phases may have occurred during thermal metamorphism, but significant losses did not occur during this process. The H, L, and LL subtypes are fairly similar in Zn composition.

ACKNOWLEDGEMENTS

The authors would like to thank: NASA-JSC - Cecilia Satterwhite, Kevin Righter; Musee Nationale Histoire Naturele, Paris - Brigitte Zanda; Smithsonian Institution – Linda Welzenbach, Tim McCoy; American Museum of Natural History – Joseph Boesenberg, Denton Ebel; Arizona State University – Laurence Garvie; National Institute of Polar Research, Tokyo – Naoya Imae; Natural History Museum, Vienna - Franz Brandstaetter, Ludovic Ferriere. We also thank Jean-Gabriel Fraboulet for assistance in processing some of the samples.

REFERENCES

Albarede, F. (2004). The stable isotope geochemistry of copper and zinc. *Rev. Mineral. Geochem.* 55, 409–427.

Alexander C M O'D (1995). Rims, matrix, and the bulk compositions of ordinarychondrites. *Meteoritics* 30, 479.

Bennet ME, McSween HY (1996). Shock features in iron-nickel metal and troilite of L-group ordinary chondrites. *Meteor. Planet. Sci.* 31, 255-264.

Binns RA (1967). Structure and evolution of noncarbonaceous chondrites. *Earth Planet. Sci. Lett.* 2, 23-28.

Biswas S, Walsh TM, Ngo NT, Lipchutz ME (1981). Trace element contents of selected Antarctic meteorites-II. Comparison with non-Antarctic specimens. *Proc. Sixth Symp. Antarctic Meteorites,* 22l-228.

Brearley AJ, Jones RH (1998). Chondritic meteorites. In: Papike JJ, ed., *Rev. Mineralogy 36: Planetary Materials*. Mineralogical Soc. Amer., Washington DC.

Chen H, Savage P, Teng F-Z, Helz RT, Moynier F **(**2013). Zinc isotope fractionation during magmatic differentiation and the isotopic composition of the bulk Earth. *Earth Planet. Sci. Lett.* 369-370, 34-42.

Clayton RN, Mayeda TK, Goswami JN, Olsen EJ (1991). Oxygen isotope studies of ordinary chondrites. *Geochim. Cosmochim. Acta* 55, 2317-2337.

Corrigan CM, Cohen BA, Hodges K, Lunning N, Bullock E (2012). 3.9 billion years ago and the asteroid belt: impact melts in ordinary chondrites. 43rd Annual LPSC, abstract #1577.

Davis AM, Hashimoto A, Clayton RN, Mayeda TK (1990). Isotope mass fractionation during evaporation of Mg_2Si0_4. *Nature* 347, 655-658.

Dougherty JR, Brannon JC, Nichols RH, Podosek FA (1999). Thoroughly anomalous Cr in the ordinary chondrite Semarkona. 30th Annual LPSC, abstract #1451.

Ebihara M, Ozaki H, Fukatsu S. (1993). Cu, Zn, and In in ordinary chondrites. *Meteoritics* 28, 343-4.

Ghidan OY, Loss, RD (2011). Isotope fractionation and concentration measurements of Zn in meteorites determined by the double spike, IDMS-TIMS techniques. *Meteor. Planet. Sci.* 46, 830–842.

Herzog G, Moynier F, Albarède F, Berezhnoy A (2009). Isotopic and elemental abundances of copper and zinc in lunar basalts, glasses, and soils, a terrestrial basalt, Pele's hair, *Geochim. Cosmochim. Acta* 73, 5884-5904.

Humayun M, Clayton RN (1995). Potassium isotope cosmochemistry: Genetic implications of volatile element depletion. *Geochim. Cosmochim. Acta,* 59, 2131-2148.

Ikramuddin M, Matza S, Lipschutz ME (1977). Thermal metamorphism of primitive meteorites.-V. Ten trace elements in Tieschitz H3 chondrite heated at 400-1000°C. *Geochim. Cosmochim. Acta* 41, 1247-1256.

Jochum KP, Palme H (1993). Fractionation of volatile elements by heating of solid Allende: implications for the source material of Earth, Moon, and the eucrite parent body. *Meteoritics* 28, 373-4.

Kallemeyn GW, Rubin AE, Wang D, Wasson JT (1989). Ordinary chondrites: bulk compositions, classification, lithophile-element fractionations, and composition-petrographic type relationships. *Geochim. Cosmochim. Acta* 53, 2747-2767.

Laul JC, Ganapathy R, Anders E, Morgan JW (1973). Chemical fractionations in meteorites - VI. Accretion temperatures of H-, LL- and E-chondrites, from abundance of volatile trace elements. *Geochim. Cosmochim. Acta* 37, 329-357.

Lodders K (2003). Solar system abundances and condensation temperatures of the elements. *Astrophys. J.* 591, 1220–1247.

Luck JM, Ben Othman D, Albarède F (2005). Zn and Cu isotopic variations in chondrites and iron meteorites: Early solar nebula reservoirs and parent-body processes. *Geochim. Cosmochim. Acta* 69, 5351-5363.

Moynier F, Blichert-Toft J, Luck JM, Telouk P, Albarède F (2007). Comparative stable isotope geochemistry of Ni, Cu, Zn, and Fe in chondrites and iron meteorites. *Geochim. Cosmochim. Acta* 71, 4365-4379.

Moynier F, Beck P, Jourdan F, Yin Q-Z, Reimold U, Koeberl C (2009) Isotopic fractionation of zinc in tektites. *Earth Planet. Sci. Lett.* 277, 482–489.

Moynier F, Beck P, Yin QZ, Ferroir T, Barr at JA, Paniello R, Telouk P, Gillet P (2010). Volatilization induced by impacts recorded in Zn isotope composition of ureilites. *Chem. Geol.* 276, 374-379.

Moynier F, Paniello RC, Beck P, Gounelle F, Podosek F, Albarède F, Zanda B (2011). Nature of volatile depletion and genetic relationships in enstatite chondrites and aubrites inferred from Zn isotopes. *Geochim. Cosmochim. Acta* **75**, 297-307.

Paniello RC, Moynier F, Beck P, Barrat JA, Podosek F, Pichat S (2012a). Zinc isotopes in HEDs: clues to the formation of 4-Vesta, and the unique composition of Pecora Escarpment 82502. *Geochim. Cosmochim. Acta* 86, 76-87.

Paniello RC, Day JMD, Moynier F (2012b). Zinc isotopic evidence for the origin of the Moon. *Nature* 490, 376–379.

Podosek FA, Ott U, Brannon JC, Neal CR, Bernatowicz TJ, Swan P, Mahan SE (1997). Thoroughly anomalous Cr in Orgueil. *Meteoritics* 32, 617-627.

Rotaru M, Birck JL, Allegre CJ (1992). Clues to early solar system history from chromium isotopes in carbonaceous chondrites. *Nature* 358, 465-470.

Rubin AE (1992). A shock-metamorphic model for silicate darkening and compositionally variable plagioclase in CK and ordinary chondrites. *Geochim. Cosmochim. Acta* 56, 1705-1714.

Schaefer L, Fegley B (2010). Volatile element chemistry during metamorphism of ordinary chondritic material and some of its implications for the composition of asteroids. *Icarus* 205: 483-496.

Stoffler D, Keil K, Scott ERD (1991). Shock metamorphism of ordinary chondrites. *Geochim. Cosmochim. Acta* 55, 3845-3867.

Van Schmus WR, Wood JA (1967). A chemical-petrologic classification for the chondritic Meteorites. *Geochim. Cosmochim. Acta* 31: 747–765.

Walsh TM, Lipschutz ME (1982). Chemical studies of L chondrites- II. Shock-induced trace element mobilization. *Geochim. Cosmochim. Acta* 46, 2491-2500.

Wang M-S, Lipschutz ME (2007). Trace elements in primitive meteorites—VII Antarctic unequilibrated ordinary chondrites. *Geochim. Cosmochim. Acta* 71, 1062–1073.

Wang K**,** Moynier F, Barrat JA, Zanda B, Paniello RC, Savage PS (2013). Homogeneous distribution of Fe isotopes in the early solar nebula. *Meteor. Planet. Sci.*, 48, 354-364.

Welzenbach LC, McCoy TJ, Grimberg A, Wieler R (2005). Petrology and noble gases of the regolith breccia MAC 87302 and implications for the classification of Antarctic meteorites. 36th Annual LPSC, abstract #1425.

Wittmann A, Friedrich JM, Troiano J, Macke RJ, Britt DT,Swindle TD, Weirich JR, Rumble D, Lasue J, Kring DA (2011). H/L chondrite LaPaz Icefield 031047 – A feather of Icarus? *Geochim. Cosmochim. Acta* 75: 6140–6159.

Wulf AV, Palme H, Jochum KP (1995). Fractionation of volatile elements in the early solar system: evidence from heating experiments on primitive meteorites. *Planet. Space Sci.* 43, 451-468.

6. Enstatite Chondrites and Achondrites

Manuscript citation: Moynier F, Paniello RC, Beck P, Gounelle F, Podosek F, Albarède F, Zanda B (2011). Nature of volatile depletion and genetic relationships in enstatite chondrites and aubrites inferred from Zn isotopes. *Geochim. Cosmochim. Acta* **75**, 297-307.

Introduction

The enstatite meteorites include two types of chondrites, EH and EL (for high and low iron, respectively), and one type of achondrite, the aubrites (Table 6-1), in which the dominant mineral is enstatite. These meteorites formed under highly reducing conditions and thus contain some minerals not commonly found in Earth materials (Mittlefehdt et al.1998), including unusual metallic and sulfide phases. The parent bodies for these meteorites are not known, but there is evidence that the aubrite parent body is related to the EH and EL chondrite parent bodies, having similar mineral composition (Watters and Prinz 1979) and oxygen isotope composition (Clayton et al. 1984).

The enstatite chondrites show evidence of thermal and/or shock metamorphism similar to the ordinary chondrites, and the same metamorphic scale has been applied to them, so that EH3-6 and EL3-6 are now recognized (Keil 1989, Zhang et al. 1995).

Enstatite chondrites have been shown to isotopically very similar to the Earth, fueling speculation of a possible enstatite chondritic origin of the Earth (Javoy et al. 2010, Savage and Moynier 2013) although this is somewhat controversial (Fitoussi and Bourdon 2012).

The unusually reduced nature of the enstatite meteorite group, along with reports of variable Zn volatility in reducing versus oxidizing environments (Wulf 1995), the metamorphic sequences of

the enstatite chondrites, and the possible link to Earth's chondritic origin made the enstitite group interesting for study of zinc isotopes.

	Ant.	Non-Ant.	Falls	Total
Enstatite				
EH chondrites	102	69	9	171
EL chondrites	52	69	8	121
Total chondrites	*154*	*138*	*17*	*292*
Achondrites	43	35	9	78
Total Enstatite	*197*	*173*	*26*	*370*

Table 6-1. Enstatite meteorites by subtype. Ant. = Antarctic.

REFERENCES

Clayton RN, Mayeda TK, Rubin AE (1984). Oxygen isotope compositions of enstatite chondrites and aubrites. *Proc Lun Plan Sci Conf* 15, C245-249.

Fitoussi C, Bourdon B (2012). Silicon isotope evidence against an enstatite chondrite earth. *Science* 335, 1477.

Javoy M, Kaminski, E.; Guyot, F.; Andrault, D.; Sanloup, C.; Moreira, M.; Labrosse, S.; Jambon, A.; Agrinier, P.; Davaille, A.; Jaupart, C. (2010). The chemical composition of the Earth: Enstatite chondrite models. *Earth Planet. Sci. Lett.* 293, 259-268.

Keil K (1989). Enstatite meteorites and their parent bodies. *Meteoritics* 24, 195-208.

Mittlefehldt DW, McCoy TJ, Goodrich CA, Kracher A (1998). Non-chondritic meteorites from asteroidal bodies. In: Planetary Materials, Papike JJ,ed. Rev. Mineral. Volume 36.

Savage PS, Moynier F (2013). Silicon isotopic variation in enstatite meteorites: Clues to their origin and Earth-forming material. *Earth Planet. Sci. Lett.* 361, 487-496.

Watters TR, Prinz M (1979). Aubrites: their origin and relationship to enstatite chondrites. *Proc Lun Plan Sci Conf* 10, 1073-1093.

Wulf AV, Palme H, Jochum KP (1995). Fractionation of volatile elements in the early solar system: evidence from heating experiments on primitive meteorites. *Planet. Space Sci.,* Vol. 43, 451-468.

Zhang Y, Benoit PA, Sears DWG (1995). The classification and complex thermal history of the enstatite chondrites. *J. Geophys. Res.* 100, 9417-9438.

Nature of volatile depletion and genetic relationships in enstatite chondrites and aubrites inferred from Zn isotopes

Frédéric Moynier[1], Randal C. Paniello[1], Matthieu Gounelle[2], Francis Albarède[3], Pierre Beck[4], Frank Podosek[1] and Brigitte Zanda[2]

[1] Department of Earth and Planetary Sciences and McDonnell Center for Space Sciences, Washington University in St Louis, One Brookings Drive, St Louis, MO 63130, USA

[2] Laboratoire de Minéralogie et de Cosmochimie du Muséum, CNRS & MNHN, UMR 7202, CP52, 61 rue Buffon, 75 005 Paris, France.

[3] Laboratoire de Sciences de la Terre, Ecole Normale Supérieure de Lyon, France

[4]Laboratoire de Planétologie de Grenoble ,Universite of Grenoble, France

Abstract:

Enstatite meteorites include the undifferentiated enstatite chondrites and the differentiated enstatite achondrites (aubrites). They are the most reduced group of all meteorites. The oxygen isotope compositions of both enstatite chondrites and aubrites plot along the terrestrial mass fractionation line, which suggests some genetic links between these meteorites and the Earth as well.

For this study, we measured the Zn isotopic composition of 25 samples from the following groups: aubrites (main group and Shallowater), EL chondrites, EH chondrites and Happy Canyon (impact melt breccia). We also analyzed the Zn isotopic composition and elemental abundance in separated phases (metal, silicates, and sulfides) of the EH4, EL3 and EL6 chondrites. The different groups of meteorites are isotopically distinct and give the following values (‰): Aubrite main group ($-7.08<\delta^{66}Zn<-0.37$); EH3 chondrites ($0.15<\delta^{66}Zn<0.31$); EH4 chondrites ($0.15<\delta^{66}Zn<0.27$); EH5 chondrites ($\delta^{66}Zn=0.27\pm0.09$; n=1); EL3 chondrites ($0.01<\delta^{66}Zn<0.63$); the Shallowater aubrite ($1.48<\delta^{66}Zn<2.36$); EL6 chondrites ($2.26<\delta^{66}Zn<7.35$); and the impact melt enstatite chondrite Happy Canyon ($\delta^{66}Zn=0.37$).

The aubrite Peña Blanca Spring ($\delta^{66}Zn= -7.04‰$) and the EL6 North West Forrest ($\delta^{66}Zn=7.35‰$) are the isotopically lightest and heaviest samples, respectively, known so far in the Solar System. In comparison, the range of Zn isotopic composition of chondrites and terrestrial samples ($-1.5 <\delta^{66}Zn<1‰$) is much smaller (Luck et al. 2005; Herzog et. 2009).

EH and EL3 chondrites have the same Zn isotopic composition as the Earth, which is another example of the isotopic similarity between Earth and enstatite chondrites. The Zn isotopic composition and abundance strongly support that the origin of the volatile element

depletion between EL3 and EL6 chondrites is due to volatilization, probably during thermal metamorphism. Aubrites show strong elemental depletion in Zn compared to both EH and EL chondrites and they are enriched in light isotopes (δ^{66}Zn down to -7.04‰). This is the opposite of what would be expected if Zn elemental depletion was due to evaporation, assuming the aubrites started with an enstatite chondrite-like Zn isotopic composition. Evaporation is therefore not responsible for volatile loss from aubrites. On Earth, Zn isotopes fractionate very little during igneous processes, while differentiated meteorites show only minimal Zn isotopic variability. It is therefore very unlikely that igneous processes can account for the large isotopic fractionation of Zn in aubrites. Condensation of an isotopically light vapour best explains Zn depletion and isotopically light Zn in these puzzling rocks. Mass balance suggests that this isotopically light vapor carries Zn lost by the EL6 parent body during thermal metamorphism and that aubrites evolved from an EL6-like parent body. Finally, Zn isotopes suggest that Shallowater and aubrites originate from distinct parent bodies.

1. Introduction

Enstatite meteorites include the undifferentiated enstatite chondrites and the differentiated enstatite achondrites known as aubrites. The enstatite meteorites are the most reduced group of meteorites (Larimer 1968; Keil, 1989; 2010): their metal contains dissolved Si and a fraction of the lithophile elements such as Ca, Mn and Mg are found in sulfides for lack of oxygen. In the $\delta^{17}O$ vs $\delta^{18}O$ plot, both enstatite chondrites and aubrites plot along the terrestrial mass fractionation line and close to the Earth mantle (Clayton and Mayeda, 1996).

Enstatite chondrites are divided into two groups: the Fe-rich EH chondrites and the Fe-poor EL chondrites. Each of these groups comprises several petrographic types according to their degree of thermal equilibration: EH3,4,5 chondrites and EL3,5,6 chondrites. The genetic relationship between EL and EH is still unresolved (Keil, 1989; 2010; Kong et al., 1997). Based on the inverse variation of moderately volatile element abundances with petrographic type between EH chondrites and EL chondrites, Kong et al. (1997) proposed that both meteorite families originated from a single parent body. In contrast, Keil (1989) considered that they were derived from two separate parent bodies based on the absence in each group of clasts from the other group and, from a detailed petrographic study, Lin and El Goresy (2002) considered that EL3 and EH3 could not have evolved of the one from the other**.** Both Mn-Cr and I-Xe systematics indicate older ages for EH4 chondrites (~4565 Ma) than EL6 chondrites (~4560 Ma) (Kennedy et al., 1988; Shukolyukov and Lugmair, 2004). ^{53}Mn has been detected in aubrites and one external isochron gives an age of ~4561-4563 Ma for the end of the planetary differentiation of the aubrite parent body (Shukolyukov and Lugmair, 2004).

Aubrites are FeO-poor orthopyroxenites, which again formed under very reducing conditions (Keil, 1989). They contain an unusual assemblage of highly reduced minerals such as

Si-bearing Fe-Ni metal, Ti-bearing troilite, niningerite: (Mg,Mn,Fe)S, caswellsilverite: $NaCrS_2$, schreibersite: $(Fe,Ni)_3P$, alabandite: (Mn,Fe,Mg)S, oldhamite: CaS, and daubreilite: $FeCr_2S_4$ which is the main carrier of Zn in aubrites (Keil, 2010 and references therein). Elements that are lithophile under moderate fO_2 conditions are hosted in chalcophile or siderophile minerals, notably oldhamite (CaS) (Graham and Henderson, 1985; Keil, 1989; 2010). All the aubrites but Shallowater are brecciated and seem to have formed within the same parent body. Shallowater is the only unbrecciated aubrite and has been suggested to have originated from a parent body distinct from all the others (Keil et al., 1989).

The large variability in the abundances of moderately volatile elements such as Zn observed in enstatite meteorites is conspicuous (Table 1). Zinc abundances decrease in the sequence (average concentrations in parenthesis): EH chondrites (~290 ppm; Lodders and Fegley, 1998), Shallowater (~32 ppm; Biswas et al., 1980), EL chondrites (19 ppm; Lodders and Fegley, 1998), aubrites main group (0.5-2 ppm; Wolf et al., 1983, Lodders et al., 1993). In addition, Zn abundances show also some variations within each group with a trend of decreasing concentrations with stronger degrees of metamorphism: for example the average Zn concentration of un-metamorphosed EL3 chondrites (213 ppm; Kong et al., 1997) are much higher than for the highly metamorphosed EL5,6 chondrites (6 ppm, Kong et al., 1997). Likewise, the Zn concentration for the EH5 chondrite St Mark's (48-100 ppm, Kong et al., 1997) is less than the mean for EH chondrites (290 ppm, Lodders and Fegley, 1998).

Nebular processes or volatilization during thermal metamorphism have both been proposed as possible causes of the loss of moderately volatile elements (Biswas et al., 1980; Kallemeyn and Wasson, 1986; Kong et al., 1997). Volatilization is expected to fractionate isotopes (Richter, 2004). Comparing the isotope compositions of volatile elements in meteorites may therefore help

understand the physical and chemical conditions of the evaporation process. Zinc is a moderately volatile element with a 50% condensation temperature T_{50}(Zn) of ~730K (Lodders, 2003) and may be even more volatile under conditions relevant to the metamorphism of ordinary chondrites (Schaefer and Fegley, 2010).

The Zn isotope variability in terrestrial rocks is relatively narrow (~0.3‰ per amu, for review see Albarede, 2004). Luck et al. (2005) showed that the different ordinary (OC) and carbonaceous chondrites (CC) groups have distinct Zn isotopic compositions with a total range of ~0.35‰ per amu but that the relative depletion of volatiles elements in CC correlates with isotopically lighter, not heavier, Zn. In contrast, the very large isotopic variability of Zn in lunar soils (up to 3‰ per amu) (Moynier et al., 2006; Herzog et al., 2009) and their depletion in light Zn isotopes are consistent with vaporization upon impact by micrometeorites or sputtering at the lunar surface. Albarede et al. (2007) extended the study of isotopic fractionation of Zn to shocked rocks from a terrestrial impact site, Meteor Crater, Arizona, USA. They observed a negative correlation between isotope compositions and shock grade in seven Coconino sandstone samples and concluded that, on Earth, vaporization at high temperature by impacts fractionates the isotopic compositions of rather heavy elements to a measurable extent. Likewise, tektites (hypervelocity impact glasses) were enriched in heavy isotopes of Zn, most likely by evaporation upon melting during impact (Moynier et al., 2009a). Zn isotopic composition of meteorites has been shown to follow a mass dependent fractionation line in meteorites, with no evidence of nucleosynthetic anomalies (Moynier et al. 2009b).

Preliminary data by Mullane et al. (2005ab) indicate a strong isotope fractionation of Fe and Zn in enstatite chondrites and aubrites. Here, we return to this issue and investigate Zn isotope fractionation in aubrites (aubrite main group and Shallowater), and in EL, and EH

chondrites by multiple-collector inductively-coupled plasma mass-spectrometry (MC-ICP-MS). In this study, we assess to what extent igneous processes such as partial melting and fractional crystallization, and impact-related processes such as brecciation, collisional disruption, impact-melting and the incorporation of foreign xenoliths, have affected the Zn isotope compositions of enstatite meteorites.

2. Samples and analytical methods:

2.1. Sample description:

Twenty-five samples representing the four main enstatite-meteorite groups (EH, EL, aubrites and Shallowater) were studied. They include 8 samples from the aubrite main group (Aubres, Bishopville, Bustee, Cumberland Falls, Khor Temiki, Mayo Belwa, Norton County, Peña Blanca Spring), and Shallowater, which may be from a different parent body (Keil, 1989; Keil et al., 1989). We also analysed 16 enstatite chondrites EL3 (2), EL6 (8), EH3 (3), EH4 (1), EH5 (1) plus Happy Canyon. The latter sample was initially classified as an aubrite (Olsen et al., 1977) but has been re-classified as an impact melt enstatite chondrite (McCoy et al., 1995). All the aubrites are brecciated; Bustee and Khor Temiki are regolith breccias, and the remaining aubrites in this study are fragmental breccias (Keil, 1989). In contrast, Shallowater is unbrecciated (Keil et al., 1989).

To assess the Zn isotopic heterogeneity of the samples, we also analysed different pieces of the same meteorite for Norton County (3), Shallowater (3), Kota-Kota (2), Qingzhen (2), Indarch (4), PCA 90120 (2) and Happy Canyon (2).

We also report the Zn isotopic composition of the geostandard USGS BCR-2, a basalt from the Columbia River, 29 miles east of Portland, Oregon, USA.

2.2 Methods:

Fragments of meteorites of ~500-1000 mg were cleaned in double-distilled water for five minutes in an ultrasonic bath. The leaching solution was discarded, then the residue was dried and crushed to a homogeneous fine powder. For enstatite chondrites ~50-100mg were dissolved under pressure in Parr bombs in HNO_3/HF for several days to ensure a total dissolution of the most refractory phases. For aubrites, fragments of ~500 mg were dissolved in HNO_3/HF in closed Teflon beakers.

In addition to the whole-rock dissolution, three samples (Indarch, EH4; PCA 90120, EL3 and Blithfield, EL6) were subjected to phase separation (magnetic and non-magnetic) and sequential dissolution on the non-magnetic phase. First, magnetic and non-magnetic fractions were separated with a hand magnet. One split of the non-magnetic fraction was dissolved in HNO_3/HF. A second split of the non-magnetic fraction was first dissolved in cold 3N HCl for 6 hours (dissolution of sulfides) and the residue was dissolved in HNO_3/HF (dissolution of silicates). For all samples, the magnetic phase was dissolved in aqua-regia.

Zinc was purified by anion-exchange chromatography using the procedure described by Moynier et al. (2006). The samples were loaded in 1.5N HBr on 0.25 ml AG-1X8 (200-400 mesh) ion-exchange columns and Zn was taken down in 0.5N HNO_3. The Zn fraction was further purified by eluting the samples twice on a 100 µl column with the same eluting solutions.

Zinc isotopic compositions were measured on the Nu Plasma High Resolution Multi Collection-Inductively Coupled Plasma-Mass Spectrometer (MC-ICP-MS) of the Ecole Normale Supérieure de Lyon, France, following the procedure described in Moynier et al. (2006). The yield was found to be better than 95 % and the blank of ~10 ng is negligible with respect to the total amount of Zn in the samples (>2 μg). Isotope ratios are expressed as deviations relative to a standard in parts per 1000:

$$\delta^{x}\mathrm{Zn}\ (‰) = \left(\frac{\left({}^{x}\mathrm{Zn}/{}^{64}\mathrm{Zn} \right)_{\mathrm{sample}}}{\left({}^{x}\mathrm{Zn}/{}^{64}\mathrm{Zn} \right)_{\mathrm{standard}}} - 1 \right) \times 1000 \qquad (1)$$

with x = 66 or 68. The reference material used is the Zn "Lyon" standard JMC 3-0749 L (Maréchal et al., 1999). The "Lyon" standard is the most broadly used reference material to normalize Zn isotope data (see Albarede, 2004 for a review). Replicate analyses of the same samples carried out during different analytical sessions define an external reproducibility of ± 0.09‰ for δ^{66}Zn and ± 0.27‰ for δ^{68}Zn (see Moynier et al., 2006 and Herzog et al., 2009 for extensive discussion of our analytical precision).

3. Results

3.1 Isotopic composition of the whole-rock meteorites

Isotope ratios are given in Tables 1, 2 and 3 and plotted in Figure 1. The overall range of values for each group is consistent with the preliminary findings of Mullane et al. (2005ab). As expected from mass-dependent isotopic fractionation, all the samples plot onto a straight line of slope 1.94 in a δ^{68}Zn vs. δ^{66}Zn diagram (Figure 1). The isotopically heaviest sample is the EL6 chondrite North West Forrest (δ^{66}Zn=7.35‰) and the lightest sample is the aubrite Peña

Blanca Spring ($\delta^{66}Zn$=-7.08‰). The different groups of meteorites are isotopically distinct (see Figure 2) and give the following values (‰):

FIGURE 1

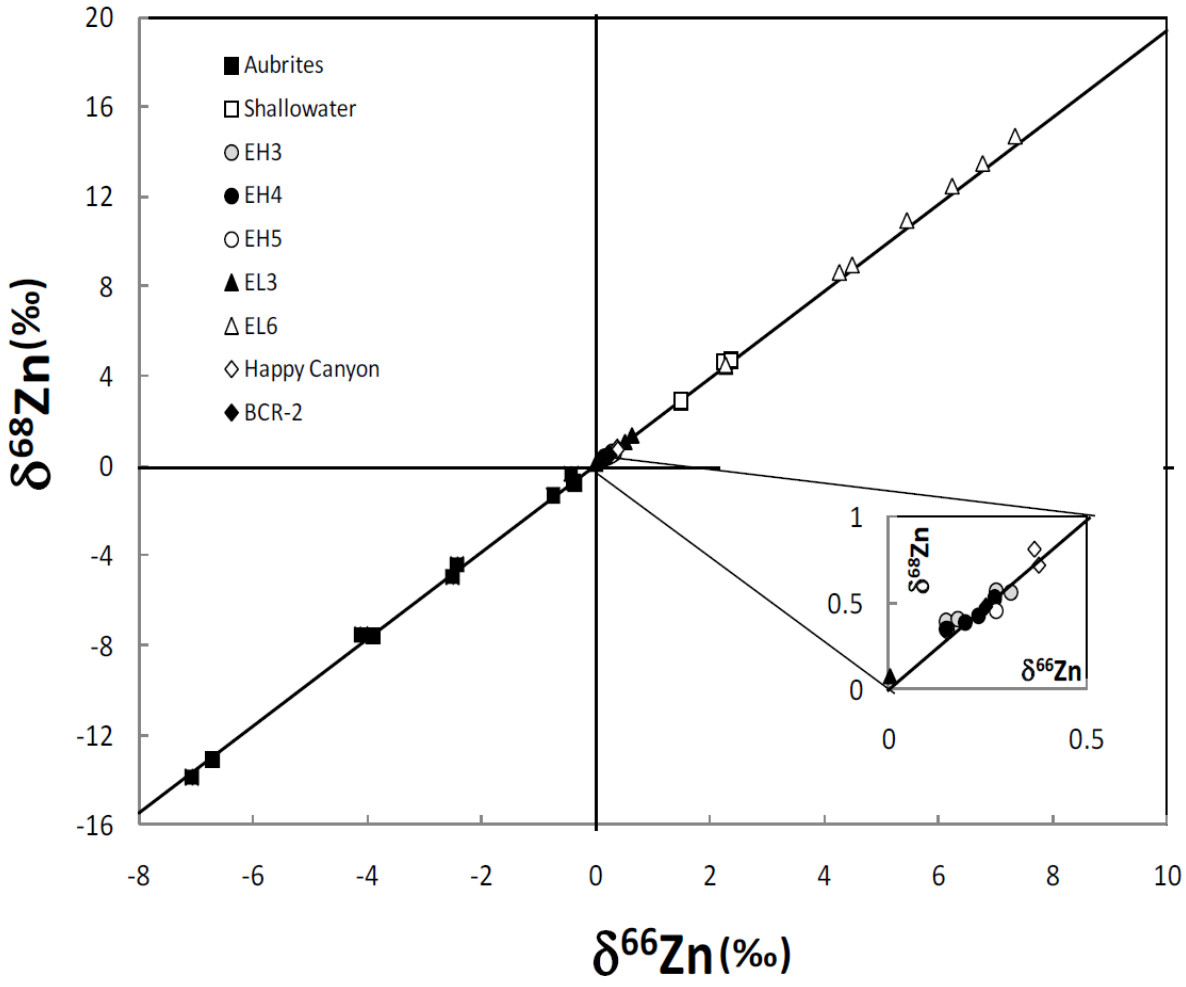

FIGURE 1: $\delta^{68}Zn$ vs $\delta^{66}Zn$. All data fall onto the mass-dependent fractionation line of slope 1.94. The sample outside the mass-dependent fractionation line has been excluded from the discussion. Both meteoritic and terrestrial samples plot on the same line, implying that the Zn from all the analyzed samples evolved from a single, isotopically homogeneous reservoir.

FIGURE 2

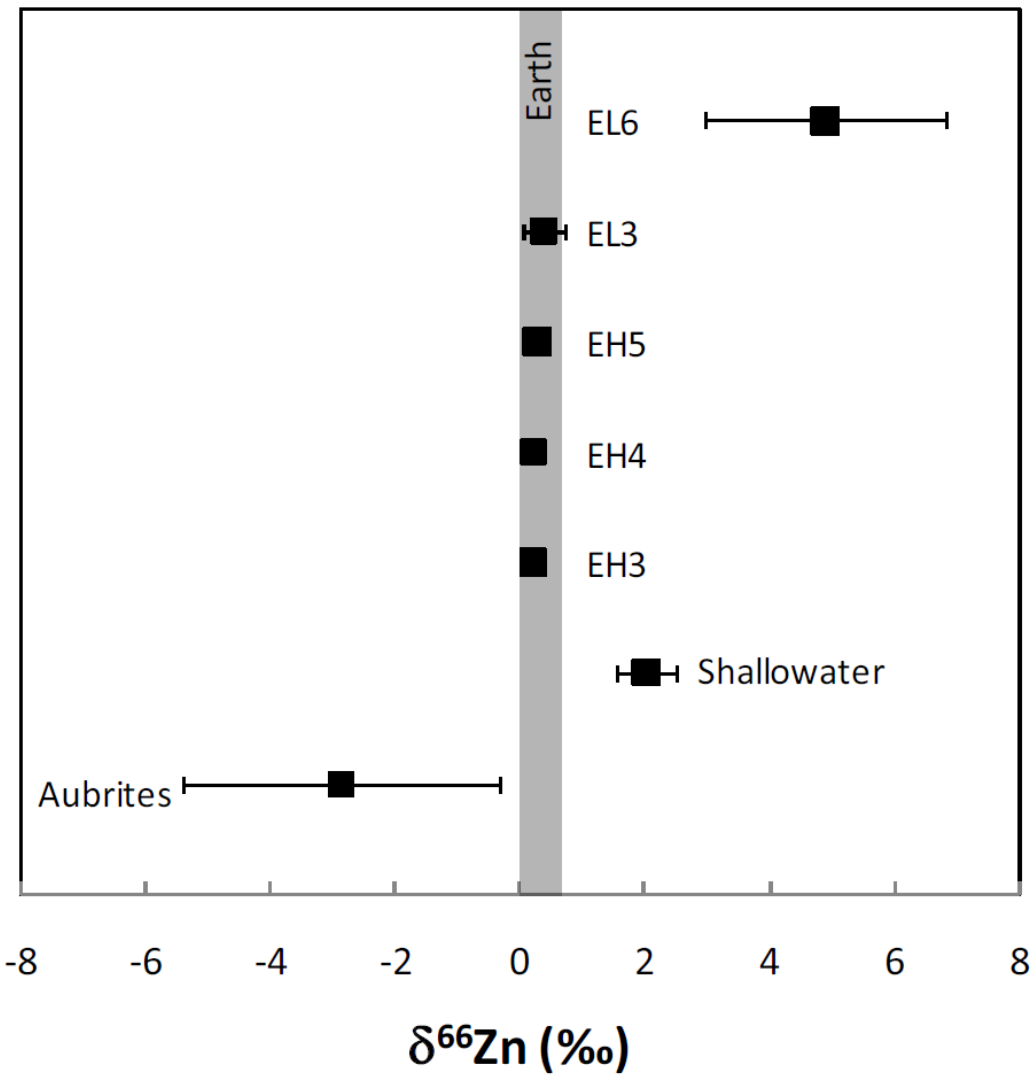

FIGURE 2: $\delta^{66}Zn$ isotopic composition for the different groups of meteorites. The different groups of meteorites are isotopically distinct. The EL6 are isotopically heavy, the aubrites isotopically light and the EH and EL3 have a normal terrestrial Zn isotopic composition.

Aubrite main group (-7.08<δ^{66}Zn<-0.37); EH3 chondrites (0.15<δ^{66}Zn<0.31); EH4 chondrites (0.15<δ^{66}Zn<0.27); EH5 chondrites (δ^{66}Zn=0.27±0.09‰; n=1); EL3 chondrites (0.01<δ^{66}Zn<0.63); the Shallowater aubrite (1.48<δ^{66}Zn<2.36); EL6 chondrites (2.26<δ^{66}Zn<7.35); and the impact melt enstatite chondrite Happy Canyon (δ^{66}Zn=0.378).

The terrestrial standard BCR-2 (δ^{66}Zn=0.25±0.02‰; n=14) has a typical "terrestrial" isotopic composition (Ben Othman et al., 2006) and confirms the results from Herzog et al. (2009) and Viers et al. (2007).

3.2 Replicate analyses of different pieces of the same meteorite

The δ^{66}Zn of the three Norton County samples (-0.44‰, -2.43‰, -4.11‰) show a large spread. One piece of Shallowater is slightly different from the others (1.48‰ vs 2.25‰ and 2.38‰). The different pieces of all the other meteorites (Kota-Kota, Qingzhen, Indarch, PCA 90120, Happy Canyon) are all identical within error. These results demonstrate the contrasting isotopic homogeneity of enstatite chondrites and the heterogeneity of aubrites, which are coarse-grained, with large enstatite crystals and with the sulfides infiltrating the grain boundaries

3.3 Isotopic composition of the sequential leaches from the same samples

The sequential dissolution was conducted to understand the elemental distribution of Zn between the different phases of the enstatite chondrites and to test whether the different phases

were at isotopic equilibrium. The amounts of sample available and the Zn contents (few ppm) were too small for analyzing the Zn isotopic composition of separated minerals.

A first observation is that Zn is not hosted in the same phases and has different isotopic compositions among EH4, EL3 and EL6 chondrites (Table 3). In the EH4 group, Zn is evenly distributed between silicates and magnetic phases, whereas sulfides contain negligible fractions of Zn. This observation is consistent with those of Kong et al. (1997) in the magnetic and non-magnetic assemblages of enstatite chondrites. However, El Goresy et al. (1988) found that most of Zn of EH3 is hosted in sulfides. A possible solution for this discrepancy is that there is a redistribution of Zn between EH4 and EH3 or that Zn bearing sulfides where associated with metal and therefore were sampled with the magnetic fraction. In EL3 chondrites, most of the Zn is hosted in sulfides (79%), with a smaller fraction residing in the magnetic assemblages. Silicates are essentially devoid of Zn. In EL6 chondrites, most of the Zn is hosted in silicates (68.9%), while sulfides account for most of the rest (26.4%) with a small fraction residing in the magnetic assemblages (4.7%). In addition, these results confirm the large variations of the Zn contents known among the different groups of enstatite chondrites (Kallemeyn and Wasson, 1986; Kong et al., 1997; Wang and Lipschutz, 2005) and gives the following values; EH4 (270 ppm); EL3 (100 ppm), and EL6 (5 ppm).

The isotopic compositions of the mineral assemblages of the enstatite chondrites vary among the different groups. The different assemblages (magnetic, silicates, sulfides) of the EH4 chondrite Indarch are isotopically indistinguishable from each other (table 3 and Fig. 3) and from the bulk rock (table 2). The magnetic assemblage of the EL3 chondrite PCA 90120 is slightly enriched in light isotopes (δ^{66}Zn= -0.07‰) with respect to the other assemblages

(δ^{66}Zn=0.45±0.56‰), which are indistinguishable within error. Finally the EL6 chondrite Blithfield, shows very large isotopic variations among the different assemblages: silicates, which harbor the most Zn, are highly enriched in heavy isotopes (δ^{66}Zn=6.99‰); sulfides are isotopically lighter (δ^{66}Zn=2.07‰) and the magnetic assemblages have a relatively unfractionated isotope composition (δ^{66}Zn=0.39‰) compared to our terrestrial standard. A mass

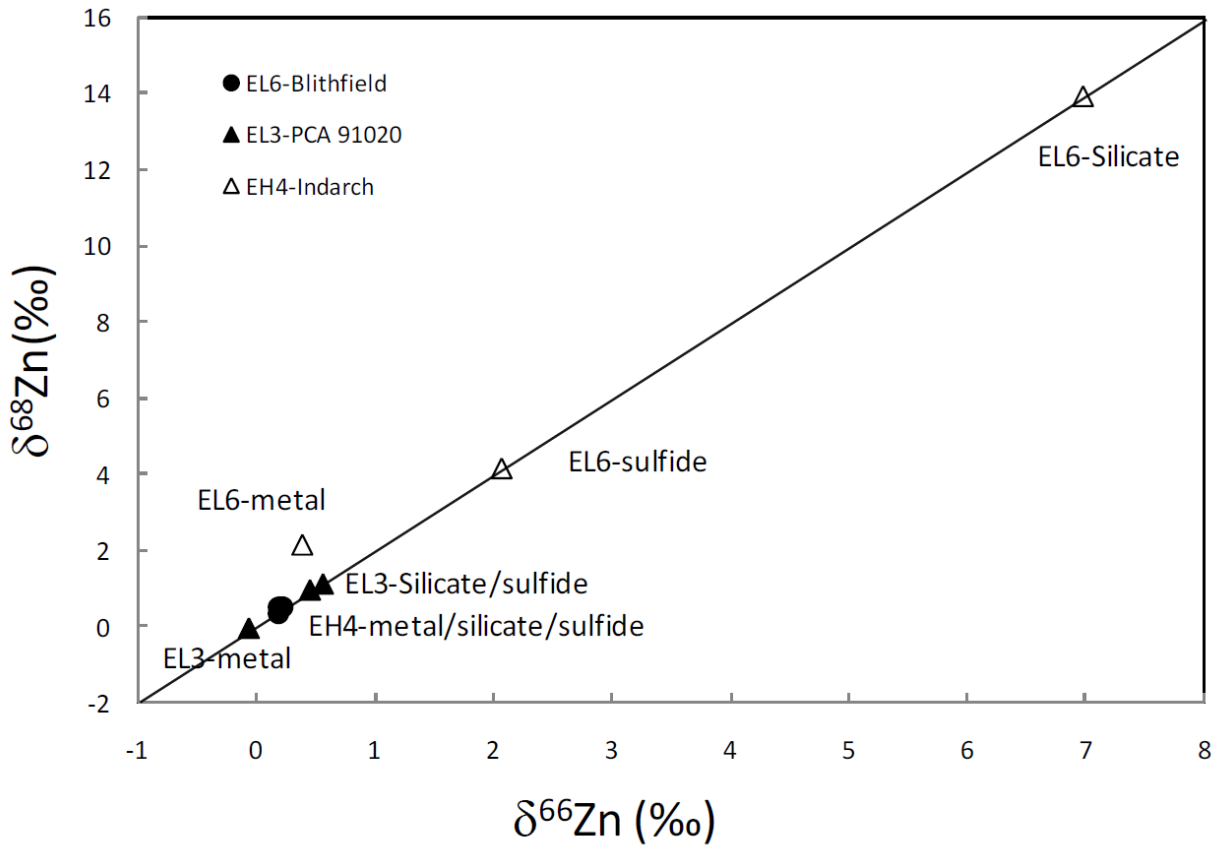

FIGURE 3: δ^{68}Zn vs δ^{66}Zn for the separated phases (silicates, metal and sulfides) of Indarch (EH4); PCA 91020 (EL3) and Blithfield (EL6). The percentage of the total Zn hosted by the different phases is indicated between parentheses. The three phases of Indarch have the same isotopic composition; the metal of PCA 91020 is slightly lighter than the silicates and sulfides. The silicates of Blithfield (EL6) are highly isotopically heavier than the sulfides and metal.

balance calculated from the separated assemblages gives $\delta^{66}Zn$=5.17‰ which compares well with the value for the bulk sample ($\delta^{66}Zn$=5.45‰).

4. Discussion

4.1. Enstatite meteorites are the rocks with the most extreme Zn isotopic compositions in the Solar System

The aubrite Peña Blanca Spring ($\delta^{66}Zn$=-7.04‰) and the EL6 chondrite North West Forrest ($\delta^{66}Zn$=+7.35‰) represent the planetary objects with the isotopically lightest and heaviest Zn known so far, respectively.

The Zn isotope of terrestrial rocks is very homogeneous, with $\delta^{66}Zn$ typically measured between 0.20‰ and 0.40‰ in igneous rocks (Marechal, 1998; Ben Othman et al., 2006; Cloquet et al., 2008) and up to 0.70‰ in some sedimentary rocks and ores (Albarede, 2004). Some tektites are enriched in the heavy isotopes and contain the most fractionated terrestrial Zn ($\delta^{66}Zn$ up to +2.49‰) (Moynier et al., 2009a). Manganese nodules from the circum-arctic also show heavy Zn isotope compositions with $\delta^{66}Zn$ values up to +1.16‰ (Maréchal et al., 2000), which probably reflects the preferential uptake of light isotopes by biological activity in the upper water column, a process not relevant to the present work. Natural samples with isotopically light Zn ($\delta^{66}Zn$ down to -0.90‰) are not very common, and the largest effects seem to be almost limited to biological material (Weiss et al., 2005; John et al., 2007; Viers et al., 2007; Moynier et al., 2009c).

The range of $\delta^{66}Zn$ variations in ordinary (-1.30‰ to 0.55‰) and carbonaceous (0.16‰ to 0.52‰) chondrites (Luck et al., 2005; Moynier et al., 2007) is narrow with respect to the range

in enstatite chondrites (-0.01‰ to +7.35‰) (see Fig. 4), which emphasizes the unusual character of the processes affecting the parent bodies of the latter.

4.2 Origin of the Zn isotopic fractionation in enstatite chondrites

The very narrow range in $\delta^{18}O$ among and between EH, EL and aubrites (Clayton et al., 1984; Clayton and Mayeda, 1996; Miura et al., 2009) indicates that these samples were not subjected to low- or intermediate-temperature aqueous alteration on the parent body nor to terrestrial weathering.

The unfractionated Zn isotopic compositions of the different petrologic types of EH chondrites with respect to terrestrial values (EH3 ($\delta^{66}Zn$=0.21±0.07‰); EH4 ($\delta^{66}Zn$=0.21±0.03‰); EH5 chondrites ($\delta^{66}Zn$=0.27±0.09‰) contrasts with the observations on other most chondritic groups. $\delta^{66}Zn$ in ordinary chondrites (-1.3‰ to 0.5‰; Luck et al., 2005), CI (0.46-0.52‰), and CM (0.33-0.55‰) and in the Earth are definitively distinct. CO (0.16-0.26‰) and CV (0.27-0.37‰) are the only chondrites, together with EH, having the same Zn isotopic composition than Earth. These results are consistent with the enstatite-chondrite 'coincidence' observed for many isotopes between the Earth and EH chondrites: oxygen: (Clayton et al., 1984), ^{54}Cr (Trinquier et al., 2007); ^{50}Ti (Trinquier et al., 2009); Xe and Kr (Miura et al., 2009); ^{62}Ni (Regelous et al., 2008) and which has been taken as indicating that the Earth formed from enstatite chondrites (Javoy, 1995; Javoy et al., 2010), or may alternatively attest that enstatite chondrites represent fragments of the proto-Earth which were eventually dislodged from the terrestrial orbit.

The Zn isotopic compositions of the two EL3 chondrites, PCA 91020 and MAC 88184, also have terrestrial values, whereas all EL6 chondrites are both enriched in heavy isotopes and highly depleted in

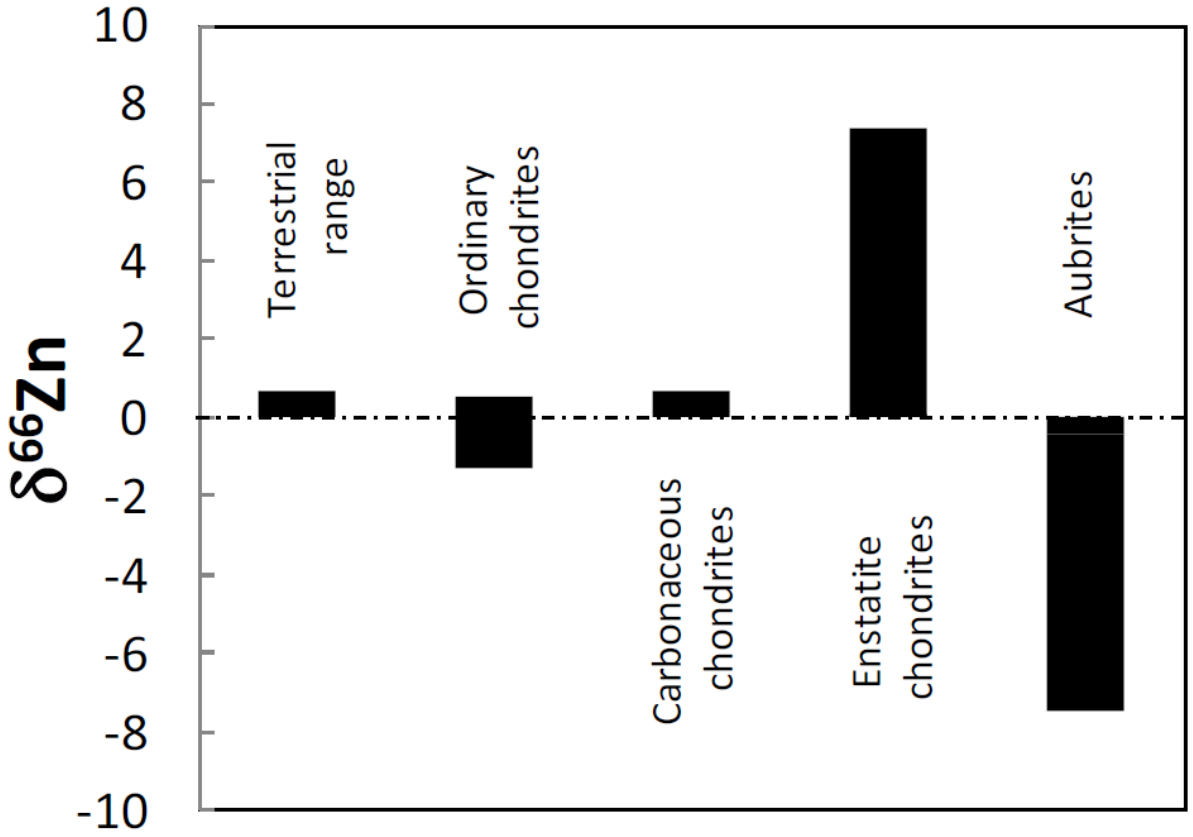

FIGURE 4: δ^{66}Zn range for terrestrial samples; ordinary, carbonaceous, enstatite chondrites and aubrites (this study). The enstatite chondrites show the largest range of Zn isotopic variations among chondritic materials.

Zn (loss of >98% when compared to EL3 chondrites). If isotope fractionation is due to volatilization upon impact, Zn should become isotopically heavier in the residue as the Zn content decreases. It is therefore remarkable that un-equilibrated EL and EH shared the same initial Zn concentration and isotope compositions. Whereas thermal metamorphism does not seem to have modified the concentrations and Zn isotope compositions of EH chondrites, EL chondrites lost most of their Zn in the process and loss preferentially affected the light isotopes to a degree unknown in any other planetary sample, including lunar soils. Impact should produce high-pressure phases, which have never been reported or observed in any EH or EL chondrites. EL6 chondrites contain the mineral sinoite (Si_2N_2O), which has been claimed to have formed by impact melting of unknown material (Rubin et al. 2009). However, this mineral may not have survived impact melting because N_2 would have been lost from the silicate-sulfide-metal melt as gas.

FeS activity in sphalerite in a kamacite-troilite-sphalerite assemblage is known to be a function of temperature and pressure. For the low pressure conditions of the nebula, the composition of the sphalerites allows the closure temperature and cooling rate of enstatite chondrites to be estimated (El Goresy and Ehlers, 1987; 1988; Kissin, 1989). Closure temperatures are higher and cooling rates are faster for EH with respect to EL (Kissin, 1989; Lin and El Goresy, 2002; Zhang and Sears, 1996). This is reminiscent of the Pb-Pb chronological evidence which indicates that L ordinary chondrites cooled in ~30 Ma, whereas the thermal evolution of H ordinary chondrites was completed in <5 Ma (Gopel et al., 1994; Amelin et al., 2005; Bouvier et al., 2007). This suggests that the cause for the depletion of EL in volatile elements and the state of Fe oxidation may be related to protracted cooling and metamorphic conditions on their parent body, a process which is not observed for the EH parent body. The

metamorphic conditions prevailing on the EL asteroid are clearly anhydrous and the loss of volatile elements is likely associated with the migration of sulfidic fumaroles (Biswas et al., 1980; Wang and Lipschutz, 2005).

An alternative explanation for the large difference in δ^{66}Zn between EL3 and EL6 would be if these meteorites had different parent bodies with originally distinct Zn concentrations and δ^{66}Zn. According to the phase relations experimentally determined in the system FeS-MgS-MnS system by Skinner and Luce (1971) a thermal metamorphic event would never change the MgS-MnS ratio as observed in EL6.

4.3 Origin of the Zn isotopic fractionation in aubrites

a. The Zn depletion in aubrites is not due to evaporation

Aubrites are breccias and it has been suggested that their parent body has been involved in a collision sufficiently powerful to result in a global disruption of the parent body, and that the material was subsequently reassembled, to form a "rubble pile" asteroid (Okada et al., 1988; Keil, 1989). Therefore, impact and impact-related processes may be of either local or global significance. Local processes include mechanical mixing of material from different areas of the original parent body, or the incorporation of chondritic xenoliths. Collisional disruption and gravitational reassembly of the aubrite parent body is categorized as a global process. Each of these local or global processes may have influenced the isotopic composition of the aubrites.

Aubrites are strongly depleted in Zn compared to both EH chondrites and EL chondrites (Wolf et al., 1983) and yet they are enriched in light isotopes (δ^{66}Zn down to -7.08‰). This is the exact opposite of what we would expect if the depletion in Zn was due to volatilization, assuming the aubrites started with an enstatite chondrite-like Zn isotopic composition. Zn

isotopic data for aubrites are therefore inconsistent with Zn and other volatile depletion being due to the loss of a vapor phase, and alternative mechanisms accounting for aubrite enrichment in light isotopes must be found.

b. Zn depletion in aubrites is not due to silicate crystal-melt fractionation

Aubrites are cumulate rocks probably formed through fractional crystallization from a Mg-rich parent magma (Okada et al., 1988). It is generally assumed that the aubrite protolith was similar in composition to material of enstatite chondrite composition (Casanova et al., 1993). None of the enstatite chondrites analyzed here has a Zn isotopic composition similar to aubrites. On Earth, igneous processes are insufficient to fractionate Zn isotopes to a large extent (Ben Othman et al., 2006). In addition, other differentiated meteorites do not seem to show a broad range of δ^{66}Zn values, or the magnitude is small when compared to aubrites: HED (-1.76‰ to 1.67‰, Paniello et al., 2009), ureilites (0.25-1.04‰ Moynier et al., 2008). Therefore, igneous processes do not seem to account for the inordinately large isotopic fractionation observed in aubrites, and we will now examine the effect of sulfide migration.

c. Zn isotope fractionation between metal, silicates and sulfides

In enstatite chondrites, Zn is distributed among silicate phases, reduced metal, and sulfides, which may contribute to Zn isotope fractionation to some extent. Based on a detailed study of the mineralogy of Peña Blanca Spring (Lodders et al., 1993), Zn appears mainly in alabandite (< 800 ppm), oldhamite (< 160 ppm), troilite (< 65 ppm), and enstatite (12 ppm). Although enstatite has rather low Zn concentration with respect to other minerals, its high abundance in aubrites (> 90%) makes it the major contributor to the Zn inventory of the sample. In enstatite

chondrites the phases hosting Zn are different in EH4, EL3, and EL6 chondrites (Table 3). In EH4 chondrites Zn is evenly distributed among metal and silicates; in EL3 chondrites most of the Zn is hosted in sulfides, while in EL6 chondrites about 2/3 of the Zn is hosted in the silicates and 1/3 in the sulfides. Our result in EH4 is in agreement with Kong et al. (1997) but disagrees with El Goresy and Ehlers (1989) who observed a large abundance of sphalerite, (Zn,Fe)S, in Indarch. A possible explanation for this discrepancy is that we sampled the Zn-bearing sulfide together with the magnetic phases which would confirm the observation of El Goresy et al. (1988) that Zn-bearing sulfides are associated with kamacite in EH3. If the aubrite parent body has the composition of one of these enstatite chondrite groups, metal/sulfide segregation into the core and preferential loss of Zn associated with sulfidic fumaroles with respect to silicates would cause Zn in the aubrite parent body to become fractionated. This is consistent with the observation by Luck et al. (2005) that Zn in sulfides from the Canyon Diablo iron meteorite is isotopically lighter by ~1‰/amu with respect to Zn in metal.

Isotopic fractionation of Zn among mineral phases varies between the different groups of enstatite chondrites (Table 3): EH4 chondrites are isotopically homogeneous, Zn in the metal of EL3 chondrites is slightly lighter than in coexisting sulfides and silicates, whereas Zn in sulfides and metal from EL6 chondrites is isotopically much lighter than in the silicates, which host the most of the Zn. Since the different phases of EH4 chondrites are isotopically homogeneous, the preferential removal of any of these phases would not affect the isotopic composition of the residue. Segregation of slightly isotopically light Zn in metal as in EL3 chondrites does not explain the isotopically light Zn of aubrites as the segregation of the core would only make mantle Zn isotopically heavier. The same is true for EL6 chondrites; both sulfides and metal are isotopically lighter than silicates, and removing both sulfides and metal would leave Zn in the

silicate residue isotopically heavy. Fractionation of any of these phases does not provide a satisfactory interpretation for isotopically light Zn in aubrites.

d. Differentiation of the Aubrite from an EL6-type parent body

Biswas et al. (1980) heated Abee, an EH4 chondrite, at temperatures of 1000 to 1400 °C under moderate vacuum (10^{-2} atm) in order to simulate the loss of volatile elements during the thermal metamorphism of enstatite chondrites. Under such condition, Zn is essentially lost at 1100°C (see Fig.1 in Biswas et al. 1980). Since the aubrite parent body has been heated to higher temperature in order to melt and differentiate, it must have lost most of its original Zn by evaporation under very reducing conditions (Biswas et al., 1980; Lodders et al., 1993). In addition, aubrites represent cumulates from a melt (Keil, 1989) and making the conservative assumption that all the Zn in aubrites is hosted in orthopyroxene, literature orthopyroxene/melt Zn partition coefficients of 2.1 (Klemme et al., 2006) suggests that the parent melt was itself depleted in Zn. The low concentration of Zn in aubrites is a strong hint that these rocks have been contaminated by vapors and melts and that their Zn isotope compositions reflect that of this mobile phase and not that of the original magma. As discussed in section 4.2, EL6 lost isotopically light Zn during open system metamorphism. Such a process must have liberated isotopically light Zn into the interstitial medium and the exosphere. Because aubrites are extremely Zn-poor, even a subtle contamination by light Zn evolved from an EL6-like parent body can account for their concentrations and δ^{66}Zn values.

4.4 Shallowater and Happy Canyon: evaporation induced by impacts?

Zinc in Shallowater is isotopically heavier than in any other aubrite (δ^{66}Zn=1.48-2.36‰) and therefore the Zn isotopes support the view that the Shallowater parent body is different from the asteroid parent to the other aubrites. Keil (1989) proposed that the original asteroid consisted of partially or completely molten enstatite covered with a solid carapace, which was disrupted by low-velocity impact with a solid body of enstatite chondrite- like material. Material from the impactor occurs as the interstitial assemblage to the unbrecciated enstatite crystals (Keil, 1989). Evaporation of Zn with enrichment in heavy isotopes is the best explanation for the enrichment of heavy isotopes compared to chondrites.

Happy Canyon, which was initially classified as an aubrite (Olsen et al., 1977), has now been re-classified as an impact melt enstatite chondrite (McCoy et al., 1995). **Its** Zn isotope composition (δ^{66}Zn=0.38±0.02‰) is similar to that of the bulk Earth, EH chondrites, and EL3 chondrites, but is clearly different from the values in aubrites, which are all very negative and in EL6, in which Zn is isotopically heavier. Happy Canyon contains up to 70 vol.% impact-melt material, which is intermixed with unmelted target clastic material (up to 30 vol.%) (McCoy et al., 1995). Impact-melting should have increased the δ^{66}Zn of Happy Canyon with respect to the original material (aubrites, EL, or EH chondrites). A genetic connection is consistent with a parent body resembling aubrites (δ^{66}Zn = 2.90‰), EH3, 4 and 5 (0.21-0.27‰), and EL3 chondrites (0.38‰). Happy Canyon meteorite may therefore be related to either the EH, the unequilibrated EL, or the aubrite parent bodies. Derivation from EL6 material or a connection with Shallowater, in which Zn is isotopically heavier, is unlikely.

5. Conclusions

We measured the Zn isotopic composition of 5 EH(3,4,5) chondrites, 10 EL(3,6) chondrites, 8 aubrites, Shallowater and Happy Canyon and discovered the most extreme range of mass-dependent fractionation yet measured in natural samples. EH chondrites and EL3 chondrites have normal terrestrial Zn isotopic compositions whereas EL6 chondrites are highly enriched in heavy isotopes. The Zn isotopic composition and abundance show that volatile element depletion in EL3 chondrites and EL6 chondrites is due to volatilization (fumarolic activity), probably during the protracted cooling and thermal metamorphism of the parent body. Aubrites are strongly depleted in Zn compared to both EH chondrites and EL chondrites (Wolf et al., 1983) and their Zn is isotopically very light. Evaporation therefore fails to explain the depletion of aubrites in volatiles. On Earth, igneous processes do not fractionate Zn isotopes to a large extent, while other differentiated meteorites do not seem to show substantial Zn isotope variability. Igneous processes do not explain the very large isotopic fractionation observed in aubrites either. We propose that the Zn isotope compositions of aubrites reflect that of a mobile phase which has contaminated these rocks and not that of the original magma. This mobile phase may contain Zn lost from the EL parent body during the protracted cooling and thermal metamorphism. This model therefore strengthens the connection between the parent bodies of aubrites and EL chondrites.

ACKNOWLEDGEMENTS

We thank Philippe Telouk for maintaining the MC-ICP-MS in Lyon in perfect condition and Joyce Brannon for taking care of the clean lab in St Louis. We thank Joel Baker, Ahmed El Goresy and an anonymous reviewer for thorough and constructive reviews.

We acknowledged the support of the Programme National de Planétologie (INSU-CEA) and the Agence Nationale de la Recherche (FA) and NASA LASER #NNX09AM64G (FM). We also are indebted to Joseph Boesenberg and Denton Ebel (American Museum of National History, NewYork), Timothy McCoy (US National Museum of Natural History, Smithsonian Institution,Washington DC), Caroline Smith (The Natural History Museum, London), Alex Bevan (Western Australian Museum , Perth), Jim Karner and Carl Agee (University of New Mexico, Albuquerque), Franz Brandstatter (Naturhistorisches Museum, Vienna), James Holstein and Clarita Nunez (The Field Museum, Chicago), Meenakshi Wadhwa (Arizona State University, Tempe), Cecilia Satterwhite (NASA Johnson Space Center, Houston) and the Comité de Gestion (Museum Nationale d'Histoire Naturelle, Paris) for their generous donations of meteorite samples for this work and their confidence in our analytical and scientific capabilities.

REFERENCES

Albarède, F. (2004) The stable isotope geochemistry of copper and zinc. In: Johnson, C. M., Beard, B. L., and Albarede, F. Eds.), *Geochemistry Of Non-Traditional Stable Isotopes*. Mineralogical Society of America. 55, 409-425.

Albarède, F., Bunch, T. E., Moynier, F., and Douchet, C. (2007) Isotope fractionation during impact: Earth versus the moon. *Meteoritics Planet. Sci.* 42, A11-A11.

Amelin, Y., Krot, AN, Hutcheon, ID, and Ulyanov, AA (2002) Lead isotopic ages of chondrules and calcium–aluminum-rich inclusions, *Science* **297**, 1678–1683.

Amelin, Y., Ghosh, A., and Rotenberg, E. (2005) Unraveling the evolution of chondrite parent asteroids by precise U-Pb dating and thermal modeling. *Geochim. Cosmochim. Acta* 69, 505-518.

Ben Othman, D., Luck, J. M., Bodinier, J. L., Arndt, N. T., and Albarède, F. (2006) Cu-Zn isotopic variations in the Earth's mantle. *Geochim. Cosmochim. Acta* 70, 46.

Biswas, S., Walsh, T., Bart, G., and Lipschutz, M. E. (1980) Thermal metamorphism of primitive meteorites. XI - The enstatite meteorites: Origin and evolution of a parent body. *Geochim. Cosmochim. Acta* 44, 2097-2110.

Bouvier, A., Blichert-Toft, J., Moynier, F., Vervoort, J. D., and Albarede, F. (2007) Pb-Pb dating constraints on the accretion and cooling history of chondrites. *Geochim. Cosmochim. Acta* 71, 1583-1604.

Casanova, I., Keil, K., and Newsom, H. E. (1993) Composition of Metal in Aubrites - Constraints on Core Formation. *Geochim. Cosmochim. Acta* 57, 675-682.

Clayton, R. N., Mayeda, T. K., and Rubin, A. E. (1984) Oxygen isotopic composition of enstatite chondrites and aubrites. *J. Geophys. Res.* 89, 245-249.

Clayton, R. N. and Mayeda, T. K. (1996) Oxygen isotope studies of achondrites. *Geochim. Cosmochim. Acta* 60, 1999-2017.

Cloquet, C., Carignan, J., Lehmann, M. F., and Vanhaecke, F. (2008) Variation in the isotopic composition of zinc in the natural environment and the use of zinc isotopes in biogeosciences: a review. *Anal. Bio. Chem.* 390, 451-463.

El Goresy, A. and Ehlers, K. (1987) Sphalerite Relations in EH-Chondrites - Textures, Compositions, Diffusion Profiles and Their Relevance to Temperature and Pressure History. *Meteoritics* 22, 370-371.

El Goresy, A. and Ehlers, K. (1988) Critical-Review of the Sphalerite Cosmo-Barometer. *Chem. Geol.* 70, 31-31.

Gopel, C., Manhes, G., and Allegre, C. J. (1994) U-Pb systematics of phosphates from equilibrated ordinary chondrites. *Earth Planet. Sci. Lett.* 121, 153-171.

Graham, A. and Henderson, P. (1985) Rare earth elements abundance in separated phases of Mayo Belwa, an enstatite achondrite. Meteoritics 20, 141-149.

Herzog, G. F., Moynier, F., Albarede, F., and Berezhnoy, A. A. (2009) Isotopic and elemental abundances of copper and zinc in lunar samples, Zagami, Pele's hairs, and a terrestrial basalt. *Geochim. Cosmochim. Acta* 73, 5884-5904.

Jacobsen, B.. Yin, QZ, Moynier, F., Amelin, Y., Krot, AN, Nagashima, K.,. Hutcheon, ID, Palme, H. (2008) ^{26}Al-^{26}Mg and ^{207}Pb-^{206}Pb systematics of Allende CAIs: Canonical solar initial ^{26}Al/^{27}Al ratio reinstated. *Earth Planet. Sci. Lett.* 272:353-364.

Javoy, M. (1995) The integral enstatite chondrite model of the Earth. *J Geophys. Res. Lett.* 22, 2219-2222.

Javoy, M., Kaminski, E., Guyot, F., Andrault, D., Sanloup, C., Moreira, M., Labrosse, S., Jambon, A., Agrinier, P., Davaille, A., and Jaupart, C. (2010) The chemical composition of the Earth: Enstatite chondrite models. *Earth Planet. Sci. Lett.* in press.

John, S. G., Geis, R., Saito, M., and Boyle, E. A. (2007) Zn isotope fractionation during high-affinity zinc transport by the marine diatom Thalassiosira oceanica. *Limnol. Oceanogr.* 52, 2710-2714.

Kallemeyn, G. W. and Wasson, J. T. (1986) Compositions of enstatite (EH3, EH4,5 and EL6) chondrites Implications regarding their formation. *Geochim. Cosmochim. Acta* 50, 2153-2164.

Keil, K. (1989) Enstatite meteorites and their parent bodies. *Meteoritics* 24, 195-208.

Keil, K., Ntaflos, T., Taylor, G. J., Brearley, A. J., and Newsom, H. E. (1989) The Shallowater aubrite - Evidence for origin by planetesimal impacts. *Geochim. Cosmochim. Acta* 53, 3291-3307.

Keil, K. (2010) Enstatite achondrite meteorites (aubrites) and the histories of their asteroidal parent bodies. *Chemie der Erde* in press.

Kennedy, B. M., Hudson, B., Hohenberg, C. M., and Podosek, F. A. (1988) I-129/I-127 Variations among Enstatite Chondrites. *Geochim. Cosmochim. Acta* 52, 101-111.

Kissin, S. A. (1989) Application of the Sphalerite Cosmobarometer to the Enstatite Chondrites. *Geochim. Cosmochim. Acta* 53, 1649-1655.

Klemme, S., Gunther, D., Hametner, K., Prowatke, S., and Zack, T. (2006) The partitioning of trace elements between ilmenite, ulvospinel, armalcolite and silicate melts with implications for the early differentiation of the moon. *Chem. Geol.* 234, 251-263.

Krot, A.N., Amelin, A., Bland, P., Ciesla, F., Connelly, J., Davis, A.M., Huss, G.R., Hutcheon, I., Makide, K., Nagashima, K., Nyquist, L., Russell, S.S.,. Scott, E.R.D , Thrane, K. Yurimoto, H., Yin, Q.Z. (2009) Origin and chronology of chondritic components: A review. *Geochim. Cosmochim. Acta* 73, *4963-4997*

Kong, P., Mori, T., and Ebihara, M. (1997) Compositional continuity of enstatite chondrites and implications for heterogeneous accretion of the enstatite chondrite parent body. *Geochim. Cosmochim. Acta* 61, 4895.

Larimer, J. W. (1968) An experimental investigation of oldhamite, CaS; and the petrologic significance of oldhamite in meteorites. *Geochim. Cosmochim. Acta* 32, 965-982.

Lin, Y. and El Goresy, A. (2002) A comparative study of opaque phases in Qingzhen (EH3) and MacAlpine Hills 88136 (EL3): Representatives of EH and EL parent bodies. *Meteoritics Planet. Sci.* 37, 577-599.

Lodders, K., Palme, H., and Wlotzka, F. (1993) Trace elements in mineral separates of the Pena Blanca Spring aubrite - Implications for the evolution of the aubrite parent body. *Meteoritics* 28, 538-551.

Lodders, K. and Fegley Jr, B., 1998. *The Planetary Scientist's Companion.* Oxford Univ. Press.

Lodders, K. (2003) Solar System Abundances and Condensation Temperatures of the Elements. *Astrophys. J.* 591, 1220-1247.

Luck, J. M., Othman, D. B., and Albarede, F. (2005) Zn and Cu isotopic variations in chondrites and iron meteorites: Early solar nebula reservoirs and parent-body processes. *Geochim. Cosmochim. Acta* 69, 5351-5363.

Maréchal, C., 1998. Géochimie des isotopes du Cuivre et du Zinc. Méthode, variabilités naturelles, et application océanographique. PhD, Ecole Normale Supérieure de Lyon.

Maréchal, C., Télouk, P., and Albarède, F. (1999) Precise analysis of copper and zinc isotopic compositions by plasma-source mass spectrometry. *Chem. Geol.* 156, 251-273.

Maréchal, C., Douchet, C., Nicolas, E., and Albarède, F. (2000) The abundance of zinc isotopes as a marine biogeochemical tracer. *Geochem., Geophys., Geosyst.* 1, 1999GC-000029.

McCoy, T. J., Keil, K., Bogard, D. D., Garrison, D. H., Casanova, I., Lindstrom, M. M., Brearley, A. J., Kehm, K., Nichols, R. H., Jr., and Hohenberg, C. M. (1995) Origin and history of impact-melt rocks of enstatite chondrite parentage. *Geochim. Cosmochim. Acta* 59, 161-175.

Miura, Y. N., Hidaka, H., Nishiizumi, K., and Kusakebe, M. (2009) Noble gaz and oxygen isotope studies of aubrites: A clue to origin and histories. *Geochim. Cosmochim. Acta* 71, 251-270.

Moynier, F., Albarède, F., and Herzog, G. (2006) Isotopic composition of zinc, copper, and iron in lunar samples. *Geochim. Cosmochim. Acta* 70, 6103-6117

Moynier, F., Blichert-Toft, J., Telouk, P., Luck, J. M., and Albarède, F. (2007) Comparative stable isotope geochemistry of Ni, Cu, Zn, and Fe in chondrites and iron meteorites. *Geochim. Cosmochim. Acta* 71, 4365-4379.

Moynier, F., Beck, P., Jourdan, F., Yin, Q.-Z., Reimold, U., and Koeberl, C. (2009a) Isotopic fractionation of zinc in tektites. *Earth Planet. Sci. Lett.* 277, 482-489.

Moynier F., Dauphas N., and Podosek F. A. (2009b) Search for ^{70}Zn anomalies in meteorites. *Astrophys. J.* 700, L92-L95.

Moynier, F., Pichat, S., Pons, M. L., Fike, D., Balter, V., and Albarède, F. (2009c) Isotopic fractionation and transport mechanisms of Zn in plants. *Chem. Geol.* 267, 125-130.

Moynier, F., Yin, Q. Z., Gillet, P., Beck, P., Ferroir, T., Barrat, J. A., and Albarède, F. (2010) Volatilization induced by impacts recorded in Zn isotope composition of ureilites. *Chemical Geology.* doi:10.1016/j.chemgeo.2010.07.005

Mullane, E., Russell, S. S., and Gounelle, M. (2005a) Aubrites: An Iron and Zinc Isotope Study. *Lunar Planet. Sci. XXXVI.* Lunar Planet. Inst., Houston, #1251.

Mullane, E., Russell, S. S., and Gounelle, M. (2005b) Enstatite Chondrites: An Iron and Zinc Isotope Study. *Lunar Planet. Sci. XXXVI.* Lunar Planet. Inst., Houston, #1250.

Okada, A., Keil, K., Taylor, G. J., and Newsom, H. (1988) Igneous history of the aubrite parent asteroid - Evidence from the Norton County enstatite achondrite. *Meteoritics* 23, 59-74.

Olsen, E. J., Bunch, T. E., Jarosewich, E., Noonan, A. F., and Huss, G. I. (1977) Happy Canyon - A new type of enstatite achondrite. *Meteoritics* 12, 109-123.

Paniello, R. C., Moynier, F., Podosek, F. A., and Beck, P. (2009) Zinc isotopic composition of achondrites. *Meteoritics Planet. Sci.* 72, 5251.

Regelous, M., Elliott, T., and Coath, C. D. (2008) Nickel isotope heterogeneity in the early Solar System. *Earth Planet. Sci. Lett.* 272, 330-338.

Richter, F. M. (2004) Timescales determining the degree of kinetic isotope fractionation by evaporation and condensation. *Geochim. Cosmochim. Acta* 68, 4971-4992.

Rubin, A. Hubert, H., and Wasson, J. (2009) Possible impact-induced refractory-lithophile fractionations in EL chondrites. *Geochim. Cosmochim. Acta* 73, 1523-1537

Schaefer, L. and Fegley, B. (2010) Volatile element chemistry during metamorphism of ordinary chondritic material and some of its implications for the composition of asteroids. *Icarus* 205, 483-496.

Skinner, B. and Luce, F. (1971) Solid solutions of the type (Ca, Mg, Mn, Fe)S and their use as geothermometers for the enstatite chondrites *.American Mineralogist,* 56, 1269-1297

Shukolyukov, A. and Lugmair, G. W. (2004) Manganese-chromium isotope systematics of enstatite meteorites. *Geochim. Cosmochim. Acta* 68, 2875-2888.

Trinquier, A., Birck, J.-L., and Allègre, C. J. (2007) Widespread ^{54}Cr Heterogeneity in the Inner Solar System. *Astrophys. J.* 655, 1179-1185.

Trinquier, A., Elliott, T., Ulfbeck, D., Coath, C., Krot, A. N., and Bizzarro, M. (2009) Origin of Nucleosynthetic Isotope Heterogeneity in the Solar Protoplanetary Disk. *Science* 324, 374-.

Viers, J., Oliva, P., Nonelle, A., Gelabert, A., Sonke, J., Freydier, R., Gainville, R., and Dupre, B. (2007) Evidence of Zn isotopic frationation in a soil-plant system of a pristine tropical watershed (Nsimi, Cameroon). *Chem. Geol.* 239, 124-137.

Wang, M. and Lipschutz, M. E. (2005) Thermal metamorphism of primitive meteorites-XII. The enstatite chondrites revisited. *Environ. Chem.* 2, 215-226.

Weiss, D. J., Mason, T. F. D., Zhao, F. J., Kirk, G. J. D., Coles, B. J., and Horstwood, M. S. A. (2005) Isotopic discrimination of zinc in higher plants. *New Phytologist* 165, 703-710.

Wolf, R., Ebihara, M., Richter, G. R., and Anders, E. (1983) Aubrites and diogenites - Trace element clues to their origin. *Geochim. Cosmochim. Acta* 47, 2257-2270.

Zhang, Y. H. and Sears, D. W. G. (1996) The thermometry of enstatite chondrites: A brief review and update. *Meteoritics Planet. Sci.* 31, 647-655.

TABLE CAPTIONS

Table 1: Zn abundance and $\delta^{66}Zn$ in aubrites and enstatite chondrites. [a] Lodders and Fegley 1998; [b]Biswas et al. 1980; [c]Wolf et al. 1983; [d]Lodders et al. (1993); [e]Kong et al. (1997)

Table 2: Isotopic composition of Zn in enstatite meteorites and a terrestrial standard (BCR-2). The isotopic composition is represented using the δ notation (parts per 1000 deviation from a terrestrial Zn standard JMC 3-0749 L). The Zn concentrations are in ppm. The external reproducibility (2σ) of $\delta^{66}Zn$ and $\delta^{68}Zn$ are ±0.09‰ and ±0.27‰, respectively. MNHN=Museum National d'Histoire Naturelle, Paris. USNM=United States National Museum, Washington DC. NHM=The National History Museum, London. ASU=Arizona State University, Tempe. UNM= University of New Mexico, Albuquerque, FM=The Field Museum, Chicago. AMNH=American Museum of National History, New York. NMW= Naturhistorisches Museum, Vienna. JSC=Johnson Space Center, NASA, Houston. WAM=Western Australia Museum, Perth.

Table 3: Isotopic composition, concentration and distribution of Zn in separated phases of Indarch (EH4), PC91020 (EL3) and Blithfield (EL6). The magnetic and non-magnetic were separated first with a hand magnet. From the non-magnetic part, the sulfides were first leached out from the silicates in cold 3N HCl.

FIGURE CAPTIONS

FIGURE 1: $\delta^{68}Zn$ vs $\delta^{66}Zn$. All data fall onto the mass-dependent fractionation line of slope 1.94. The sample outside the mass-dependent fractionation line has been excluded from the discussion. Both meteoritic and terrestrial samples plot on the same line, implying that the Zn from all the analyzed samples evolved from a single, isotopically homogeneous reservoir.

FIGURE 2: Zn isotopic composition for the different groups of meteorites. The different groups of meteorites are isotopically distinct. The EL6 are isotopically heavy, the aubrites isotopically light and the EH and EL3 have a normal terrestrial Zn isotopic composition.

FIGURE 3: $\delta^{68}Zn$ vs $\delta^{66}Zn$ for the separated phases (silicates, metal and sulfides) of Indarch (EH4); PCA 91020 (EL3) and Blithfield (EL6). The percentage of the total Zn hosted by the different phases is indicated between parentheses. The three phases of Indarch have the same isotopic composition; the metal of PCA 91020 is slightly lighter than the silicates and sulfides. The silicates of Blithfield (EL6) are highly isotopically heavier than the sulfides and metal.

FIGURE 4: $\delta^{66}Zn$ range for terrestrial samples; ordinary, carbonaceous, enstatite chondrites and aubrites (this study). The enstatite chondrites show the largest range of Zn isotopic variations among chondritic materials.

Table 1

Group	Zn Concentration	δ^{66}Zn
EH	290[a]	0.15 to 0.31
Shallowater	32[b]	1.48 to 2.36
EL	19[a]	0.01 to 7.35
Aubrites	0.5-2[c,d]	-7.08 to -0.37
EL3	213[e]	0.01 to 0.63
EL5,6	6[e]	2.26 to 7.35
EH5	48-100[e]	0.15 to 0.18

Table 2

Name	Museum code	Mass (mg)	Group	f/f	δ^{66}Zn	δ^{68}Zn
Peña blanca spring	MNHN 3409PE	271.0	Aub	Fall	-7.08	-13.88
Mayo Belwa	MNHN 3158PE	259.0	Aub	Fall	-3.91	-7.57
Bishopville	MNHN 178PE	224.0	Aub	Fall	-0.75	-1.32
Cumberland Falls	USNM 2558	540.0	Aub	Fall	-0.37	-0.81
Khor Temiki	NHM 1934,781	443.2	Aub	Fall	-2.51	-4.95
Bustee	NHM 32100	451.9	Aub	Fall	-0.40	-0.73
Aubres	NHM 63552	417.5	Aub	Fall	-6.72	-13.10
Norton County piece 4	ASU 523.3	332.2	Aub	Fall	-0.44	-0.37
Norton County piece 1	UNM	390.0	Aub	Fall	-4.11	-7.52
Norton County piece 2	UNM	380.1	Aub	Fall	-2.43	-4.40
Shallowater piece 1	USNM 1206	321.0	Aub	Find	1.48	2.88
Shallowater piece 2	ASU 318.9	183.5	Aub	Find	2.25	4.65
Shallowater piece 3	ASU 318.9	183.0	Aub	Find	2.36	4.71
Sahara 97096	MNHN	68.9	EH3	Find	0.31	0.56
Kota Kota piece 1	NHM 1905,355	148.2	EH3	Find	0.15	0.39
Kota Kota piece 2	NHM 1905,355	71.2	EH3	Find	0.18	0.41
Qingzhen piece 1		61.2	EH3	Find	0.27	0.57
Qingzhen piece 2		65.8	EH3	Find	0.15	0.34
Indarch piece 1	FM 1404	58.4	EH4	Fall	0.23	0.42
Indarch piece 2	FM 1404	60.3	EH4	Fall	0.19	0.39
Indarch piece 3	FM 1404	65.3	EH4	Fall	0.15	0.35
Indarch piece 4	FM 1404	94.3	EH4	Fall	0.27	0.53
St Mark's	AMNH	94.4	EH5	Fall	0.27	0.45
PCA 91020 piece 1	JSC	157.9	EL3	Find	0.51	1.08
PCA 91020 piece 2	JSC	166.9	EL3	Find	0.63	1.38

MAC 88184	JSC	167.8	EL3	Find	0.01	0.08
Khairpur	AMNH	192.2	EL6	Fall	2.26	4.43
Hvittis	FM 1470	151.8	EL6	Fall	6.78	13.50
Pillistfer	NMW	185.1	EL6	Fall	2.27	4.50
Eagle	USNM 6411	150.5	EL6	Fall	4.49	8.97
Atlanta	NHM 1959,1001	160.0	EL6	Find	6.25	12.49
Yilmia	WAM 12192	95.6	EL6	Find	4.27	8.64
North West Forrest	WAM 13194	106.7	EL6	Find	7.35	14.72
Blithfield	FM 1979	236.1	EL6	Find	5.45	10.95
Happy Canyon piece 1	ASU 1058f	180.0	EL6/7	Find	0.37	0.81
Happy Canyon piece 2	ASU 1058f	183.7	EL6/7	Find	0.38	0.72
BCR-2 (n=14)		105.9	Geo		0.25±0.02	0.48±0.03

Table 3

Sample name	Mass (mg)	group	$\delta^{66}Zn$	$\delta^{68}Zn$	[Zn] ppm	Mass	%Zn
Indarch magnetic	52.9	EH4	0.19	0.51	279	52.9	57.8
Indarch non magnetic	28.0	EH4	0.21	0.39	298	28	
Indarch non magnetic-silicate	17.9	EH4	0.22	0.52	270	39.6	41.9
Indarch non magnetic-sulfides	39.6	EH4	0.18	0.33	4	17.9	0.3
PCA 91020 magnetic	41.2	EL3	-0.07	-0.05	58	41.2	18
PCA 91020 non magnetic	36.0	EL3	0.52	1.16	128	36	
PCA 91020 non magnetic-silicate	45.9	EL3	0.45	0.96	10	45.9	3
PCA 91020 non magnetic-sulfides	23.4	EL3	0.56	1.12	448	23.4	79
Blithfield magnetic	26.1	EL6	0.39	2.14	1	26.1	4.7
Blithfield non magnetic	53.0	EL6	6.77	13.53	5	53	
Blithfield non magnetic-silicate	18.4	EL6	6.99	13.92	4	96.1	68.4
Blithfield non magnetic-sulfides	96.1	EL6	2.07	4.14	8	18.4	26.4